

**Magneto-Rheological Dampers for
Super-sport Motorcycle Applications**
by

John W. Gravatt

Thesis submitted to the Faculty of the
Virginia Polytechnic Institute and State University
in partial fulfillment of the requirements for the degree of

Masters of Science
In
Mechanical Engineering

Approved:

Dr. Mehdi Ahmadian, Chairman

Dr. Mary Kasarda

Dr. Harry Robertshaw

May 8, 2003
Blacksburg, VA

Keywords: magneto-rheological, damper, semiactive,
motorcycle, controllable damper, shock absorber

© 2003 John W. Gravatt

Magneto-Rheological Dampers for Super-sport Motorcycle Applications

John W. Gravatt

Abstract

In recent years, a flurry of interest has been shown for a relatively old technology called magneto-rheological fluids, or MR fluids. Multiple types of devices have been designed to implement this versatile fluid, including linear dampers, clutches, work-piece fixtures, and polishing machines. The devices have been used in automobiles, washing machines, bicycles, prosthetic limbs, and even smart structures.

This thesis focuses on another application of MR dampers, involving super-sport motorcycles. This paper introduces the topics of MR dampers and motorcycle suspensions, and why the two would be a good combination. A detailed history of MR fluids, MR dampers, and motorcycle suspension technologies is given next.

After a broad outline of MR dampers and motorcycle suspensions, the method of designing and manufacturing MR dampers is discussed. The damper design for this research is presented in detail, along with the design procedure used to make it.

Next, laboratory testing for it is covered, including the test equipment, test procedure, and the laboratory test results. Upon laboratory test completion, the field test setup and procedure are presented. The results of field tests with stock dampers and MR dampers with a variety of control systems is discussed.

The MR dampers provided a more stable ride than that of the OEM dampers. By reducing suspension displacement, settling time, and suspension oscillations, the MR dampers were able to reduce suspension geometry instability.

Lastly, concluding remarks are made on the research presented. Design flaws are discussed, as well as recommendations for future work in the same area.

Acknowledgements

I would like to thank Dr. Mehdi Ahmadian for helping me through my master's studies at Virginia Tech. Dr. Ahmadian was always an inspiration, no matter what bad news I had to tell him about my research. I thank him for being patient with me when my timelines did not hold true, and I will never forget his words of encouragement. Thanks so much for welcoming me into the AVDL lab family.

Thanks and love go to my family, who has supported me endlessly. To my mother, Sarah, thank you for understanding and giving me support and love when I needed it most. To my father, Mayo, thanks for the encouragement and support, and putting your trust in me. To my brother, Carter, thanks for the advice about the road less traveled, the one you have traversed before me, and thanks for all the supporting phone calls. To my sister, Sally, be patient with the road ahead, life is what you make of it – and good luck in your master's studies. To my whole family – you're the best family I could have!

I would like to give special thanks to Steve Grenoble and Fernando Goncalves. Steve has been a lifesaver many times during assembly and testing, helping switch forks and anything else that needed to be done. Thanks to Fernando for sacrificing his time to help me do all of my laboratory testing. Thanks to all the AVDL members for our great times at Claytor Lake – may life take you all on a fair and prosperous journey.

Last but not least, I would like to acknowledge the support of Lord Corporation, Material Division, in Cary, North Carolina for providing the MR fluid that was used in this research.

I would like to dedicate this research to my late grandfather, John R. Sutton, affectionately known as Jack. An engineer and inventor, his strive to reach seemingly impossible goals inspired me greatly.

Contents

Chapter 1 Introduction.....	1
1.1 OVERVIEW OF MOTORCYCLE SUSPENSIONS AND MR TECHNOLOGIES	1
1.1.1 A Brief History of Motorcycle Suspension Technologies.....	1
1.1.2 Magneto-rheological Fluids and Devices.....	2
1.1.3 Magneto-rheological Damper Applications for Motorcycles.....	3
1.2 OBJECTIVES	4
1.2.1 Approach	4
1.2.2 Outline	5
1.2.3 Contributions	5
Chapter 2 Background	6
2.1 MR FLUID.....	6
2.2 MR DAMPERS.....	11
2.3 MOTORCYCLE SUSPENSION TECHNOLOGY.....	14
2.4 LITERATURE SEARCH.....	17
2.4.1 Keywords: magnetorheological motorcycle	18
2.4.2 Keywords: magneto-rheological motorcycle.....	18
2.4.3 Keywords: magneto rheological motorcycle	18
2.4.4 Keywords: MR motorcycle.....	19
2.5 SUMMARY.....	19
Chapter 3 Hardware Design and Fabrication.....	20
3.1 PRINCIPLES OF MR DAMPER DESIGN.....	20
3.1.1 MR Damper Types.....	20
3.1.2 MR Damper Mathematics.....	23
3.1.3 Electromagnet Design	27
3.2 MR DAMPER DESIGN FOR MOTORCYCLE APPLICATIONS	29
3.2.1 Test Vehicle Overview	29
3.2.2 Analyzing the OEM Damper Package and Performance	30
3.2.3 Designing the MR Damper.....	32
3.3 CONTROL UNIT DESIGNS	37
3.3.1 On-Off Skyhook Control.....	37
3.3.2 Displacement-Based Control System.....	40
Chapter 4 Hardware Laboratory Testing	43
4.1 LABORATORY TEST PROCEDURE	43
4.2 OEM DAMPER TESTING	45

4.3	MR DAMPER TESTING	46
4.4	REMARKS.....	54
Chapter 5 Hardware Field Testing		55
5.1	FIELD TEST SETUP	55
5.2	PROCEDURE	58
5.3	FIELD TEST RESULTS	60
5.3.1	<i>OEM Damper Results</i>	60
5.3.2	<i>MR Damper Results</i>	62
5.3.3	<i>Performance Comparison</i>	68
5.4	SUBJECTIVE OPINION OF THE TEST RIDER	70
Chapter 6 Conclusions.....		72
6.1	SUMMARY.....	72
6.2	RECOMMENDATIONS.....	75
6.2.1	<i>Damper Design</i>	75
6.2.2	<i>Prediction Model</i>	75
6.2.3	<i>Shaft Material & Design</i>	76
6.2.4	<i>Housing Materials</i>	76
6.2.5	<i>Seals</i>	77
6.2.6	<i>Coil Manufacturing</i>	77
6.2.7	<i>Control Units</i>	78
6.2.8	<i>Control Sensors</i>	78
6.2.9	<i>Data Acquisition Units</i>	79
References.....		80
Vitae		82

List of Tables

TABLE 4.1. DAMPER FORCE CHARACTERIZATION DATA POINTS.....	44
---	----

List of Figures

FIGURE 2.1. JACOB RAINBOW’S MR FLUID EXPERIMENT [2].....	6
FIGURE 2.2. OFF-STATE MR FLUID PARTICLES (LEFT) ALIGNING IN AN APPLIED MAGNETIC FIELD (RIGHT) [ADAPTED FROM 5].....	7
FIGURE 2.3. FERROUS PARTICLE CHAINS RESIST FLUID FLOW [ADAPTED FROM 5].....	8
FIGURE 2.4. MR FLUID IN PRESSURE DRIVEN FLOW (VALVE) MODE [ADAPTED FROM 6].....	9
FIGURE 2.5. MR FLUID IN DIRECT-SHEAR MODE [ADAPTED FROM 6].....	10
FIGURE 2.6. MR FLUID IN SQUEEZE-FILM MODE [ADAPTED FROM 6].....	10
FIGURE 2.7. MR DAMPER OPERATING IN VALVE MODE.	12
FIGURE 2.8. MR DAMPER USING BOTH VALVE AND SHEAR MODES.	13
FIGURE 2.9. MOTORCYCLE SUSPENSION GEOMETRY [ADAPTED FROM 7].....	15
FIGURE 2.10. BMW “TELELEVER” SUSPENSION SYSTEM [ADAPTED FROM 11].	17
FIGURE 2.11. LITERATURE SEARCH FLOWCHART.	18
FIGURE 3.1. MONOTUBE MR DAMPER, SECTION VIEW [ADAPTED FROM 5].....	21
FIGURE 3.2. TWINTUBE MR DAMPER, SECTION VIEW [ADAPTED FROM 5].....	22
FIGURE 3.3. DOUBLE-ENDED (THROUGH-TUBE) MR DAMPER, SECTION VIEW [ADAPTED FROM 5].....	22
FIGURE 3.4. PRESSURE DRIVEN FLOW MODE.	24
FIGURE 3.5. DIRECT-SHEAR MODE.	25
FIGURE 3.6. MR DAMPER DESIGN PROGRAM PART I.....	27
FIGURE 3.7. MR DAMPER DESIGN PROGRAM PART II.	28
FIGURE 3.8. 1997 HONDA CBR900RR (LEFT) WITH OEM FORKS (RIGHT).....	29
FIGURE 3.9. 1997 HONDA CBR900RR OEM DAMPER IN DAMPER DYNAMOMETER FOR FORCE-VELOCITY CHARACTERIZATION.....	30
FIGURE 3.10. 1997 HONDA CBR900RR OEM DAMPER CURVES (ZEROED DATA).	31
FIGURE 3.11. OEM DAMPER ASSEMBLY.	31
FIGURE 3.12. OEM DAMPER AND PREDICTED MR OFF STATE DAMPER CURVES.	33
FIGURE 3.13. RETROFIT MR DAMPER MODULE MODEL (LEFT) AND PROTOTYPE (RIGHT).....	34
FIGURE 3.14. MODEL OF RETROFIT MR DAMPER COMPLETELY ASSEMBLED.....	34
FIGURE 3.15. RETROFIT MR DAMPER ASSEMBLY PROTOTYPE.	35
FIGURE 3.16. RETROFIT MR DAMPER ASSEMBLY, LABELED.	35
FIGURE 3.17. SECTION VIEW OF MR DAMPER MODULE.....	35
FIGURE 3.18. NITROGEN CHARGER ASSEMBLY (LEFT) AND THE PROTOTYPE HARDWARE (RIGHT).....	36
FIGURE 3.19. SKYHOOK CONTROL SETUP [15].....	37
FIGURE 3.20. SKYHOOK CONTROL STRATEGY.	38
FIGURE 3.21. SKYHOOK CONTROL CIRCUITS.	39
FIGURE 3.22. SKYHOOK CONTROL UNIT.	40
FIGURE 3.23. DISPLACEMENT CONTROL POLICY.	41

FIGURE 3.24. DISPLACEMENT CONTROL CIRCUIT BLOCK DIAGRAM.....	41
FIGURE 3.25. DISPLACEMENT BASED CONTROL SYSTEM ON TEST VEHICLE.	42
FIGURE 4.1. DAMPER DYNAMOMETER TEST FACILITY.	43
FIGURE 4.2. DAMPER CURVE ZEROING EXAMPLE.	45
FIGURE 4.3. COMPLETE 1997 HONDA CBR900RR OEM DAMPER CURVE.....	46
FIGURE 4.4. FORCE VS. VELOCITY CURVE FOR MR DAMPER (180PSI).	47
FIGURE 4.5. EFFECT OF ACCUMULATOR PRESSURE ON SPRING FORCE.	48
FIGURE 4.6. MONOTUBE MR DAMPER OPERATING PROPERLY [ADAPTED FROM 5].....	49
FIGURE 4.7. MR DAMPER CAVITATION CAUSED BY INSUFFICIENT ACCUMULATOR PRESSURE [ADAPTED FROM 5].	50
FIGURE 4.8. FORCE VS. VELOCITY CURVE FOR MR DAMPER (100PSI).	51
FIGURE 4.9. THEORETICAL AND EXPERIMENTAL OFF STATE MR DAMPER CURVES.	52
FIGURE 4.10. MR VS. OEM DAMPER COMPARISON.	53
FIGURE 5.1. THE DATAQ DI-700 DATA ACQUISITION UNIT [ADAPTED FROM 16].	55
FIGURE 5.2. DATA ACQUISITION SYSTEM (LEFT) AND LAPTOP COMPUTER (RIGHT).	56
FIGURE 5.3. SENSOR MOUNTING LOCATIONS.....	57
FIGURE 5.4. INFRARED DATA STORAGE TRIGGER (LEFT) AND EMITTERS (RIGHT).	58
FIGURE 5.5. TEST COURSE.....	58
FIGURE 5.6. EQUIVALENT SUSPENSION INPUT GRAPH SHOWING SUSPENSION INPUT VERSUS COURSE DISTANCE.	59
FIGURE 5.7. DATA ACQUISITION SETUP (LEFT) AND VEHICLE TEST (RIGHT)	59
FIGURE 5.8. TIME DOMAIN OEM SUSPENSION PERFORMANCE AT 15 MPH.	61
FIGURE 5.9. FREQUENCY DOMAIN OEM SUSPENSION PERFORMANCE AT 15MPH.	62
FIGURE 5.10. TIME DOMAIN PERFORMANCE OF MR SUSPENSION IN OFF-STATE AT 15 MPH.	63
FIGURE 5.11. FREQUENCY DOMAIN PERFORMANCE OF MR SUSPENSION IN OFF-STATE AT 15 MPH.	64
FIGURE 5.12. TIME DOMAIN PERFORMANCE OF MR SUSPENSION WITH SKYHOOK CONTROL AT 15 MPH.	65
FIGURE 5.13. FREQUENCY DOMAIN PERFORMANCE OF MR SUSPENSION WITH SKYHOOK CONTROL AT 15 MPH.....	66
FIGURE 5.14. TIME DOMAIN PERFORMANCE OF MR SUSPENSION WITH DISPLACEMENT CONTROL AT 15 MPH.....	67
FIGURE 5.15. FREQUENCY DOMAIN PERFORMANCE OF MR SUSPENSION WITH DISPLACEMENT CONTROL AT 15 MPH.....	68
FIGURE 5.16. FREQUENCY DOMAIN COMPARISON OF DISPLACEMENT DATA AT 15 MPH.	69
FIGURE 5.17. OEM AND MR DAMPER PERFORMANCE COMPARISON.	70
FIGURE 6.1. PERFORMANCE COMPARISON OF OEM AND MR DAMPERS.....	74

Chapter 1

Introduction

Since the introduction of the first motorcycle, suspension designers have sought to build suspension systems that can provide both rider comfort and high-speed performance. The purpose of this chapter is to inform the reader of traditional and current motorcycle suspension technologies, and to provide a brief description of magneto-rheological (MR) fluids and their use in new suspension technology. This research pertains to the use of MR technologies in the evolving field of motorcycle suspension systems.

1.1 Overview of Motorcycle Suspensions and MR Technologies

Motorcycle suspension designers have historically sought a good compromise between a comfortable ride and performance handling. Unfortunately, this compromise generally leads to a suspension design that is good for a mix of performance and comfort, yet does not excel at either of the two. Magneto-rheological suspension technologies offer a new component for suspension design that can bridge this shortcoming.

1.1.1 A Brief History of Motorcycle Suspension Technologies

When the first motorcycle was manufactured by Daimler-Benz in 1885, suspension was not a priority. Sporting iron-banded wooden wheels and a rigid chassis, the motorcycle was nicknamed the “bone crusher” due to its lack of a comfortable ride [1]. The first type of suspension introduced on motorcycles was a seat with springs underneath. Soon motorcycle developers realized that a more useful suspension was in order for motorcycle designs, and the emphasis of the development was placed on front suspension.

Initially front suspension consisted of a sliding fork with springs. While boasting more comfort than the original rigid fork design, the new suspension tended to oscillate indefinitely because of its lack of damping capability. The decades between the 1920s and 1940s saw an increase in motorcycle suspension designs; these included leading link designs and frame mounted swing-arms [1]. With the addition of a damper, the simple

sliding sprung fork design proved to be the most robust motorcycle front suspension design available.

Most modern motorcycle suspensions are still based on a telescopic cartridge fork design, which houses both the spring and damper unit. This design proved to be lightweight, inexpensive, and sturdy enough to handle the loads of today's motorcycles. Damper technology, however, has continuously evolved. Monotube dampers have given way to twintube dampers, while fixed orifice damper valving has been replaced by rider-adjustable compression and rebound adjusters. The end goal has been to provide the rider with better ride performance while maintaining comfort.

1.1.2 Magneto-rheological Fluids and Devices

In recent years, a family of fluids known as magneto-rheological fluids has gained increased recognition for its many applications. Magneto-rheological fluids (referred to as "MR" fluids) demonstrate a change in apparent viscosity when exposed to a magnetic field. Jacob Rainbow, an inventor at the US National Bureau of Standards, developed the first MR fluids in the late 1940s [2]. Upon introduction, there was keen interest in the technology for devices like automatic transmissions and clutches, but the activity dropped off shortly thereafter. Resurgence in interest in MR fluids occurred in the early 1990s when Dave Carlson of Lord Corporation began to experiment with the fluid for a variety of devices, including vehicle suspensions.

Jacob Rainbow's original MR fluids consisted of nine parts by weight of carbonyl iron to one part of a carrier fluid, namely silicon oil or hydrocarbon-based oil. To increase the fluid stability and reduce settling, grease or another thixotropic solution was added [2]. This original solution proved to be as strong as modern day MR fluids. Modern fluids use micron sized iron particles coated with an anticoagulant in a carrier fluid of hydrocarbon-based oil, silicon-based oil, or water. The fluids also contain a number of anti-settling agents to prevent the fluid from hardening [2].

Magneto-rheological fluids are activated by the application of a magnetic field across the fluid. The induced field causes alignment of the iron particles in column-type structures parallel to the field lines [3]. This resulting structure resists fluid flow, causing a change in fluid apparent viscosity. While the viscosity of the carrier fluid does not

actually change, the shear strain rate and yield stress of the fluid increase with an increasing field [3]. This variable MR fluid yield stress is advantageous in applications such as dampers and shock absorbers.

Recent renewed interest in MR fluids has been apparent in automobile suspension technologies. Lord Corporation pioneered the use of the fluid in the 1990s, introducing a MR damper for truck seat suspension called the “Motion Master.” Shortly after, Lord developed a rotary MR brake for treadmill applications, as well as dampers for automobile use. Current manufacturers of MR dampers include Lord Corporation, Delphi, and Carrera Shocks, Inc. Cadillac and Corvette models introduced an electronic ride control system in 2003, which boasted the use of MR dampers [17].

1.1.3 Magneto-rheological Damper Applications for Motorcycles

MR technology offers excellent properties that can be utilized in motorcycle suspension design. Changing fork fluid viscosity is one of the most popular ways to tune a motorcycle suspension. With a MR damper system, changing the fluid viscosity is accomplished by adjusting the magnetic field intensity. The range of adjustability is virtually infinite within the off state and saturation state, making MR damper technologies an excellent replacement for conventional motorcycle front suspension dampers. While MR dampers are becoming common in automobile primary suspensions, motorcycle applications are rare.

MR technologies are not limited to simple rebound and compression adjustments though. Utilizing proper control techniques, such as a skyhook or groundhook control methods, MR dampers can drastically increase the damper’s efficiency by reacting to road inputs and minimizing suspension oscillation [13]. Use of MR dampers with an effective control policy allows the suspension to offer both comfort and performance in the same package. Motorcycle suspension performance no longer needs to be hindered by compromise between comfort and performance—adaptive control techniques like skyhook control can offer the great performance *and* great comfort at the same time.

1.2 Objectives

The primary objectives of this research are to:

1. research the MR damper designs to adapt for use in motorcycle front suspensions,
2. design and manufacture retrofit MR damper modules for a motorcycle front suspension,
3. design and manufacture control circuits to operate the MR damper replacements,
4. test the MR damper replacements and control circuit in laboratory and field testing,
5. provide an analysis of the effectiveness of MR dampers for motorcycle applications, and
6. provide recommendations for future design and manufacture of MR dampers for motorcycle applications.

1.2.1 Approach

This research focuses on the design and manufacture of MR dampers and control circuits for use in motorcycle front suspensions. A monotube design was chosen for the MR dampers to replace the vehicle's original equipment manufacturer (OEM) passive twintube dampers. The dampers were manufactured in house and subjected to laboratory dynamic testing to determine the MR damper curves, which were then compared to the OEM suspension damper curves.

Three control circuits were designed and built for field-testing. The first design was a simple DC power supply for the initial ride on the new system. The second design was an analog skyhook control system that utilized accelerometer inputs from the vehicle's wheel and body. The skyhook control system determined both the absolute velocity of the body and the relative velocity of the damper to regulate the damper between its full on and off states. The third control system design was a displacement based control design which used high damping for small displacements, low damping for large displacements, and high damping for a bottoming prevention measure. All control

system designs were field tested to determine their effectiveness for a motorcycle front suspension technology.

1.2.2 Outline

Chapter 2 contains background information on the history and uses of MR fluids, current and previous MR dampers and damper designs, and current motorcycle suspension technology. Current and previous work on MR dampers with applications in motorcycle suspension will also be discussed. Chapter 3 discusses the design and fabrication of the MR dampers and control circuits used in this research. Chapter 4 discusses hardware testing techniques, test setup, and test results for all laboratory testing. Chapter 5 includes testing techniques, test setup, and test results for all field-testing. Chapter 6 summarizes the work done discussed in this paper as well as recommendations for future design and testing of MR dampers for motorcycle front suspensions.

1.2.3 Contributions

The research discussed in this paper will be a great contribution to the motorcycle industry. MR damper technologies would be a great advance in current motorcycle suspension systems, offering greater ease of adjustment, damper adjustment on-the-go, and the possibility of great comfort combined with excellent performance in the same package. Semiactive suspension systems will provide a base for the next generation of motorcycle suspension systems.

Chapter 2

Background

This chapter explains in detail the technical background of MR fluids, their use in MR dampers, and some commercially available MR dampers. Motorcycle suspension technologies will be examined, highlighting some of the problems with modern motorcycle suspension systems. Current and previous research related to the application of MR dampers on motorcycles will be discussed in the literature review.

2.1 MR Fluid

Magneto-rheological fluids are fluids that exhibit a change in rheological properties when a magnetic field is induced through the fluid [3]. In essence, the fluid's flow characteristics, namely apparent viscosity, change. Jacob Rainbow, who worked for the US National Bureau of Standards, first introduced MR fluids in the 1940s [3]. In an early demonstration, Rainbow was able to suspend a 117 pound woman from a swing using the activated fluid, as shown in Figure 2.1 [2]. This experiment proved the strength and

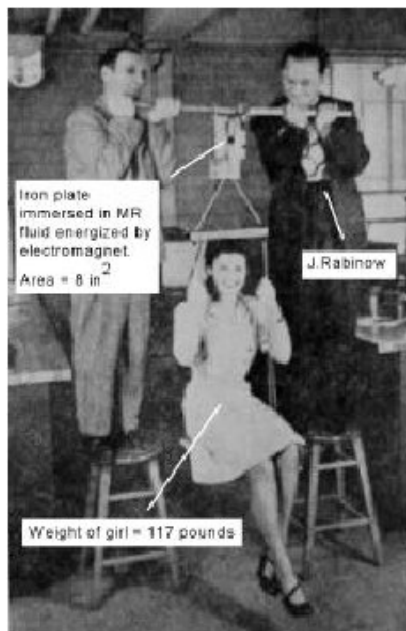


FIGURE 2.1. JACOB RAINBOW'S MR FLUID EXPERIMENT [2].

capabilities of the new MR fluid. For this experiment to succeed, the fluid's yield strength needed to be over 100 kPa.

Initially MR fluids drew significant interest in the 1940s and early 1950s, but soon the new technology lost popularity [3]. In the early 1990s, Lord Corporation pioneered the use of MR fluids in the Motion Master™ Damper and began improving the MR solution characteristics.

MR fluids are quite similar to electrorheological (ER) fluids and ferrofluids in composition: all three fluids are a non-colloidal suspension of polarizable particles [4]. While MR and ER fluids usually contain carbonyl iron on the order of a few microns in size [3], ferrofluids use nanometer-sized iron oxide particles. Ferrofluid particles are too small to demonstrate any yield strength; instead they tend to be only attracted to and flow toward a magnetic field. MR fluids, on the other hand, demonstrate very high yield strengths when a field is induced, usually on the order of 20 to 50 times the strength of ER fluids [4].

With no applied magnetic field (off state), MR fluids behave with Newtonian-like characteristics [6]. Applying an external magnetic field through the fluid activates MR fluids, causing the micron-sized particles to form magnetic dipoles along the lines of magnetic flux, as shown in Figure 2.2.

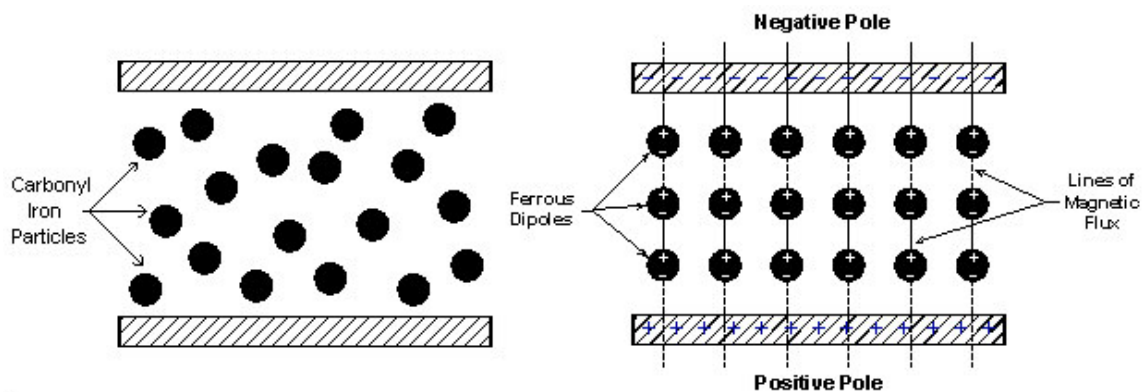


FIGURE 2.2. OFF-STATE MR FLUID PARTICLES (LEFT) ALIGNING IN AN APPLIED MAGNETIC FIELD (RIGHT) [ADAPTED FROM 5].

The dipoles align parallel to the induced magnetic flux lines to form chain-like structures of iron particles between the north and south pole [6]. The ferrous particles

that form each of the chains resist movement out of their respective flux lines, and the amount of resistance is proportional to the intensity of the applied magnetic field. The reluctance of the ferrous dipole chains to move result in a restriction of the fluid flow, as seen in Figure 2.3.

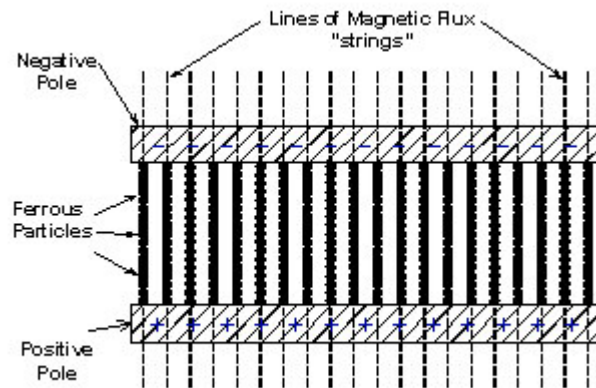


FIGURE 2.3. FERROUS PARTICLE CHAINS RESIST FLUID FLOW [ADAPTED FROM 5].

The flow restriction resulting from the alignment of the ferrous dipoles causes a change in the apparent viscosity of the fluid. The term “apparent” is used to modify the fluid because the carrier fluid’s physical viscosity does not change – rather, the MR mixture acts as if it is thickening due to the resistance of the dipole chains. The apparent viscosity can be varied infinitely between its off-state and saturation state, even becoming a near-solid. At saturation, the ferrous dipoles are fully aligned and any additional field intensity will cause no change in the apparent viscosity [5].

MR fluid also develops a yield stress as it thickens, based on the amount of mechanical energy required to yield the ferrous dipole chains. This behavior can be compared to a Bingham plastic with variable yield strength [3].

MR fluids can be used in three principal modes of operation: pressure driven flow (valve) mode, direct-shear mode, and squeeze-film mode [6]. In pressure driven flow (valve) mode, the two magnetic poles are fixed, and a pressurized flow of MR fluid moves between them. In direct-shear mode, the two magnetic poles move relative to each other, and the MR fluid is “sheared” between them. Squeeze-film mode involves a layer of MR fluid which is squeezed between the two magnetic poles [6].

Pressure driven flow mode, commonly known as valve mode, has two fixed magnetic poles through which pressurized MR fluid flows, as shown in Figure 2.4. Upon application of a magnetic field, the MR particles align parallel to the applied field lines and resist the flow of the pressurized MR fluid [5, 6]. The name “valve mode” is commonly used since, in the essence, this mode resembles the operation of a valve. Via the application of higher intensity fields, the flow resistance increases, much like closing a sink faucet valve. The pressure driven flow mode is probably the most common mode used in MR dampers, such as Lord Corporation’s “MR Damper” (RD-1005-3), but can be used in other applications in which a variable flow resistance is required.

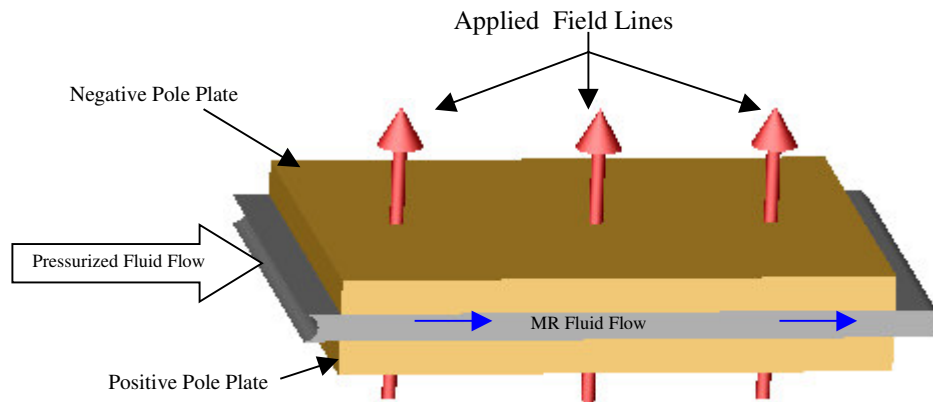


FIGURE 2.4. MR FLUID IN PRESSURE DRIVEN FLOW (VALVE) MODE [ADAPTED FROM 6].

Operation in direct-shear mode requires that the two magnetic pole plates move relative to each other, thus “shearing” the fluid between them, as depicted in Figure 2.5. An applied magnetic field aligns MR particles perpendicular to the pole plates while the shearing motion attempts to bend the particle chains along the flux lines [5, 6]. Again, as the field intensity increases, the MR fluid’s resistance to shearing increases. The direct-shear mode of MR fluids can be used in low force dampers, and has also found uses as magnetic brakes and clutches, such as Lord Corporation’s “MR Rotary Brake” (MRB-2107-3).

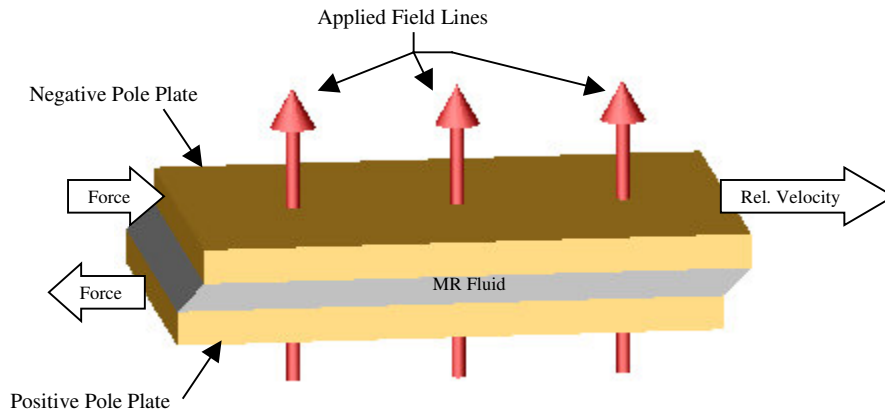


FIGURE 2.5. MR FLUID IN DIRECT-SHEAR MODE [ADAPTED FROM 6].

Squeeze-film mode, the third mode of MR fluid use, is used via squeezing the two magnetic pole plates together on a thin film of MR fluid, as shown in Figure 2.6. The application of force on the plates parallel to the direction of flux lines pressurizes the chain-like structures of MR fluid particles. The intensity of the induced field determines the ability of the MR fluid particle columns to resist buckling.

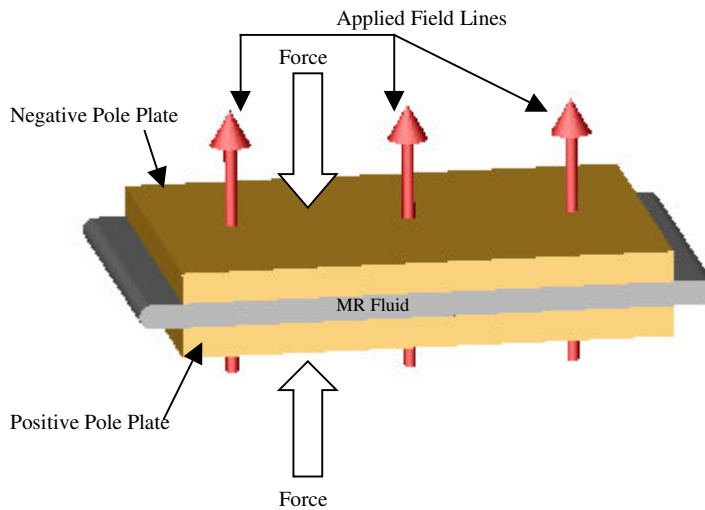


FIGURE 2.6. MR FLUID IN SQUEEZE-FILM MODE [ADAPTED FROM 6].

The adjustability of the MR fluid is heavily dependent on the size of the fluid gap in each of the fluid's operation modes. The fluid gap for the direct-shear and squeeze-film modes should be in the range of 0.005 inch to 0.025 inch, for most vehicle damper applications. The fluid gap for pressure driven flow mode depicted in Figure 2.5 should

also be between 0.005 inch and 0.025 inch [5]; however, a different orifice type (i.e., circular orifice) would have to be designed around the volume of the fluid being activated. A smaller fluid gap requires less field intensity and therefore less power to operate. This aspect is an important part of designing MR fluid devices.

Currently, Lord Corporation is the leading producer of MR fluids and devices. In early research, Lord Corporation discovered a new, undesirable property of MR fluids that had not been found in Jacob Rainbow's early work. Some initial fluids used in prototype dampers were subject to "in-use thickening (IUT)," which caused the damper's off state force versus velocity curve to gradually increase through out its cyclic lifetime, 600,000 cycles at the time [2]. The force vs. velocity curve increased as much as 250% in some cases. The IUT phenomenon was caused by the iron particles shearing into smaller, nanometer-sized particles, which increased the viscosity of the fluid. Through two years of development, Lord Corporation was able to virtually eliminate the problem of IUT, and new fluids are capable of over 10 million cycles with a negligible amount of IUT [2].

The Lord Corporation offers four variations of MR fluid: two types of hydrocarbon-based oils, a silicon-based oil, and a water-based fluid. Lord adds a proprietary mixture of wear and abrasion inhibitors as well as anti-coagulants to ensure good functionality throughout the life of the fluid [4].

2.2 MR Dampers

Magneto-rheological dampers are perhaps one of the most common applications for MR fluids. The fluid's adjustable apparent viscosity makes it ideal for use in dampers for vibration control. Real-time adjustable systems can be developed to change damping based on certain physical measurements, such as velocity or acceleration, in order to better counteract and control the system dynamics.

Typically, MR damper applications use the pressure driven flow (valve) mode of the fluid, or a combination of valve mode and direct-shear mode. Dampers that use only direct-shear mode tend to be used in applications that do not require much force from the damper.

In a typical pressure driven flow mode damper, either the movement of the piston assembly, the accumulator charge, or a combination of both pressurizes the MR fluid. As the fluid flows through the valve, the coils can be powered, causing activation regions where the fluid has been polarized, as shown in Figure 2.7.

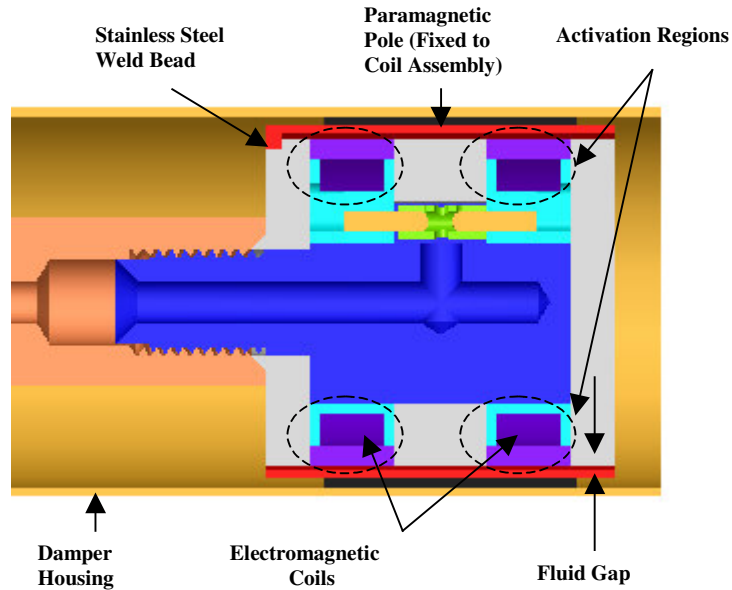


FIGURE 2.7. MR DAMPER OPERATING IN VALVE MODE.

Lord Corporation’s Motion Master damper is similar to the damper shown in Figure 2.7. Instead of using the housing as the second paramagnetic pole, a small sleeve is attached to the coil via stainless steel welds, which prevent a magnetic short between the two poles. As the coil assembly moves, the fluid in the direction of travel is pressurized, and flows through the coil/valve assembly, where it can be activated by the electromagnetic coils. Increasing field strength produces stronger MR particle chains between the two poles of the field, creating a higher resistance to the flow of the MR fluid through the valve section of the damper. This resistance provides the force mechanism for the damper. The flow resistance can be regulated between the off state (no applied field) and the saturation state, at which point the particles are fully aligned and an increase in the electromagnet current fails to produce a higher damper force at a certain velocity [5].

MR dampers can also use a combination of the pressure driven flow and direct-shear modes of the MR fluid operation. In this case, the damper housing is used as the second paramagnetic pole, and the coil assembly moves relative to the damper housing, as shown in Figure 2.8. The fluid flows through the fluid gap between the damper housing and the coil assembly, where it can be activated by the coils. While the fluid is primarily operating in pressure driven flow mode, the relative velocity between the two pole plates leads to a direct-shear mode of operation as well.

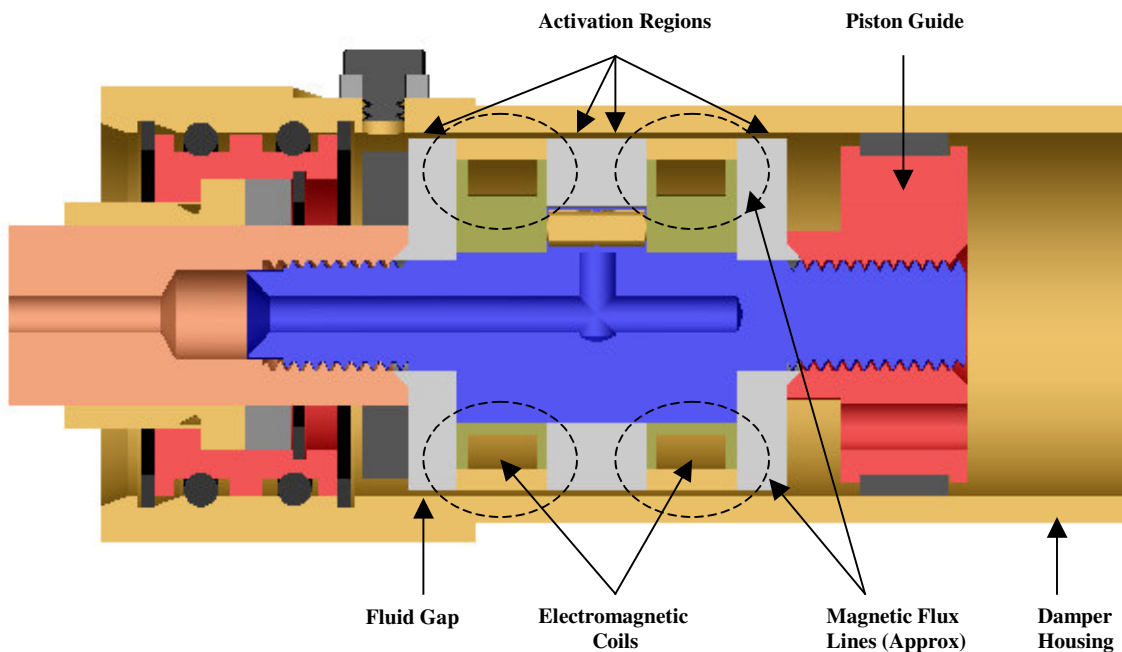


FIGURE 2.8. MR DAMPER USING BOTH VALVE AND SHEAR MODES.

The magnetic flux lines illustrated in Figures 2.7 and 2.8 do not represent the actual flux lines of the magnetic field. Since the coil assembly and the housing are made of low reluctance iron, the fluid gap has the highest reluctance of the magnetic circuit. Therefore, the flux lines will probably be normal to the flow of the fluid, as opposed to the angled flux path across the fluid gap demonstrated. Since the fluid is the highest reluctance component of the magnetic path, the fluid gap has tremendous impact on the effectiveness of the coil to control the fluid.

2.3 Motorcycle Suspension Technology

From the introduction of the world's first motorcycle in 1885 until the early 1900s, suspension for motorcycles was little more than a squishy tire and a driver seat with springs [1]. Suspension design as it seems, was merely an afterthought. With the conditions of early roads and a rigid frame, motorcycle riders were punished while riding their new motorcycles.

As technology grew, one of the primary focuses of improvement became the front suspension. While the driver was supported by a comfortable, sprung leather seat, the handlebars would thrash any rider upon hitting a bump or pothole in the road. In order to reduce the road inputs through the handlebars, motorcycle designers introduced springs into the front forks, making the first version of a telescoping fork. Simple springs for a front suspension proved to be rather inadequate, since the suspension would oscillate uninhibited after being excited by road input.

Motorcycle designers began struggling with damping the front suspension systems and introduced a number of systems to work this task. One of the earliest sprung and damped front motorcycle suspensions was known as the girder fork. Original girder fork designs used a leading link type of suspension, and was one of the earliest attempts to control the front suspension of a motorcycle. This design included a spring was mounted between the leading link and the motorcycle frame, and a friction damper which was stiff at the beginning of its travel, and softer with greater suspension travel. Leading link designs were simply a hinged carrier that carried the front wheel [1]. Girder forks proved to be unstable at higher speeds though, since the front wheel's motion was that of an arc, thereby changing the effective wheelbase of the motorcycle throughout its range of suspension travel [1].

BMW introduced the hydraulic damper for the conventional telescoping forks in 1935 [8]. Hydraulic dampers were far superior to the friction dampers used in leading link designs, such as the girder fork, and proved to have an almost opposite operation from the friction dampers. The new hydraulic dampers were soft and supple at the beginning of their stroke, but as velocity increased, their damping rate increased correspondingly. The BMW design started the trend of using damped telescoping forks for the front suspension, a design that is still the most common form of motorcycle front

suspension today. Many other motorcycle designers followed suit: Norton released a similar design in 1939, followed by the introduction of the Matchless design in 1941, and Ariel's design in 1941 [10].

Refinements to the BMW damped telescoping fork have led to today's conventional fork designs. Modern designs offer plusher rides and better performance through progressive spring rates, adjustable spring pre-load, adjustable rebound and compression damping, reduced sliding friction, and new material technology that allows lighter forks with increased rigidity. These forks, however, are still reminiscent of the original BMW design of 1935.

While the damped telescoping fork provides substantially improved front suspension performance, there are many drawbacks to the design. Telescoping forks possess an unwanted characteristic known to motorcycle suspension designers as stiction, or binding. The fork tubes have a rake angle, which is the angle between the forks and the vertical axis, as shown in Figure 2.9. Longitudinal forces acting on the wheel attempt to bend the fork tubes, and the bending causes the fork sliders to bind on each other, which is the cause of stiction in the slider bushings [8].

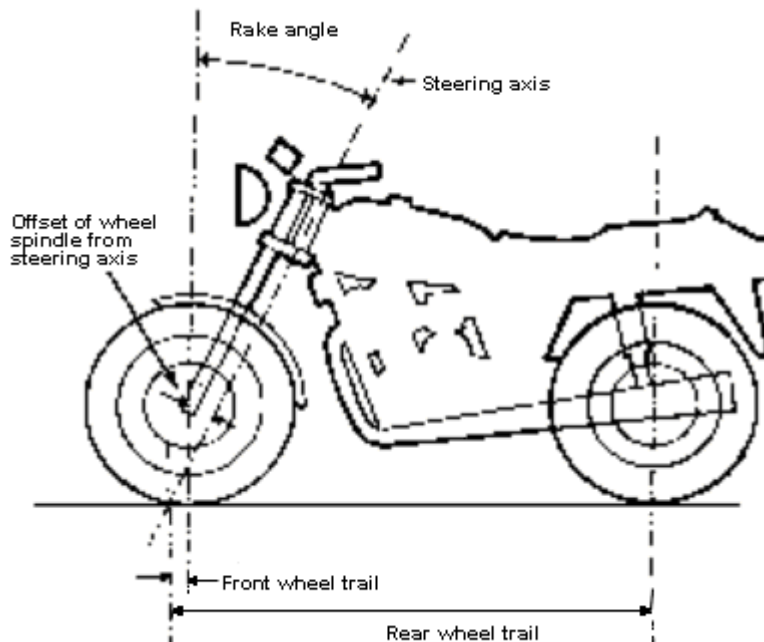


FIGURE 2.9. MOTORCYCLE SUSPENSION GEOMETRY [ADAPTED FROM 7].

The rake and trail shown in Figure 2.9 are also an important factor in stability. The trail (also known as castor) helps to keep the motorcycle in a straight line by counteracting lateral turning forces and maintaining directional stability [7]. This suspension geometry can also lead to instability in cornering. As the suspension compresses, the front of the motorcycle dives as the rear rises, causing the rake dimension to change. When the rake changes, so does the trail length, causing a subsequent shift in the amount of aligning torque. The shift in aligning torque is transmitted to the rider who has to stabilize the bike through the feedback from the handlebars. This process can lead to tire wobble, which is the beginning of a high speed, uncontrollable shift of the steering from lock to lock, usually resulting in a dismount.

Further complaints of telescoping fork designs include their inability to separate braking forces and road inputs, resulting in tremendous dive under braking [8]. Additionally, telescoping fork designs tend to experience “chatter,” or small suspension oscillations on the order of two or three Hertz. Though chatter can usually be tuned out, it is uncomfortable for the rider and can also lead to instability in cornering.

Motorcycle suspension designers have successfully tackled some of the problems in telescoping front suspension in recent years. For example, the traditional forks with a the stanchion tube on the top have given way to inverted or “upside-down” forks, where the stanchion tube mounts to the wheel. This design significantly increases the fork rigidity and also reduces stiction, two of the main problems of traditional telescoping forks. New forks have more precise rebound and compression adjustments to allow a rider to customize the suspension for the rider’s size and weight, as well as riding style.

Newer and more innovative front suspension designs have been few and far between. BMW recently introduced the “Telelever” system, which uses a pair of forks to guide the wheel, but uses a nitrogen-charged monotube shock to control the wheel’s motion. The shock is mounted to the frame at one end and a leading link A-arm at the other, allowing the shock to transmit the braking forces into the frame, rather than the handlebar [1]. The design, illustrated in Figure 2.10, has received significant praise for its stability and anti-dive capability, allowing riders to brake harder and later when beginning cornering [8].

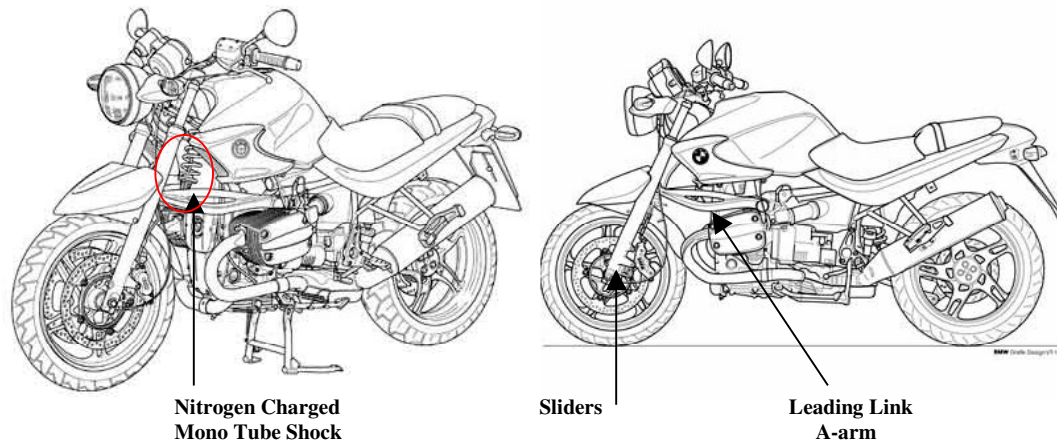


FIGURE 2.10. BMW “TELELEVER” SUSPENSION SYSTEM [ADAPTED FROM 11].

2.4 Literature Search

The following literature search was conducted to determine the current and previous research pertaining to magneto-rheological dampers in motorcycle suspension applications. Five databases were used in this literature search: the Applied Science and Technology Index, the Compendex database, the Engineering and Technology database, the LexisNexis Academic database, and the Transportation Research Information Service (TRIS) database. Primarily focusing on motorcycle applications of magneto-rheological fluid and damper technology, this search returned few results. Each database was searched for a variety of different phrases: “magneto-rheological [and] motorcycle,” “magneto-rheological [and] motorcycle,” “magneto rheological [and] motorcycle,” and “MR [and] motorcycle.” Only one database, the Engineering and Technology database, returned results. The search results primary database, Engineering and Technology, are shown in Figure 2.11.

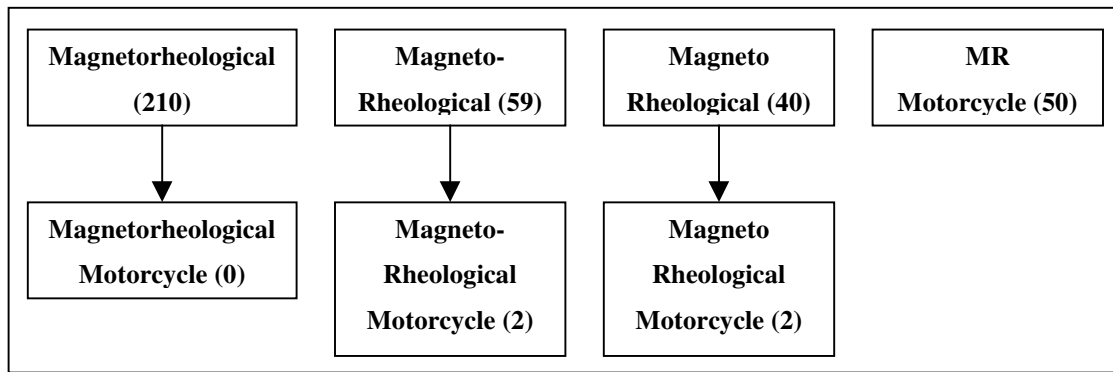


FIGURE 2.11. LITERATURE SEARCH FLOWCHART.

2.4.1 Keywords: magnetorheological motorcycle

While the keyword “magnetorheological” produced copious results, no results were related to the use of magnetorheological devices in motorcycle applications.

2.4.2 Keywords: magneto-rheological motorcycle

This search returned two results. Though both papers were based on magneto-rheological damper applications for off-road motorcycles, only one was available for viewing.

Erickson and Gordaninejad [12] discuss a theoretical model for the damping force of a MR damper and predict the force vs. displacement curve for the damper. The predicted results are then compared experimental force vs. displacement results of a modified Honda XR 400 off-road motorcycle rear shock absorber. The main purpose of the model was to validate the theoretical force vs. displacement model. No field tests were conducted in this research.

Peck [13] also researches the application of MR dampers for off-road motorcycle use. This thesis, however, was not available in its full form, as only its listing was given.

2.4.3 Keywords: magneto rheological motorcycle

This search returned two results, both identical to those found in the search for keywords “magneto-rheological motorcycle” in 2.4.2. No new results were found.

2.4.4 Keywords: MR motorcycle

This search produced 50 results, none of which were related to magneto-rheological dampers or the application of MR dampers to motorcycle technology.

2.5 Summary

Past research on magneto-rheological fluids for use in vehicle primary suspension systems has eluded motorcycles. Erickson researched using MR fluid in a rear shock absorber of an off-road motorcycle, but the research was focused on making and verifying a model of the MR damper's force versus displacement characteristics, and involved no field testing.

The author intends to complete this void by designing and building prototype MR dampers for a motorcycle front suspension, and then test the dampers against the OEM dampers in laboratory and field tests. The goal of the research is to determine the performance gains of a semiactive MR front suspension over the OEM system.

Chapter 3

Hardware Design and Fabrication

Magnet-rheological dampers are used for a variety of different applications ranging from automobile primary suspensions to smart structure vibration control. The popularity of these dampers has led to extensive research and development to produce very controllable dampers with long life spans.

The primary goal of the damper design in this research was to retrofit MR dampers into the OEM stanchion tubes. Motorcycle fork dampers are typically very thin diameter, with a body diameter of approximately one inch or less. This size constraint causes a packaging issue with the MR damper module itself.

In this chapter, the principles of design of the MR dampers, including the types of MR dampers, the mathematics involved with damper design, and the design of the electromagnetic circuit, will be discussed. Packaging issues will be considered, and the final design selected for the motorcycle application will be presented in detail.

3.1 Principles of MR Damper Design

Magneto-rheological damper design requires knowledge of fluid dynamics, electromagnetic principles, and basic machine design. The purpose of this section is to describe the guidelines of designing and manufacturing MR dampers.

3.1.1 MR Damper Types

MR dampers are much like conventional fluid dampers in basic construction, but the conventional damper valves are replaced with an electromagnetic coil to control the MR fluid behavior.

Linear MR dampers can be of three primary designs: monotube, twintube, or double-ended (also known as through-tube). The three design types reflect methods of adjusting the fluid volume to account for the volume of the damper shaft. Monotube

designs are the most common damper design; they exhibit simplicity and compactness of design and with the ability to be mounted in any orientation [5].

The monotube damper is composed of a main damper housing, a piston and piston rod assembly, and an accumulator, as shown in Figure 3.1. The main reservoir contains the piston and piston rod assembly submerged in the MR fluid, while the accumulator reservoir contains a compressed, non-oxidizing gas (usually nitrogen) [5]. As the piston rod moves into the damper housing, a volume of fluid equivalent to the volume of the intruding piston rod is displaced. The accumulator piston moves toward the bottom of the damper, compressing the nitrogen charge to account for the change in volume. As the piston rod retracts, the accumulator piston moves up the damper tube to counteract the loss of volume. The monotube damper design is the most versatile damper design since it can be mounted in any orientation without affecting the damper's performance.

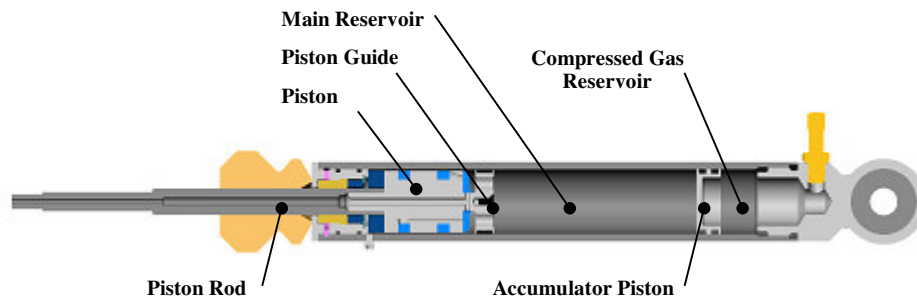


FIGURE 3.1. MONOTUBE MR DAMPER, SECTION VIEW [ADAPTED FROM 5].

The twintube damper uses inner and outer cartridges to negotiate the changing volume of MR fluid, as shown in Figure 3.2. As the piston rod enters the inner housing, the extra volume of MR fluid displaced by the piston rod is forced from the inner housing to the outer housing via the foot valve. When the piston rod retracts, MR fluid flows back into the inner housing, therefore preventing the creation of vacuum in the inner housing and cavitation of the damper. Drawbacks of this design include size and orientation – this damper must be mounted with the foot valve at the bottom to ensure no cavitation.

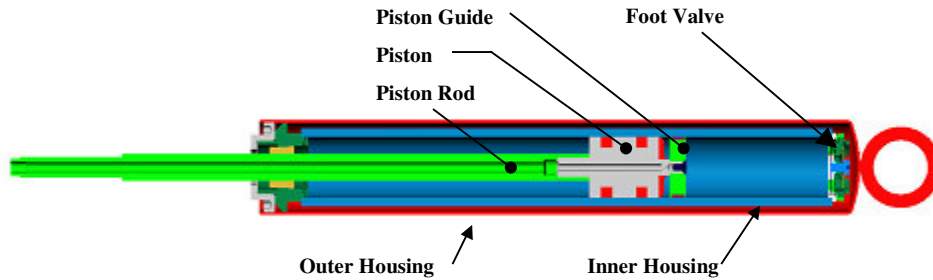


FIGURE 3.2. TWINTUBE MR DAMPER, SECTION VIEW [ADAPTED FROM 5].

Double-ended (through-tube) dampers use a third method to account for the piston rod volume. Fully extended, the piston rod protrudes through both sides of the damper housing, as shown in Figure 3.3. This method of damper design retains a constant piston rod and fluid volume within the housing, thereby eliminating the need for a second housing or accumulator.

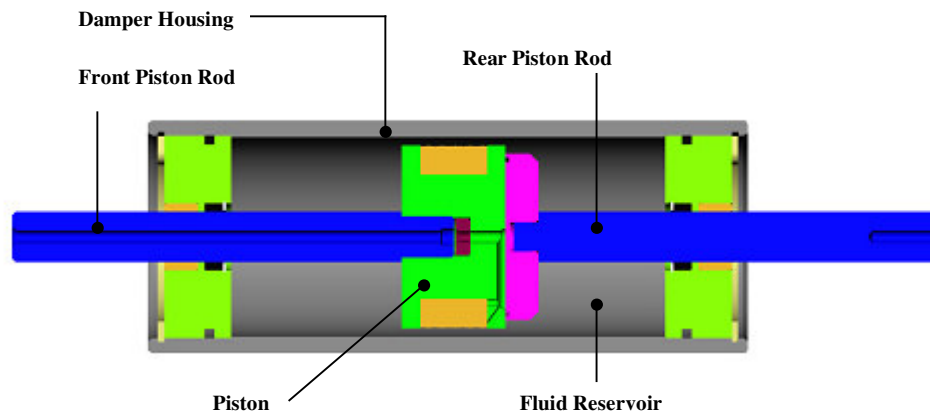


FIGURE 3.3. DOUBLE-ENDED (THROUGH-TUBE) MR DAMPER, SECTION VIEW [ADAPTED FROM 5].

The twintube and double-ended damper provide a significant advantage over the monotube design. The pressurized charge in the accumulator of the monotube design adds a spring force to the damping rod, so not only does the damper have force vs.

velocity characteristics, it also has a spring rate. The twintube and double-ended damper, however, do not demonstrate this trait, showing only force vs. velocity characteristics.

3.1.2 MR Damper Mathematics

MR fluid behaves in two distinct modes: off state and activated state. While Newtonian-like behavior is common in the off state, the fluid behaves as a Bingham plastic with variable yield strength when activated. Though the fluid does have departures from these two models, they give a good reference as to the behavior of the fluid [6].

The shear stress associated with the flow of MR fluid can be predicted by the Bingham equations [6]:

$$\tau = \tau_y(H) + \eta \dot{\gamma}, \quad \tau < \tau_y \quad (3.1)$$

In equation 3.1, τ is the fluid shear stress, τ_y is the fluid's yield stress at a given magnetic field H , η is the plastic viscosity, and $\dot{\gamma}$ is the fluid shear rate. This equation holds for fluid stresses above the field dependent yield stress [6]. However, for fluid stresses below τ_y , the MR fluid behaves as a viscoelastic material:

$$\tau = G\gamma, \quad \tau < \tau_y \quad (3.2)$$

where τ is the fluid shear stress, G is the complex material modulus, and γ is the fluid shear.

Since MR dampers generally use either the pressure driven flow (valve) mode or direct-shear mode of the fluid, there are two independent sets of equations used to determine the MR damper force in the different modes. Pressure driven flow mode has two components to the pressure drop: pressure loss due to viscous drag, and pressure loss due to the field dependent yield stress, as shown in Equation (3.3) [6]:

$$\Delta P = \Delta P_\eta + \Delta P_\tau = \frac{12\eta QL}{g^3 w} + \frac{c \tau_y L}{g} \quad (3.3)$$

In Equation (3.3), ΔP is the total pressure drop, ΔP_η is the viscous pressure loss, ΔP_τ is the field dependent yield stress pressure loss, η is the fluid viscosity, Q is the flowrate, L is the pole length, w is the pole width, g is the fluid gap, and τ_y is the field dependent yield stress. Many of these dimensions are illustrated in Figure 3.4. The variable c ranges from a minimum value of 2 (for $\Delta P_\tau/\Delta P_\eta < 1$) to a maximum value of 3 (for $\Delta P_\tau/\Delta P_\eta > 100$).

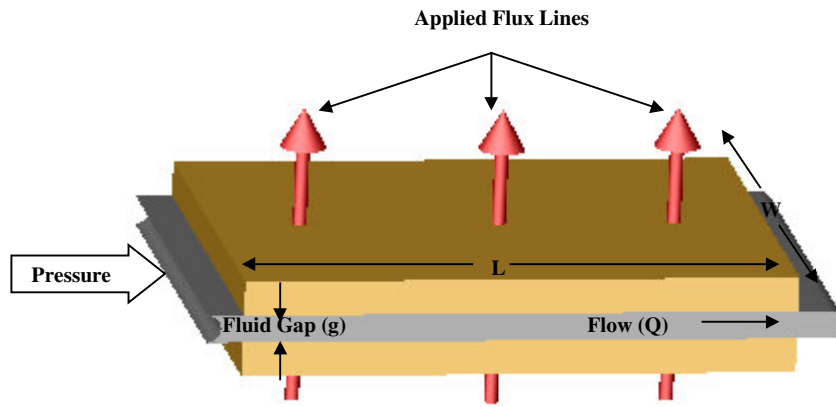


FIGURE 3.4. PRESSURE DRIVEN FLOW MODE.

The force of a direct-shear device is based on the shear stress developed along the piston surface due to a combination of the viscous effects of the fluid and the field induced yield stress [6]:

$$F = F_\eta + F_\tau = \frac{\eta SA}{g} + \tau_y A \quad (3.4)$$

In Equation (3.4), F is the damper force, η is the fluid viscosity, S is the relative velocity between poles, A is the pole area, g is the fluid gap, and τ_y is the field dependent yield stress. The physical dimensions are illustrated in Figure 3.5.

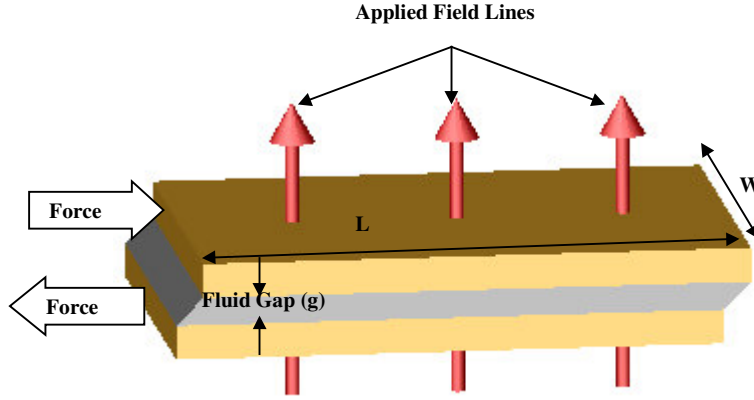


FIGURE 3.5. DIRECT-SHEAR MODE.

While Equations (3.1) to (3.4) model the amount of force that can be achieved with a certain geometry, there are also guidelines for the aspect ratios between the dimensions that relate to the of the MR fluid itself. The volume of fluid exposed to the magnetic field controls the desired MR effect [6]. Equations (3.3) and (3.4) can be manipulated to yield:

$$V = k \left(\frac{\eta}{\tau_y^2} \right) \lambda W_m \quad (3.5)$$

Where k is a constant and λ is the control ratio required to achieve a specified mechanical power, W_m [6].

For pressure driven flow mode, the equations for the variables in Equation (3.5) are:

$$k = \frac{12}{c^2} \quad (3.6)$$

$$\lambda = \frac{\Delta P_\tau}{\Delta P_\eta} \quad (3.7)$$

$$W_m = Q \Delta P_\tau \quad (3.8)$$

For direct-shear mode, the equations for the variables in Equation (3.5) are:

$$k = 1 \quad (3.9)$$

$$\lambda = \frac{F_\tau}{F_\eta} \quad (3.10)$$

$$W_m = F_\tau S \quad (3.11)$$

Equation (3.5) can be further manipulated to provide constraints and aspect ratios for efficient use of MR fluid [6]. For pressure driven flow mode:

$$wg^2 = \frac{12}{c} \left(\frac{\eta}{\tau_y} \right) \lambda Q \quad (3.12)$$

For direct-shear mode:

$$g = \left(\frac{\eta}{\tau_y} \right) \lambda S \quad (3.13)$$

3.1.3 Electromagnet Design

In order to maintain good damper adjustability, not only should the aspect ratios be considered, but the electromagnet design should also be examined. The electromagnet circuit creates the magnetic field lines that are responsible for activating the MR fluid, so proper operation of this circuit is essential.

The goal of the electromagnet design is to channel the field lines in a manner that makes them cross the fluid gap in a perpendicular fashion, as well as making sure that the fluid gap is the point of highest reluctance in the path of the field lines. Therefore, an efficient magnetic circuit must be designed to have no bottlenecks. In order to do so, the areas perpendicular to the field lines must be equal, namely the piston cross-sectional area (A_A), the piston radial root area (A_B), and the housing cross-sectional area (A_C) [5].

The Excel program shown in Figure 3.6 can be used as an aid for the piston design.

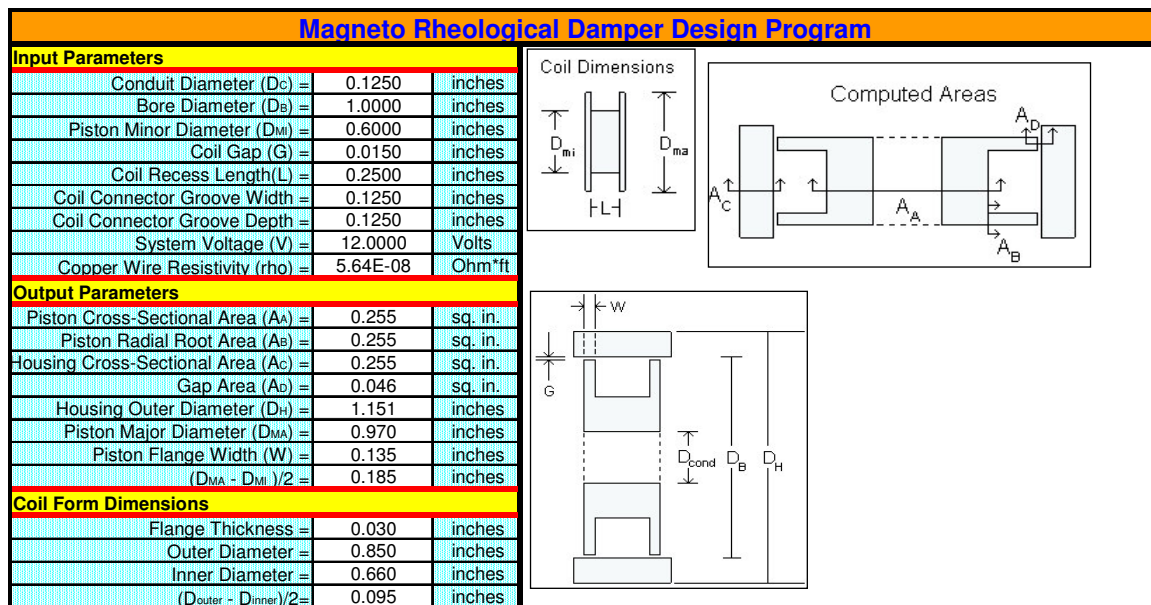


FIGURE 3.6. MR DAMPER DESIGN PROGRAM PART I.

When designing a MR damper, usually a few of the design's dimensions are known or can be determined. Some of these dimensions include the wire conduit diameter D_C , the bore diameter D_B , the fluid gap G , the coil recess length L , and the coil

connector groove width and depth. The piston minor diameter, D_{mi} , must be solved for iteratively until a desired housing outer diameter or total piston length is determined.

Once the piston dimensions have been settled, the coil form dimensions can be calculated, and the maximum number of turns of different wires sizes can be determined from the second part of the design program, shown in Figure 3.7.

Amer. Wire Gage No.	Bare Wire Dia. (in)	Insulated Wire Dia.* (in)	Wire Turns Per Row	Rows of Wire Turns	Max No. of Turns	Length of Wire (ft)	Wire Resis. (Ohm)	Max Current (Amps)	Wire Amperage (100 cir. Mils / A)	Wire Amperage (400 cir. Mils / A)	Field Intensity (Max) H (kA/m)	Field Intensity (100cm/A) H (kA/m)	Field Intensity (400cm/A) H (kA/m)
14	0.0641	0.0705	2.7	1	2.7	0	0.00	10054.88	41	11	5625.40	22.94	6.15
15	0.0571	0.0628	3.0	1	3	1	0.00	7264.27	33	8.5	4515.71	20.51	5.28
16	0.0508	0.0559	3.4	1	3.4	1	0.00	5126.89	26	6.5	3611.98	18.32	4.58
17	0.0453	0.0498	3.8	1	3.8	1	0.00	3681.65	21	5.5	2898.94	16.54	4.33
18	0.0403	0.0443	4.3	2	8.6	2	0.01	1214.89	16	4.1	2164.95	28.51	7.31
19	0.0359	0.0395	4.8	2	9.6	2	0.01	875.97	13	3.3	1742.51	25.86	6.56
20	0.0320	0.0352	5.4	2	10.8	2	0.02	626.57	10	2.5	1402.20	22.38	5.59
21	0.0285	0.0314	6.1	3	18.3	3	0.04	283.32	8	2.0	1074.34	30.34	7.58
22	0.0253	0.0278	6.8	3	20.4	4	0.06	203.38	6.4	1.6	859.71	27.05	6.76
23	0.0226	0.0249	7.6	3	22.8	4	0.08	147.12	5.0	1.3	695.07	23.62	6.14
24	0.0201	0.0221	8.6	4	34.4	6	0.16	75.58	4.0	1.0	538.73	28.51	7.13
25	0.0179	0.0197	9.6	4	38.4	7	0.22	54.46	3.2	0.83	433.34	25.46	6.60
26	0.0159	0.0175	10.9	5	54.5	10	0.40	29.89	2.5	0.65	337.59	28.23	7.34
27	0.0142	0.0156	12.2	6	73.2	13	0.68	17.59	2.0	0.50	266.83	30.34	7.58
28	0.0126	0.0139	13.7	6	82.2	15	0.96	12.52	1.6	0.40	213.33	27.25	6.81
29	0.0113	0.0124	15.3	7	107.1	19	1.56	7.69	1.3	0.33	170.62	28.85	7.32
30	0.0100	0.0110	17.3	8	138.4	25	2.58	4.65	1.0	0.25	133.43	28.68	7.17
31	0.0089	0.0098	19.4	9	174.6	31	4.11	2.92	0.8	0.20	105.67	28.58	7.24
32	0.0080	0.0088	21.6	10	216	39	6.29	1.91	0.6	0.16	85.40	28.64	7.16
33	0.0071	0.0078	24.3	12	291.6	53	10.87	1.10	0.5	0.13	66.71	30.21	7.85
34	0.0063	0.0069	27.4	13	356.2	64	16.79	0.71	0.4	0.10	52.75	29.52	7.38
35	0.0056	0.0062	30.8	15	462	84	27.63	0.43	0.314	0.078	41.58	30.06	7.47
36	0.0050	0.0055	34.5	17	586.5	106	44.07	0.27	0.250	0.063	33.09	30.38	7.66
37	0.0045	0.0050	38.4	19	729.6	133	67.73	0.18	0.202	0.050	26.78	30.54	7.56
38	0.0040	0.0044	43.2	21	907.2	164	106.34	0.11	0.160	0.040	21.21	30.08	7.52
39	0.0035	0.0039	49.4	24	1185.6	215	181.51	0.07	0.122	0.031	16.24	29.97	7.62
40	0.0031	0.0034	55.7	27	1503.9	272	293.36	0.04	0.096	0.024	12.75	29.92	7.48
41	0.0028	0.0031	61.7	30	1851	336	442.79	0.03	0.078	0.019	10.39	29.92	7.29
42	0.0025	0.0028	69.1	34	2349.4	427	706.11	0.02	0.063	0.016	8.27	30.67	7.79
43	0.0022	0.0024	78.5	39	3061.5	557	1189.70	0.01	0.048	0.012	6.40	30.45	7.61
44	0.0020	0.0022	86.4	43	3715.2	676	1747.46	0.01	0.040	0.010	5.29	30.79	7.70

* The estimated insulated wire diameter is calculated by using 110% of the bare wire diameter.
 ** American Wire Gage Information from http://www.reawire.com/ind_awgchart.asp

FIGURE 3.7. MR DAMPER DESIGN PROGRAM PART II.

Part II of the MR damper design program includes the absolute maximum amperage for the given supply voltage, and the recommended maximum amperage based on the 100 circular mils per amp and 400 circular mils per amp rule. The 100 circular mils per amp rule is a recommendation of the max current that can be carried by a certain wire gage without overheating. The 400 circular mils per amp rule is somewhat more conservative and will produce less heat than the 100 cm/A rule [14]. Choosing the wire size to use is dependent on multiple items: magnetic field required, power dissipation, and the feasibility of hand-winding the chosen number of turns. While the highest

magnetic field possible is usually desirable (more adjustability), power dissipation and coil turns have a major effect on the size of the wire chosen.

3.2 MR Damper Design for Motorcycle Applications

As described in Section 3.1, designing MR dampers requires an iterative process. Beginning with a rough design, the coil and piston dimensions are iterated to an appropriate design. The piston and coil dimensions are then used to determine a predicted off-state curve for the damper. This section outlines the process used for the test vehicle used for this research.

3.2.1 Test Vehicle Overview

The test vehicle for this research was a 1997 Honda CBR900RR, with the OEM suspension intact, as shown in Figure 3.8. The CBR900RR of this model year used conventional cartridge forks with an adjustable twintube damper. The OEM damper's adjustability includes both jounce and rebound settings, with 2.5 turns of a valve screw for each. The forks use progressive springs to prevent bottoming, and the spring pre-load is adjustable. The research presented focused solely on the front suspension of the motorcycle.

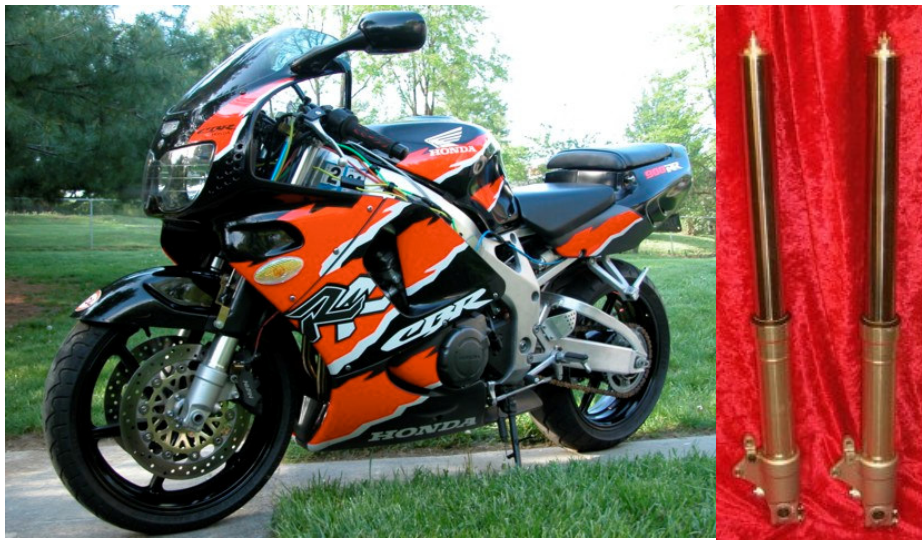


FIGURE 3.8. 1997 HONDA CBR900RR (LEFT) WITH OEM FORKS (RIGHT).

The purpose of the MR damper design was to retrofit the OEM forks with MR damper modules as replacements for the twintube dampers. Packaging and size of the MR replacement was therefore essential to the design.

3.2.2 Analyzing the OEM Damper Package and Performance

The first tasks in designing the new MR damper module were modeling the OEM damper assembly and experimentally determining the OEM damper force versus velocity curves. These initial tests determine the design envelope for the MR dampers.

Analyzing the vehicle's OEM damper performance required the design and production of a set of fixtures, for holding the OEM fork in a damper dynamometer, as shown in Figure 3.9.

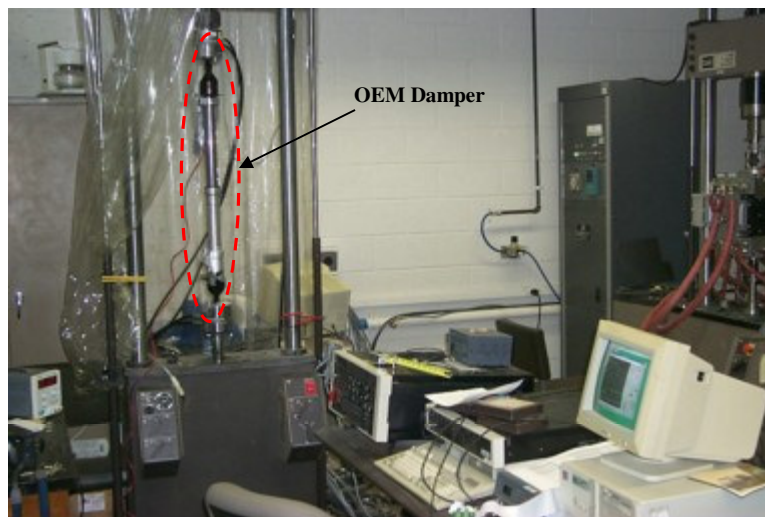


FIGURE 3.9. 1997 HONDA CBR900RR OEM DAMPER IN DAMPER DYNAMOMETER FOR FORCE-VELOCITY CHARACTERIZATION.

The OEM dampers were run through a series of tests, which will be further detailed in Chapter 4. The damper dynamometer allows us to measure the damper force at different vibrations, therefore providing a force-velocity curve for the damper, such as the one shown in Figure 3.10 for the OEM damper. It is worth noting that the damping curves in Figure 3.10 have been zeroed according to what will be described later in section 4.1. Positive velocity indicates rebound, while negative velocity indicates jounce.

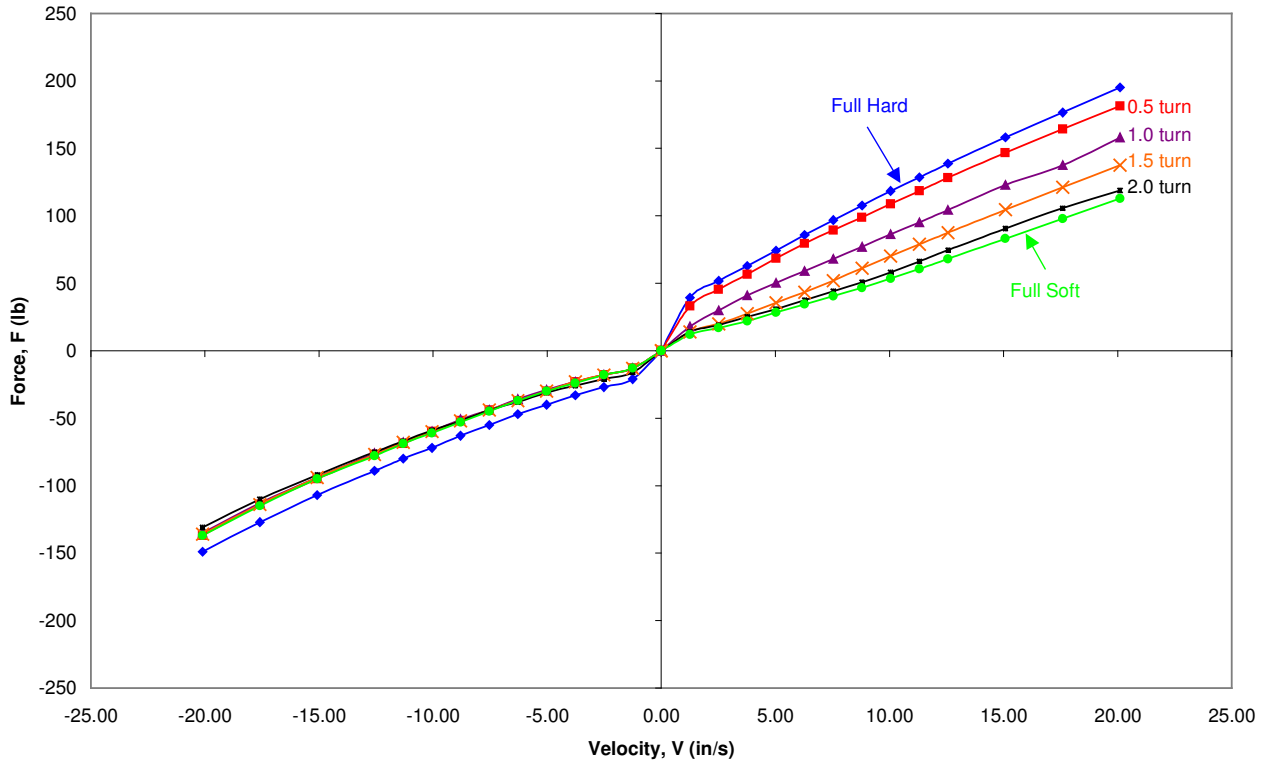


FIGURE 3.10. 1997 HONDA CBR900RR OEM DAMPER CURVES (ZEROED DATA).

Modeling the OEM dampers was the second task, involving measuring and modeling each component in CAD. This step provided the necessary packaging dimensions for which the retrofit MR dampers must fit. The model of the OEM damper modules is shown in Figure 3.11.

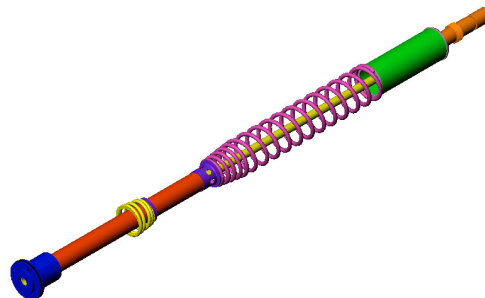


FIGURE 3.11. OEM DAMPER ASSEMBLY.

3.2.3 Designing the MR Damper

With the basic package dimensions and the OEM damper curves, the MR damper module design could be established. Research performed by Poynor [5] suggested twintube MR dampers did not work well in implementation, primarily due to magnetic circuit design problems. However, Poynor established a robust and reliable monotube MR damper design that was proven in two automobile applications. For the motorcycle application, a twintube configuration like the OEM setup was dismissed for reliability purposes, and Poynor's design was adapted for the new application.

The first step in the retrofit MR damper design involved use of the MR damper design program to iterate an initial piston design, as discussed earlier in Section 3.1.3.

Upon initial MR piston design completion, the off-state damping rate was then predicted using the following equation for a pressure driven flow mode damper, derived from the equations in Section 3.1.2 [18]:

$$F_{off} = \pi \left[\frac{3\pi D_1^3 (d + 2L) \left(1 + \frac{2g}{D_1}\right)}{4g^3} \right] \mu v_0 \frac{(D_1^2 - D_5^2)}{4} \quad (3.14)$$

The results were compared to the OEM damper curve, illustrated in Figure 3.12. If necessary, further iterations could have been made to change the off-state damping curve.

The goal of the damper design was to envelop the stock damper curves with the MR damper replacement. The tradeoffs between adjustability, damper power consumption, and off-state performance must be carefully balanced. In this motorcycle application, extra power was not readily available, so power consumption was carefully planned. While the design presented in Figure 3.12 does not completely envelop the OEM damper curves in low speed damping, the power consumption will remain at a reasonable level. The MR dampers would require less than five watts to operate, which was an acceptable level. Upon completion of the piston design, the remaining MR damper components could be designed, keeping in mind the packaging constraints.

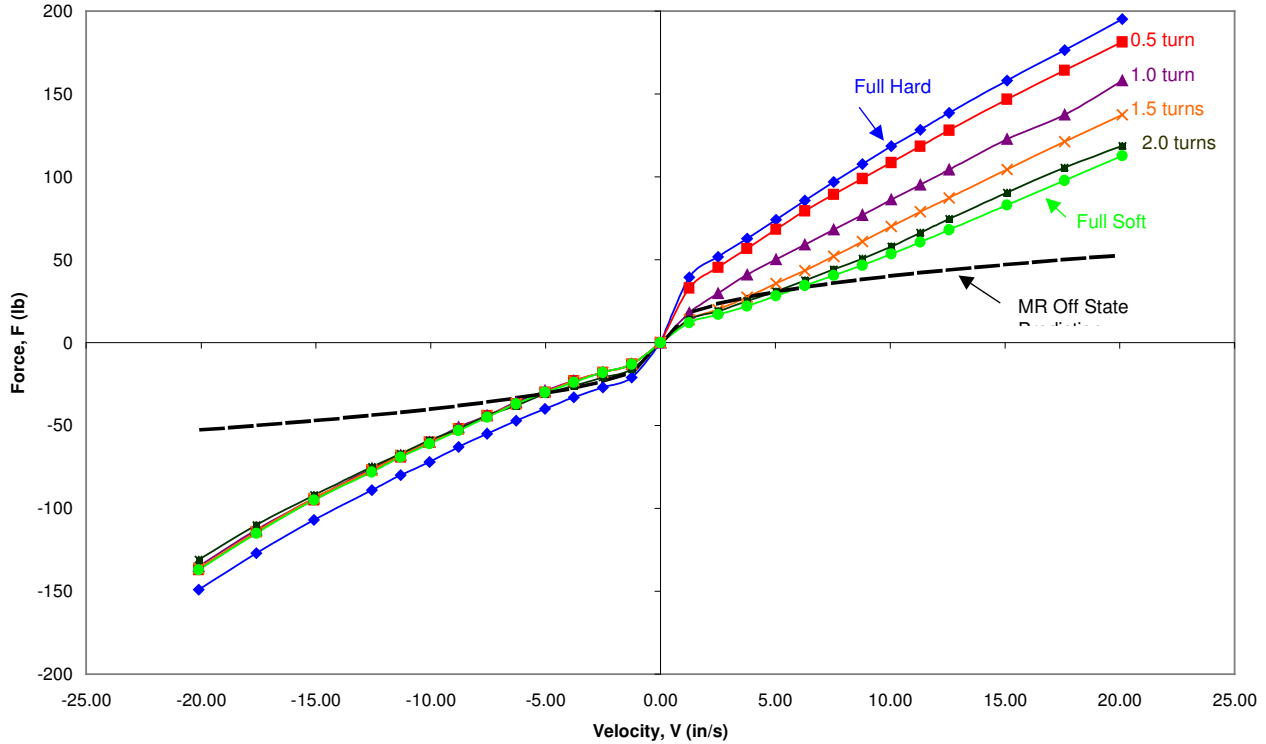


FIGURE 3.12. OEM DAMPER AND PREDICTED MR OFF STATE DAMPER CURVES.

Weight reduction was crucial in the retrofit MR damper design, as the damper resides primarily with the unsprung mass of the motorcycle. In order to aid in weight loss, all non-critical components were made of aluminum, and extra material was removed wherever possible. The piston rod extension, for example, does not contact the seal surface and does not need a smooth surface, so it was machined from 7075 aluminum. Fork stops and main spring plates were designed and constructed from aluminum and employed weight reduction holes.

Packaging issues also included the OEM fork main spring and rebound spring. To use the existing OEM fork shell, the main spring must be located in the same position to allow proper spring adjustment. A main spring plate was designed to meet the main spring constraint, allowing a change in the overall damper housing length. The OEM fork also has a rebound spring to prevent the over-extension of the fork during rebound. Considering the original rebound spring system could not be used on the MR damper due to a change in housing diameter, a new extension bumper design was required. A rubber

bumper design was used, and mounted to the MR damper housing through the use of aluminum clamps.

The final design is displayed in Figures 3.13 to 3.15, and detailed drawings are included in Appendix B. The retrofit MR damper forks weigh only one pound heavier each than the OEM forks, and require a total of five watts to operate.



FIGURE 3.13. RETROFIT MR DAMPER MODULE MODEL (LEFT) AND PROTOTYPE (RIGHT).

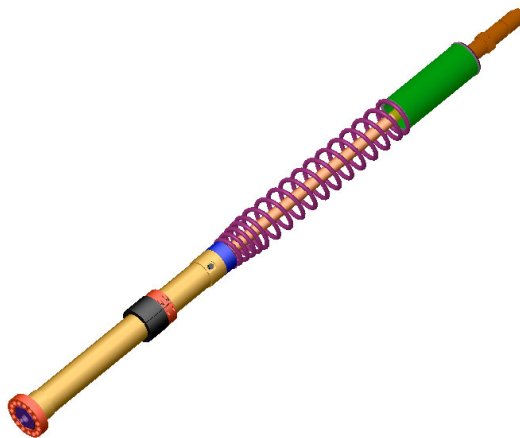


FIGURE 3.14. MODEL OF RETROFIT MR DAMPER COMPLETELY ASSEMBLED.



FIGURE 3.15. RETROFIT MR DAMPER ASSEMBLY PROTOTYPE.

The retrofit MR damper forks used a number of OEM parts, including the main spring, spring collar, joint plates, spring seat, and rebound cap. These parts are labeled in Figure 3.16. Figure 3.17 illustrates a labeled sectional view of the retrofit MR damper module.

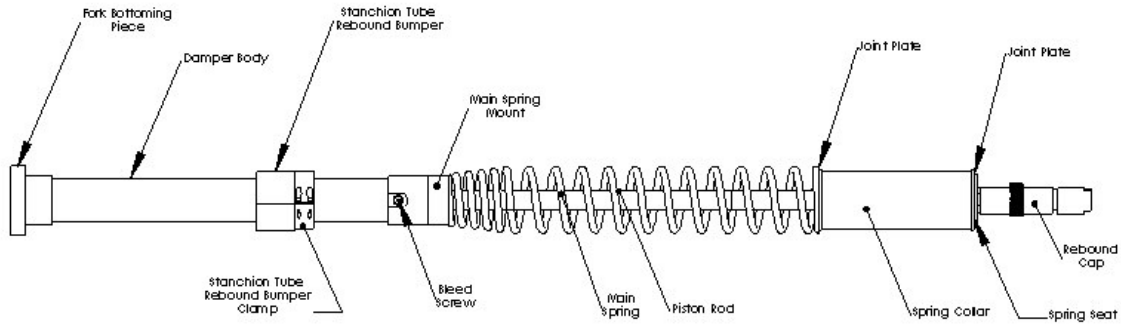


FIGURE 3.16. RETROFIT MR DAMPER ASSEMBLY, LABELED.

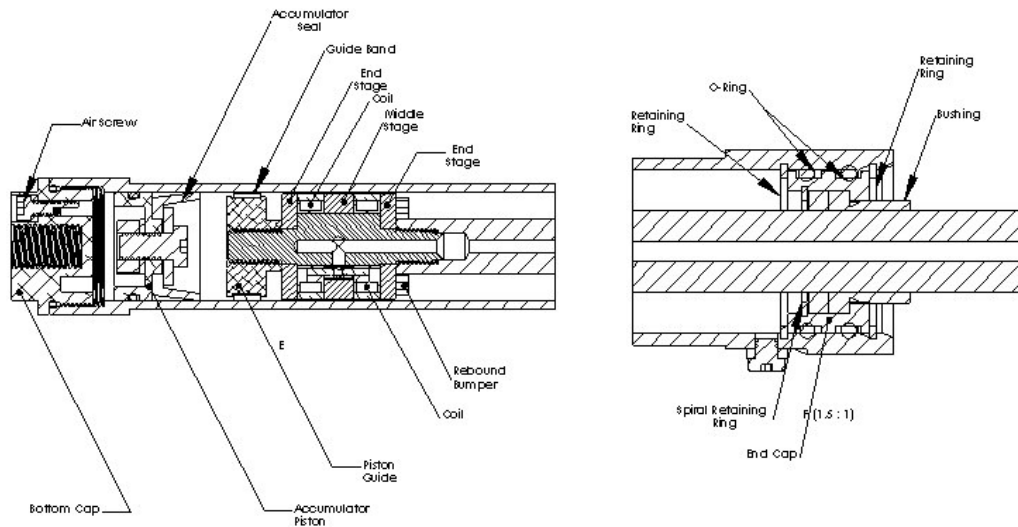


FIGURE 3.17. SECTION VIEW OF MR DAMPER MODULE.

One of the most innovative aspects of this retrofit MR damper design involved the accumulator design and the method with which to charge it. Since the OEM fork tube design required that the damper base be bolted in, and there was no room for an air valve, a new charger was required to charge the dampers before installation. The MR damper bottom cap was designed with an air screw hole offset from the damper body bolt hole. With the bottom cap screwed into the damper body, a charger assembly could be placed over the bottom of the damper and bolted to the bottom cap. A hex rod extended through a sealed hole for tightening the air screw. This charger assembly had an air valve that could be charge with a nitrogen tank. Once the desired pressure was reached, the hex rod was used to tighten the air screw, the charger was removed, and the damper could be placed in the fork tube. The CAD model and picture of this charger is shown in Figure 3.18.

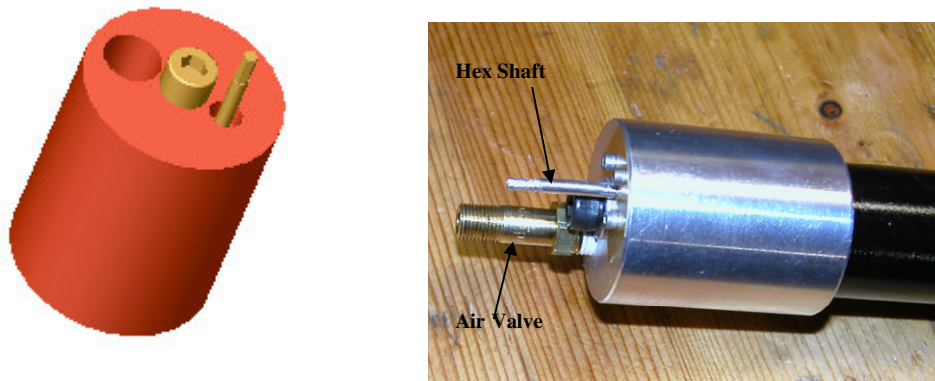


FIGURE 3.18. NITROGEN CHARGER ASSEMBLY (LEFT) AND THE PROTOTYPE HARDWARE (RIGHT).

3.3 Control Unit Designs

For this research, three control units were designed, built, and tested: a passive powering unit, a skyhook control unit, and a displacement-based control unit. This section will discuss the latter two control unit designs.

3.3.1 On-Off Skyhook Control

On-off skyhook control adjusts the MR damper between two states: a low state (off) damping, and a high state (on) damping. High and low states are usually defined by the damper's mechanical limits, i.e., the minimum and maximum amount of damping force that the damper can provide, and regulation between the two states is based on the product of the relative and body velocities.

Rather than connecting the damper between the body and the wheel, skyhook control policy dictates that the damper should theoretically connect between the vehicle body and some reference point in the sky, as shown in Figure 3.19.

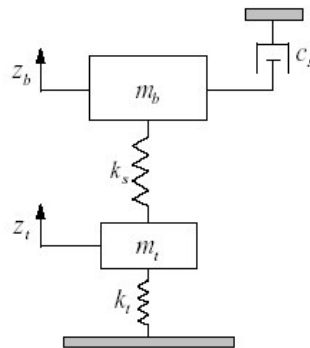


FIGURE 3.19. SKYHOOK CONTROL SETUP [15].

The purpose of the skyhook control system is to reduce the body oscillations while maintaining the wheel contact patch. In operation, there are two phases of control. Positive relative velocity allows the damper to pull down on the body (rebound), while negative relative velocity allows the damper to push up on the body (compression) [15]. When the body is moving upward with a positive velocity, the maximum amount of damping is desired to push the body down, while the minimum amount of damping is desired to continue pushing the body up. When the body is moving downward with a

negative velocity, the maximum amount of damping is desired to push the body up, and minimum damping is used to continue forcing the body downward [15]. The product of the body velocity and the relative velocity reflects this policy. When the product is greater than or equal to zero, the damper operates in high state, but when the product is negative, the damper operates in the low state mode. On-off skyhook control, therefore, work according to:

$$\dot{z}_b \times v_{rel} \geq 0; \quad c_s = \text{high state} \quad (3.15)$$

$$\dot{z}_b \times v_{rel} < 0; \quad c_s = \text{low state} \quad (3.16)$$

Skyhook control emulates the ideal body displacement control configuration of a damper attached to the body and “hooked” to a reference point in the sky [15].

Implementation of this control policy requires a method of measuring the relative velocity across the damper and the absolute body velocity. Motorola MMA1220D micro-machined +/- 8 g accelerometers were for this purpose, and the signals were integrated to achieve velocities. Figure 3.20 shows the basic control strategy used to accomplish skyhook control policy.

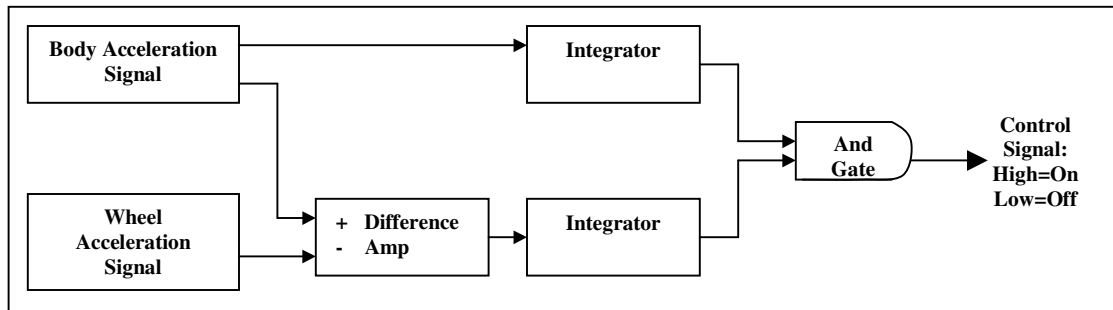


FIGURE 3.20. SKYHOOK CONTROL STRATEGY.

While control strategy is rather simplistic, the circuitry used to implement it was cumbersome. The acceleration signals were first conditioned by zero-biasing each of the inputs. The body and wheel acceleration signals were subtracted to yield a relative acceleration. Employing low input bias current, high-impedance operational amplifiers, compensated Miller integrators with a cutoff frequency of 1.5 Hz integrated the relative acceleration and body acceleration signals to produce velocity signals. The velocity signals were then signal processed through a series of followers, inverters, and comparators to condition them for the and-gate. Upon receiving either two positive signals or two negative (inverted) signals, the and-gate would change to high state (+5 volts), sending a control signal to the power unit comparator to turn on the power unit. The power unit itself used a step down DC to DC converter to reduce the system's power consumption from 34 watts to 5 watts. Figures 3.21 and 3.22 show the circuit boards that controlled the damper as well as the finished control box. A complete circuit schematic of this system can be viewed in Appendix E.

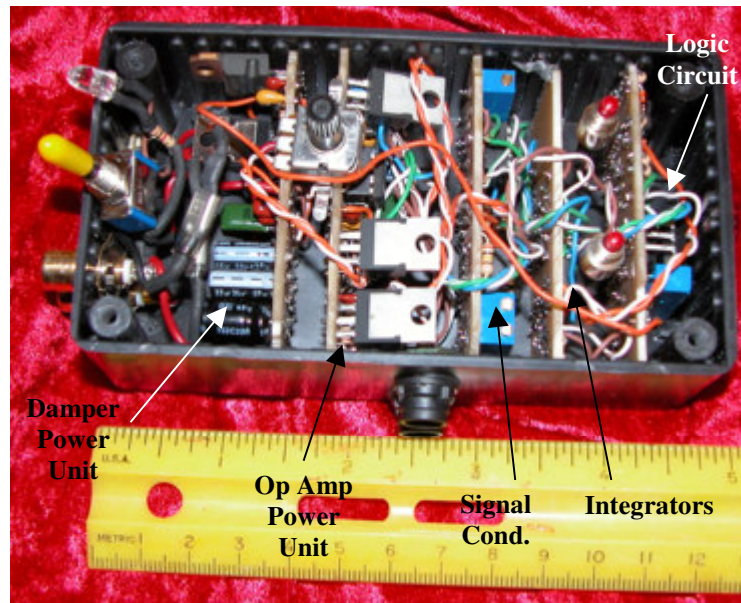


FIGURE 3.21. SKYHOOK CONTROL CIRCUITS.



FIGURE 3.22. SKYHOOK CONTROL UNIT.

3.3.2 Displacement-Based Control System

The displacement-based control system was designed to accentuate high-speed handling and performance. Utilizing the same on-off type control employed by skyhook control, this system based the control signal on the front suspension displacement. High performance suspension is usually set much stiffer, both in spring and damping rates, than those suspensions designed for a compromise of performance and comfort. Stiffer suspension allows the rider to “feel” the road better and therefore push the motorcycle closer to the edge of its performance capabilities.

Sensing the fork displacement was accomplished by a 150 mm linear potentiometer, connected between the body of the motorcycle and the wheel. When suspension displacement was within ± 0.25 inch of the normal sag (with rider), the dampers operate in their high (on) state. Once the displacement exceeded the first limit, the dampers switched to low (off) state. At ± 2.5 inches, the dampers returned to high state to prevent bottoming or hyperextension. This control system is illustrated in Figure 3.23.

The displacement-based control system was composed of analog circuitry. The system used a difference op amp circuit to zero the displacement for control purposes (the circuit must be zeroed with a rider on the motorcycle). The control signal was then conditioned by a series of followers, inverters, and comparators. A block diagram of the system function is shown in Figure 3.24. The detailed circuit drawings for this system are shown in Appendix F.

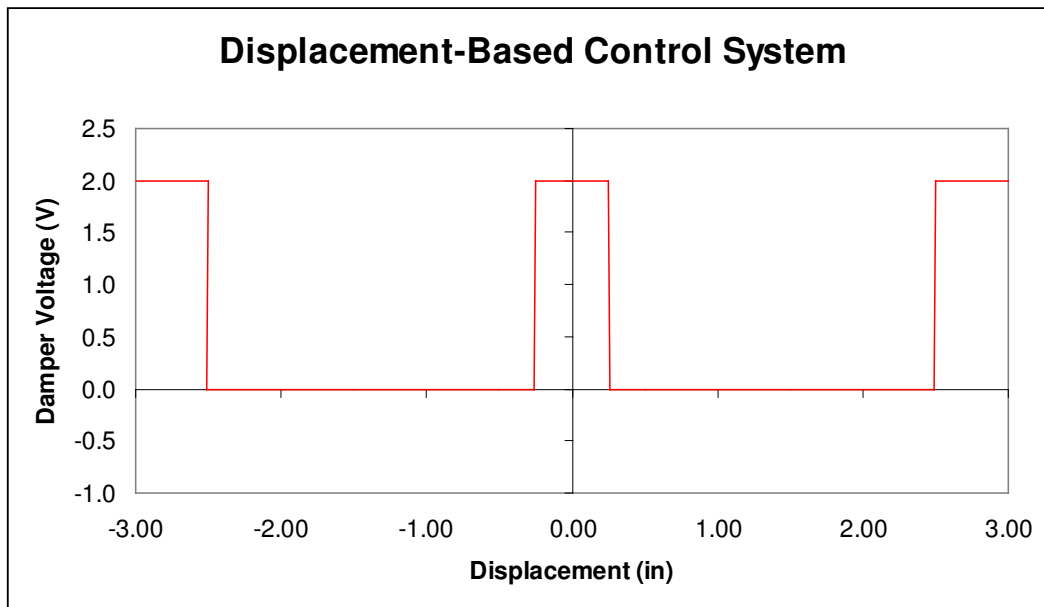


FIGURE 3.23. DISPLACEMENT CONTROL POLICY.

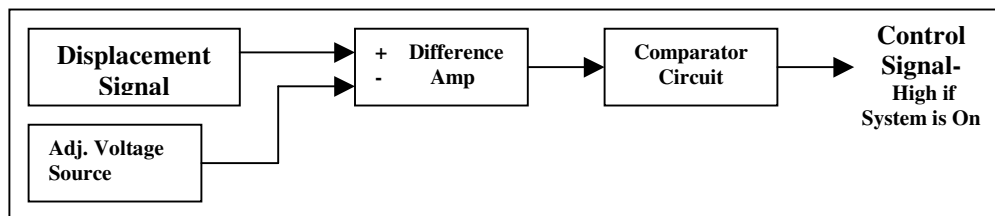


FIGURE 3.24. DISPLACEMENT CONTROL CIRCUIT BLOCK DIAGRAM

Primarily designed for high speed, smooth road applications, this control system was not intended for comfort. If a rider were to hit a pothole with this control system implemented, the first 0.25 inch of travel would be very stiff, sending a large amount of the front suspension force directly into the rider's arms and shoulders. However, this

control system should increase stability on smooth road applications. A picture of the prototype control system mounted on the test vehicle is displayed in Figure 3.25.



FIGURE 3.25. DISPLACEMENT BASED CONTROL SYSTEM ON TEST VEHICLE.

Chapter 4

Hardware Laboratory Testing

Hardware testing was performed in the laboratory before any field tests were conducted. The lab testing was used to establish the OEM and MR dampers' force versus velocity curves, ensure the MR damper prototype's functionality and reliability, and to discover any problems with the prototype setup.

4.1 Laboratory Test Procedure

The laboratory testing was accomplished via the use of a Material Test System (MTS) machine, which can provide a variety of types of displacement inputs from impulses and square waves to sinusoidal waves. The MTS machine was set to input a sinusoidal wave of a given frequency and displacement into the damper via a hydraulic actuator. The clamping system on the MTS machine also incorporates a load cell, which outputs a voltage proportional to the force of the damper. The range of forces and displacements depend on the specific load and displacement cards used in the MTS controller. The MTS machine and control system is shown in Figure 4.1.

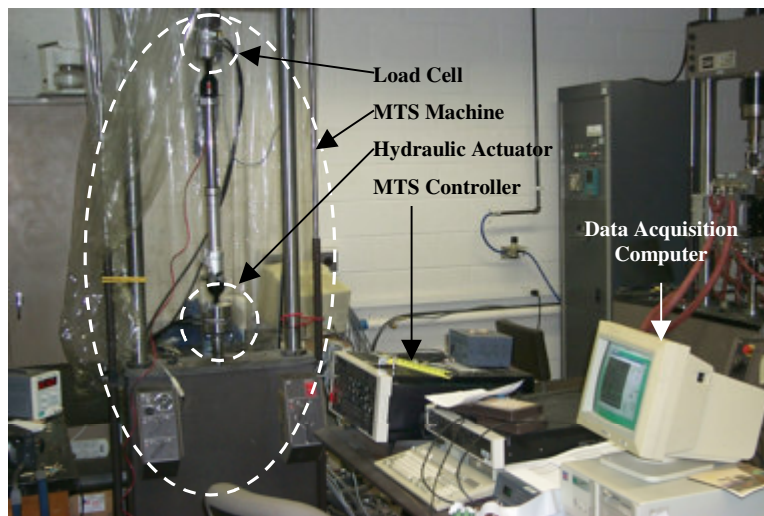


FIGURE 4.1. DAMPER DYNAMOMETER TEST FACILITY.

Test procedure was kept the same for both the OEM and MR dampers. A sinusoidal displacement input was used to excite the dampers. Frequency of the sine wave was fixed at 2 Hz, while the displacement was varied from 0 to 1.6 inch, providing a range of velocities at which to collect force data. Since the input is a sinusoidal wave in the form of Equation (4.1), the maximum velocity can be determined via its derivative, as shown in Equation (4.2):

$$x = A \sin \omega t \quad (4.1)$$

$$\dot{x} = A \omega \cos \omega t \quad (4.2)$$

In these equations, x is the damper displacement, \dot{x} is the damper velocity, A is the amplitude of the sine wave, ω is the angular velocity, and t is the time. The maximum velocity is $A\omega$, and the maximum force is at that displacement setting is attributed to the maximum velocity. The test data points are shown in Table 4.1.

TABLE 4.1. DAMPER FORCE CHARACTERIZATION DATA POINTS.

Frequency (Hz)	Displacement (in)	Max Velocity (in/s)
2.0	0.0	0.0
2.0	0.1	1.3
2.0	0.2	2.5
2.0	0.3	3.8
2.0	0.4	5.0
2.0	0.5	6.3
2.0	0.6	7.5
2.0	0.7	8.8
2.0	0.8	10.1
2.0	0.9	11.3
2.0	1.0	12.6
2.0	1.2	15.1
2.0	1.4	17.6
2.0	1.6	20.1

Motorcycle forks include the spring inside the damper, so it is necessary to factor out the spring force from the force versus velocity curve. By averaging the two lowest points in jounce and rebound, an offset force is determined. Adding the offset value to all other data points, the force versus velocity curve can be zeroed, as shown in Figure 4.2.

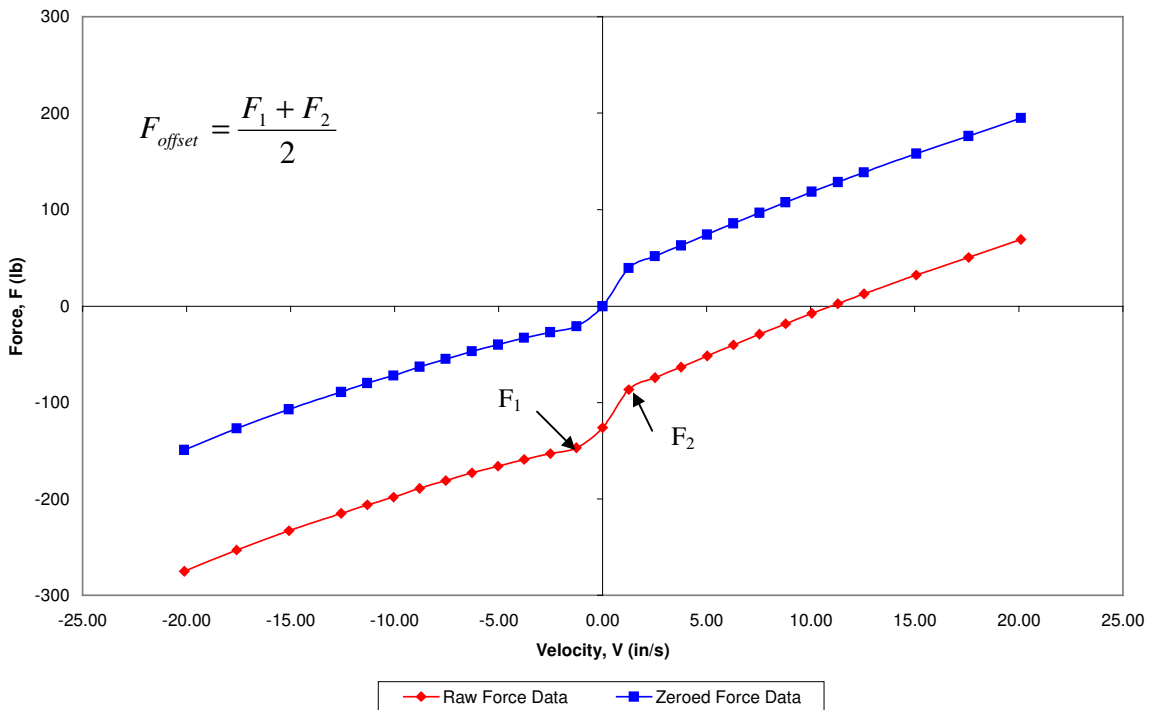


FIGURE 4.2. DAMPER CURVE ZEROING EXAMPLE.

4.2 OEM Damper Testing

As mentioned in Chapter 3, the OEM dampers were the first to be tested, as the data was essential to the design of the replacement MR dampers. The dampers were tested on the MTS machine as indicated by the test schedule in Table 4.1. The compression and rebound settings were adjusted half a turn at a time, and a test was run for each new rebound and compression combination resulting in six force versus velocity curves. The complete zeroed curve is shown in Figure 4.3.

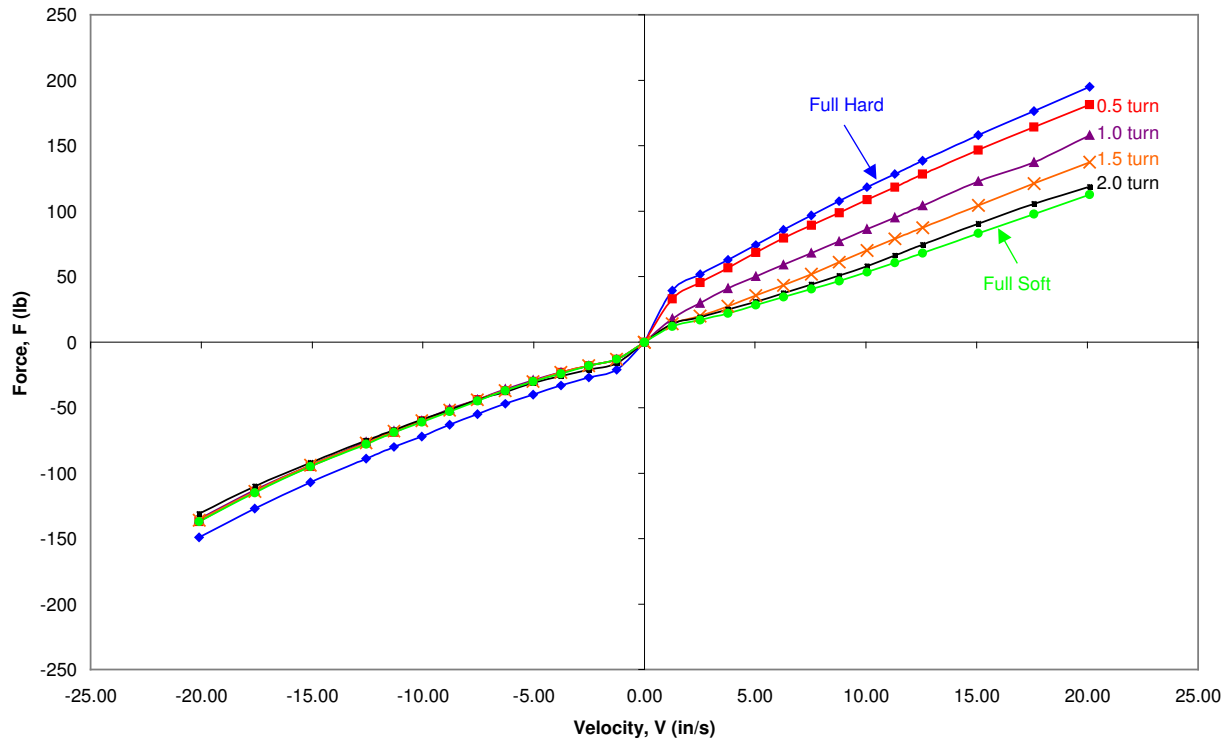


FIGURE 4.3. COMPLETE 1997 HONDA CBR900RR OEM DAMPER CURVE.

Varying the compression damping setting had little effect on the change in force, as the maximum variation between the fully soft and fully hard settings was only 12 pounds. The variability of the rebound adjustment showed a maximum difference of 85 pounds, allowing much more adjustability than the compression setting. Lack of compression adjustment shows the designer's attempt to fit in a margin of good performance and comfort, since the jounce stroke feeds the most force to the rider.

4.3 MR Damper Testing

Upon completion of the retrofit MR damper modules, testing was performed to validate the design and check for any malfunctions. Initially, the MR dampers were run through a variety of velocities and amperages to "break in" the new assemblies. Eleven tests followed, one test for every tenth of an amp from zero and one amp.

Overheating the MR dampers was a concern, so the dampers were varied between high and low amperage for every other test, i.e., test one at zero amps, test two at one

amp, test three at one-tenth amp, and so on. Every test followed the test schedule presented in Table 4.1. The first series of tests were performed with an accumulator pressure of 180 psi, and the results are shown in Figure 4.4. The MR replacement dampers performed very well in laboratory testing. The force vs. velocity curve proved excellent, with an adjustable range of approximately 90 pounds.

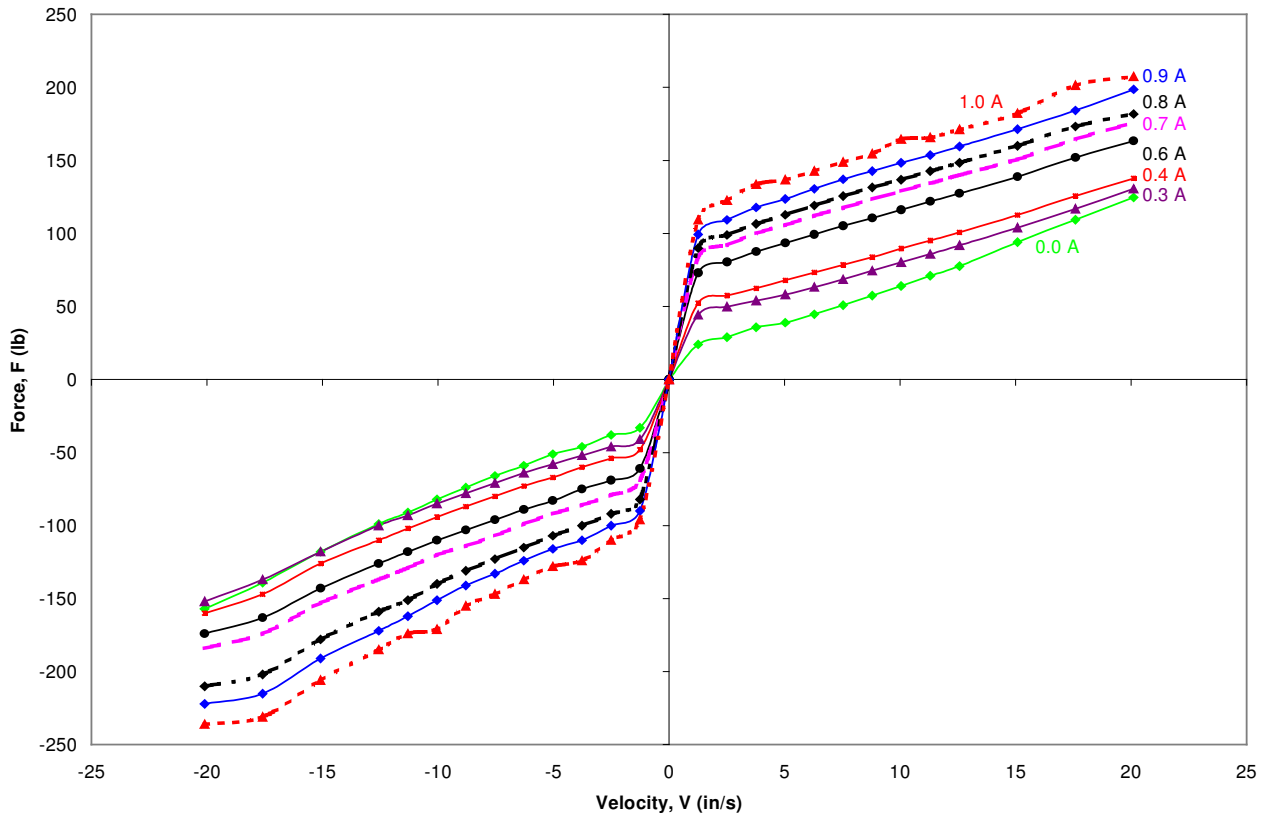


FIGURE 4.4. FORCE VS. VELOCITY CURVE FOR MR DAMPER (180PSI).

Unfortunately the MR dampers behaved as if the spring rate were twice as stiff as the original dampers. In a design oversight, the effect of the accumulator piston's spring force was not analyzed, so after completion of the first round of testing, this problem was analyzed. Piston surface areas normal to the direction of piston movement were calculated, and the pressure on these areas was calculated in order to determine the pre-load force on the piston shaft. These forces were then added to the OEM fork spring

force data to determine the effect of the accumulator spring rate. The results of this analysis are shown in Figure 4.5.

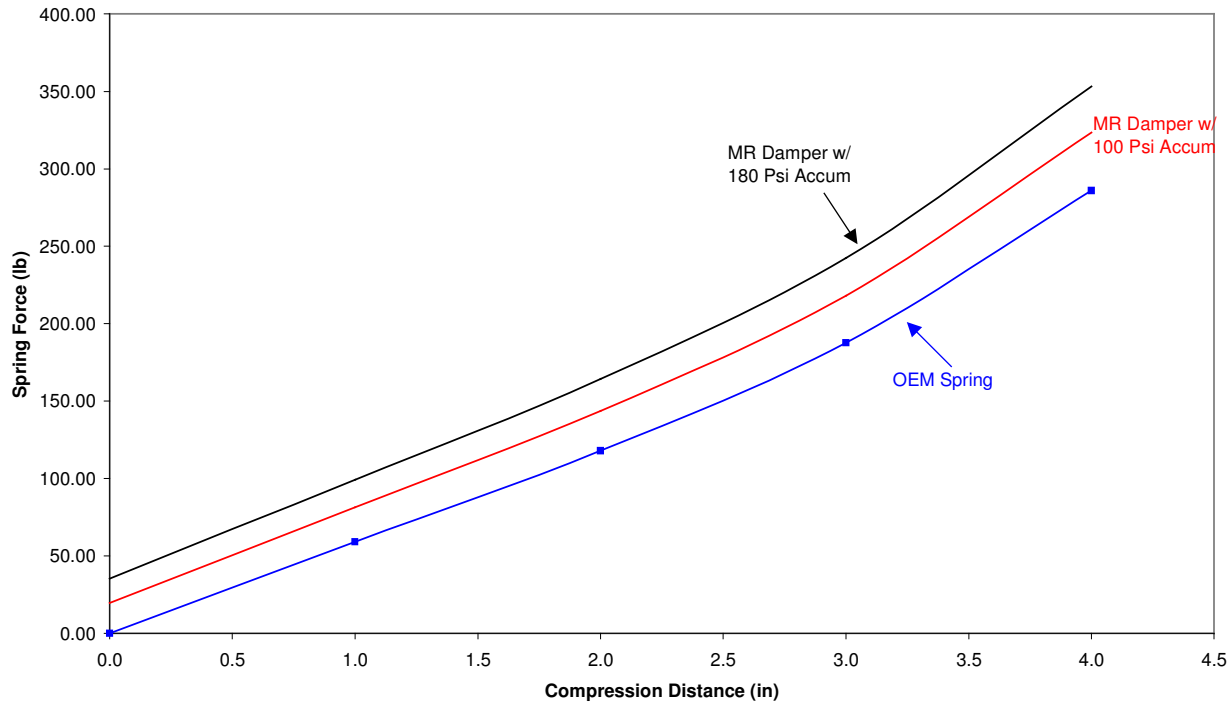


FIGURE 4.5. EFFECT OF ACCUMULATOR PRESSURE ON SPRING FORCE.

Accumulator pressure adds a significant force to the OEM spring force. This additional force was overlooked in design, but had a severe impact on ride harshness. For a 180 psi accumulator pressure, the magnitude of the additional force ranges from 35 to almost 70 pounds. Considering that this force represents only one of the two fork legs, that equates to a maximum of 140 additional pounds of spring force.

In an attempt to reduce the problem of accumulator pressure, the working accumulator pressure was reduced, while trying to avoid damper cavitation. Cavitation is undesirable in damper operation since the fluid boils at that point, introducing a compressible gas into the MR fluid [5]. These compressible bubbles cause a reduction in the amount of total damper force.

Lack of accumulator pressure can lead to another problem with the accumulator. In a properly functioning damper, when the MR piston moves into the damper, the accumulator moves down to accommodate the volume of the piston rod, as shown in Figure 4.6. When the MR piston moves out of the damper, the accumulator moves up to account for the lost piston rod volume.

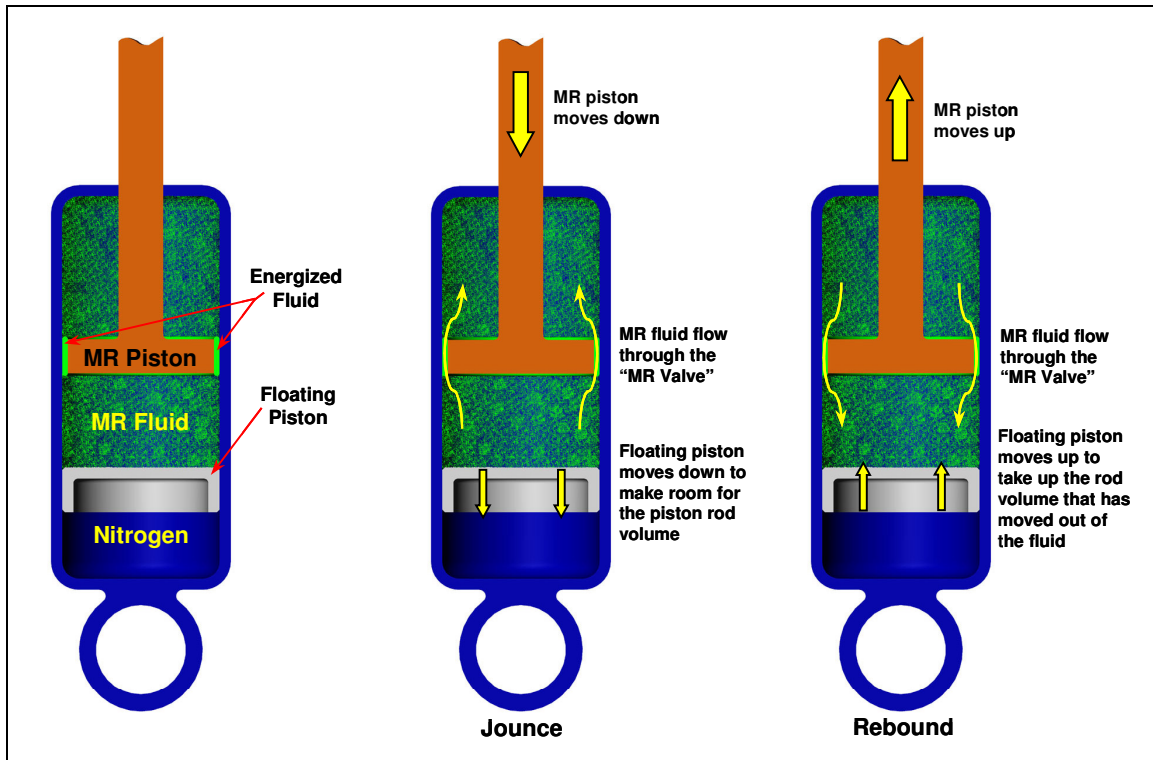


FIGURE 4.6. MONOTUBE MR DAMPER OPERATING PROPERLY [ADAPTED FROM 5].

When the accumulator pressure is too low, the activated MR fluid can act as a seal between the two sides of the piston, as shown in Figure 4.7. Since the seal around the MR piston will not allow the flow of MR fluid around it, the accumulator cannot absorb the piston rod volume. Instead, the accumulator piston moves down the same amount as the MR piston in compression, while a vacuum is created on the top side of the piston, causing cavitation. The cavitation results in a loss of damper force. Raising the accumulator pressure can solve this problem.

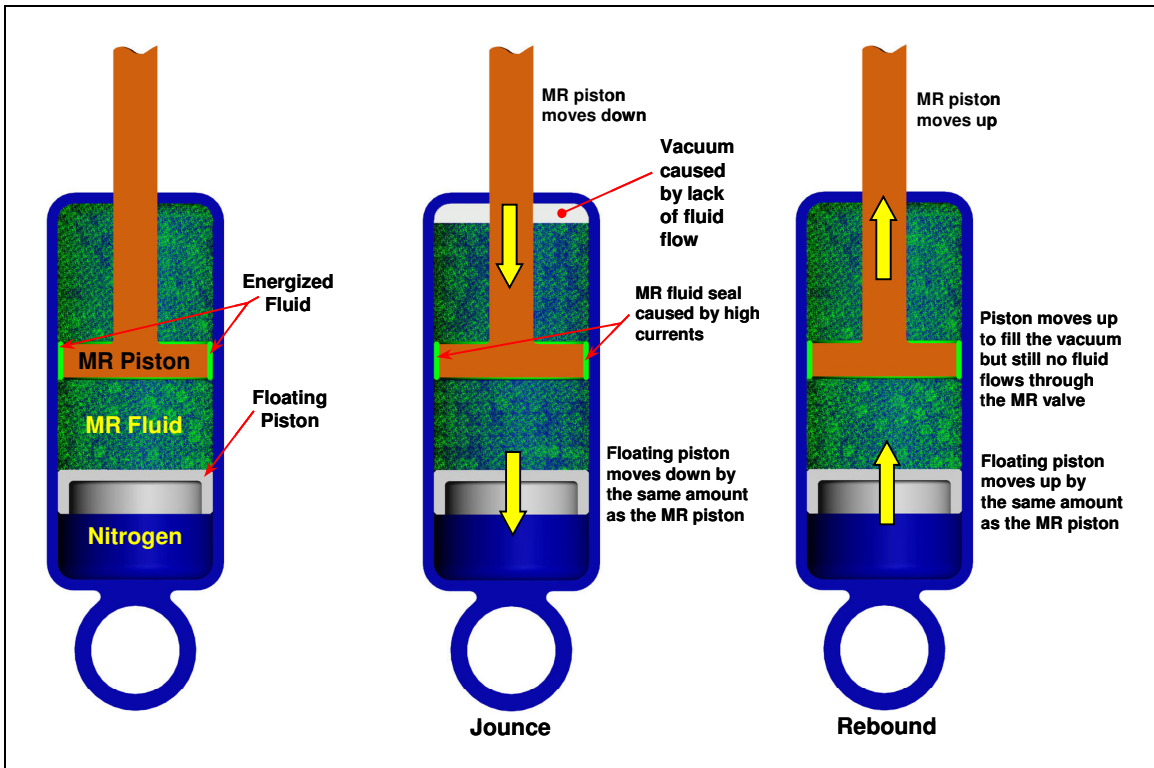


FIGURE 4.7. MR DAMPER CAVITATION CAUSED BY INSUFFICIENT ACCUMULATOR PRESSURE [ADAPTED FROM 5].

When reducing the accumulator pressure to decrease the spring force, care must be taken to avoid damper cavitation. The retrofit MR dampers were reduced to the point of cavitation during operation (roughly 80 psi) and then increased to 100 psi to ensure no cavitation. The dampers were run on the damper dynamometer to look for signs of cavitation, usually visible by a sudden drop in damper force. Upon determination that the dampers were not cavitating, the dampers were tested again with the lowered 100 psi accumulator pressure in both their on (one amp) and off (zero amp) states, as shown in Figure 4.8.

As shown in Figure 4.8, the MR dampers with a lowered 100 psi accumulator pressure produced an excellent range of adjustability. The dampers provided a maximum 105 pounds of adjustability in compression and a maximum 77 pounds of adjustability in rebound.

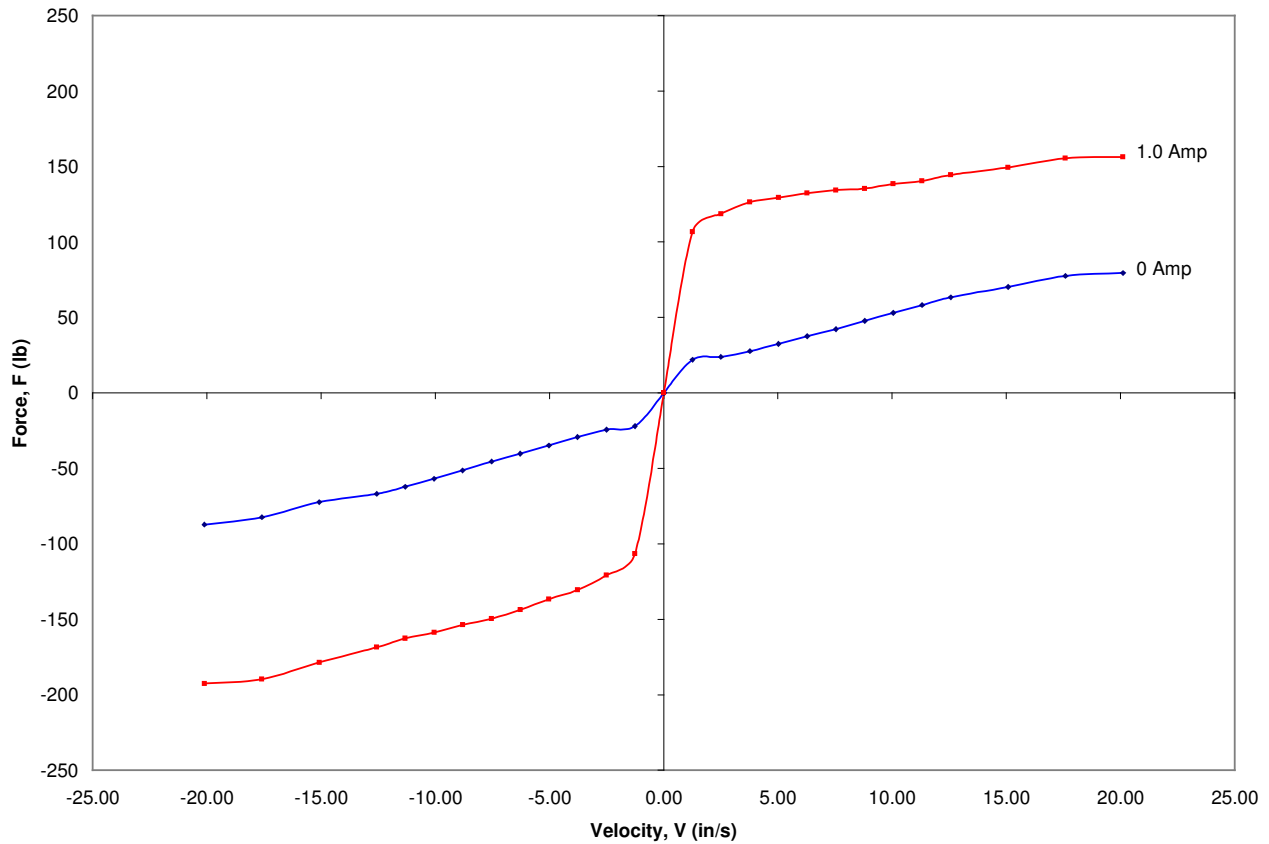


FIGURE 4.8. FORCE VS. VELOCITY CURVE FOR MR DAMPER (100PSI).

The accumulator pressure also affects the force vs. velocity data. As evident in Figure 4.6, the compression stroke achieves a higher force than does the rebound stroke for the 1.0 amp run. For the pressure driven flow mode of MR dampers, the damper force is based on the pressure differential across the piston. Accumulator pressure pressurizes the MR fluid as well, which in turn changes this effective pressure differential. The modeling equations assume that the pressure of moving the piston through the housing is not affected by the accumulator charge. As the accumulator charge increases however, there is a change in the effective pressure differential that alters the velocity-dependent damper force.

The effect of accumulator pressure is shown in Figure 4.9. This figure demonstrates the off state damper curves for the predicted model and accumulator pressures of 100 psi

and 180 psi. The force curve for the 100 psi accumulator charge held much closer to the predicted data than did the 180 psi accumulator charge.

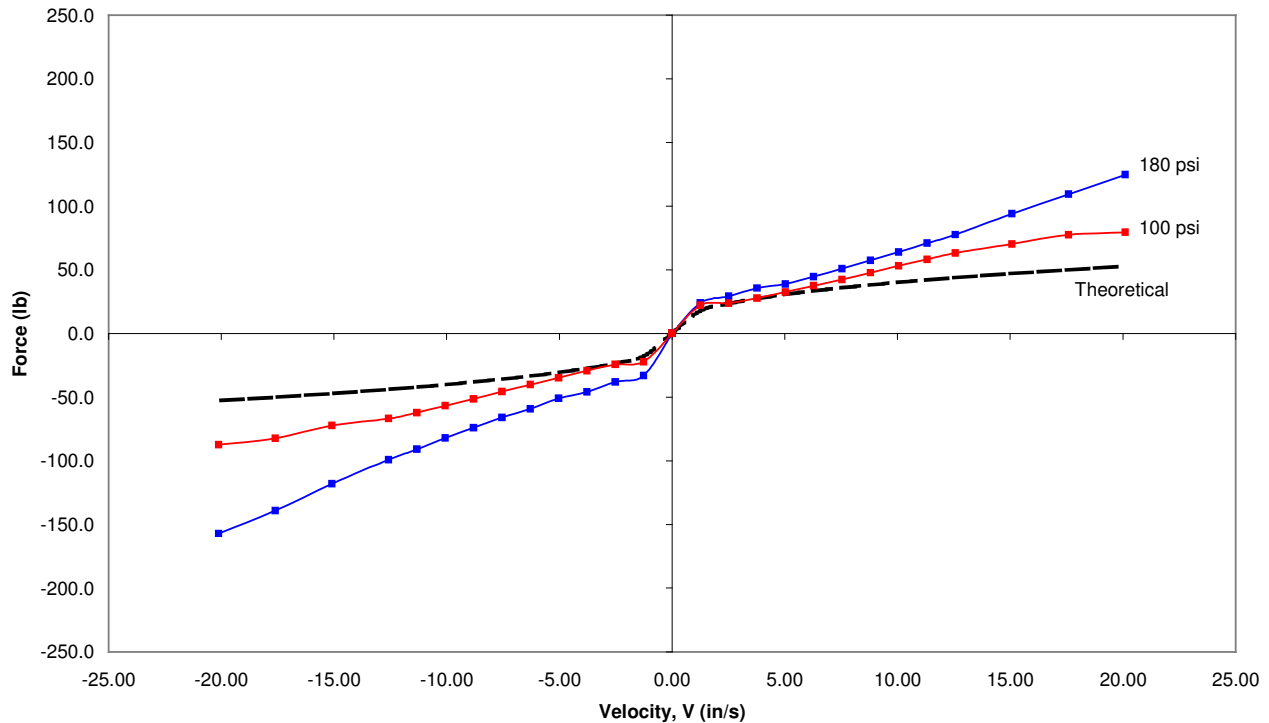


FIGURE 4.9. THEORETICAL AND EXPERIMENTAL OFF STATE MR DAMPER CURVES.

Attempting to envelop the OEM dampers' force versus velocity curve was a primary design consideration for the retrofit MR damper modules. Through a fork velocity based control system, this would allow the MR damper modules to emulate the OEM equipment should the rider desire a passive MR device. The retrofit dampers could also be used with any other type of control system desired. Displayed in Figure 4.10 is a comparison of the OEM damper and retrofit MR damper (100psi) curve limits. Each damper is infinitely adjustable within its limits.

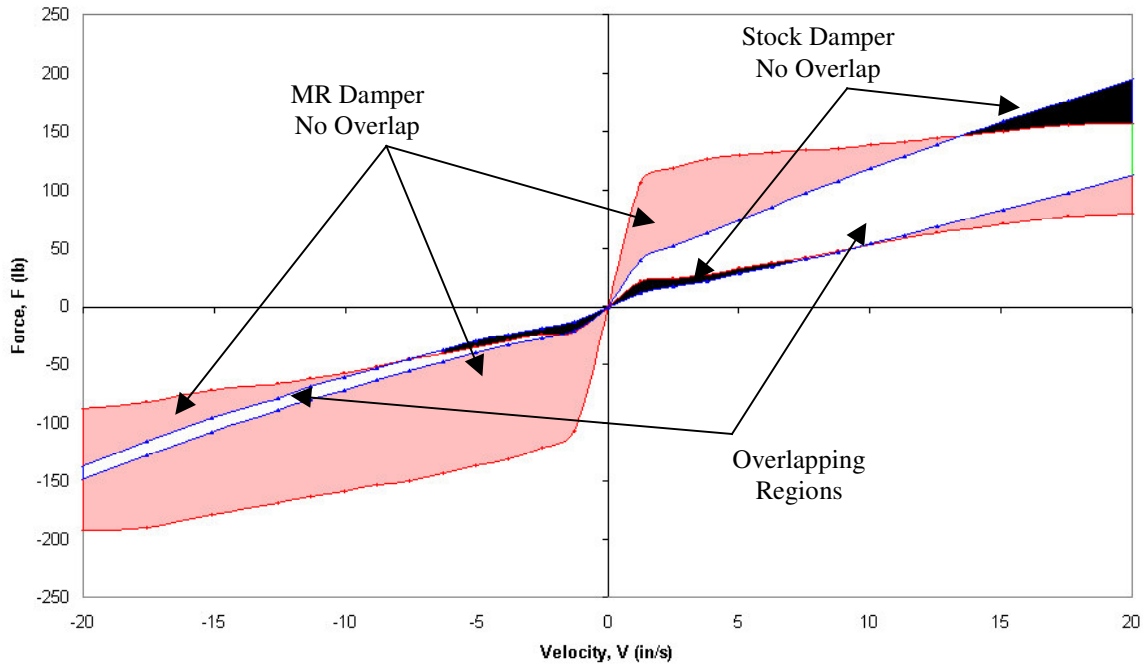


FIGURE 4.10. MR VS. OEM DAMPER COMPARISON.

The MR damper (shaded) almost completely envelops the OEM damper curve. The unshaded regions indicate the areas which both the MR and OEM dampers fill. Dark black areas indicate the OEM curve where the MR damper did not overlap. Despite the slight offset at low velocity the MR damper shows excellent coverage of the OEM curve, until high velocity in rebound, which should prove to be an excellent starting point for a very controllable front suspension. Not only was the overlay of the MR damper curves on the OEM curve a good match, the MR dampers offer much more range of adjustability, since the dampers can be adjusted to any point within the red shaded area.

4.4 Remarks

The laboratory testing was quite successful, despite the setback from the accumulator spring force. The retrofit MR dampers proved to have a good force range, as compared to the OEM damper. While the accumulator spring force problem would be more apparent in the field testing aspect of this research, it has only had a minor influence on the laboratory test results for the MR damper.

Chapter 5

Hardware Field Testing

To validate the retrofit MR damper design, field tests were conducted using both the OEM and MR dampers. Test data, including fork displacement and acceleration, was collected using an onboard data acquisition system. The test vehicle was driven over a series of bumps at established positions, and the corresponding fork responses were compared.

5.1 Field Test Setup

Field test required that the test vehicle be outfitted with an onboard data acquisition system. On a motorcycle, size and weight are primary issues, so the data acquisition system chosen must be compact and lightweight, while possessing the collection abilities required.

The DI-700 16-channel USB unit by DATAQ Instruments was chosen as the data acquisition system. The instrument, pictured in Figure 5.1, features compact size and weighs only one pound, while including 16 single-ended or 8 double-ended analog channels using a 16-bit analog to digital converter at a 1kHz throughput rate.



FIGURE 5.1. THE DATAQ DI-700 DATA ACQUISITION UNIT [ADAPTED FROM 16].

The DI-700 unit's compact size allowed mounting it in the rear compartment of the motorcycle, where it is attached to a custom wiring harness for the sensors. A small laptop computer was mounted on the gas tank to run the unit and to record the data. The final mounting of the data acquisition system and the laptop is illustrated in Figure 5.2.

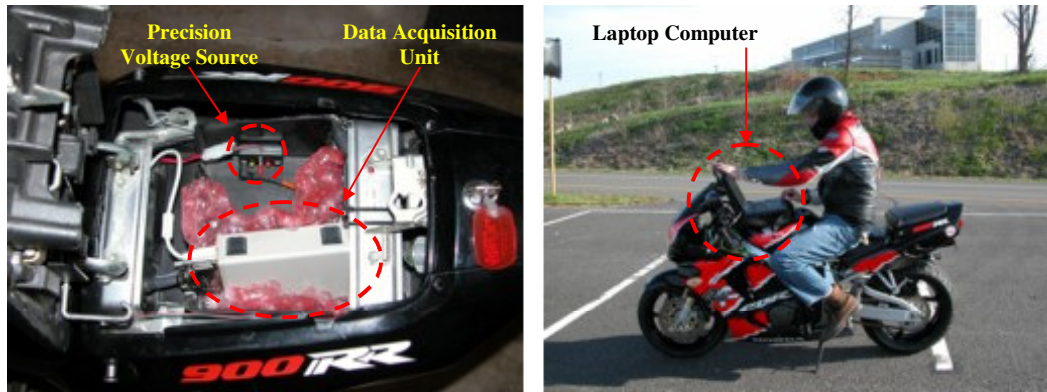


FIGURE 5.2. DATA ACQUISITION SYSTEM (LEFT) AND LAPTOP COMPUTER (RIGHT).

Three sensors were used to measure the suspension data as the test vehicle was maneuvered through the course. A $6\text{k}\Omega$ linear potentiometer from Transducers Direct™ was used to measure the fork displacement, mounted between the lower fork slider and the upper triple clamp. An Endevco™ Model 7265A-HSM3 $\pm 20\text{g}$ Accelerometer mounted to the lower fork slider was used to measure the wheel acceleration, while an Endevco™ Model 2262-25 $\pm 25\text{g}$ Accelerometer was mounted to the frame to measure body acceleration. All sensors were powered by a 10.00-volt precision power source mounted in the test vehicle's rear compartment, as shown in Figure 5.2. Schematics for the precision voltage source are shown in Appendix G.

The test vehicle employed no engine vibration damping systems. As such, frame vibration caused a significant amount of noise in the accelerometer measurements. The vibration occurred between 900 and 2400 engine rpm, or approximately 15 to 40 Hz, which is within the anticipated range of 0.5 to 20 Hz road inputs. The vibration's phase and frequency changed due to the effects of the frame structure, causing a lower frequency (8-10 Hz) vibration near the accelerometer mounting point at the front of the motorcycle. Since this vibration occurs in the middle of the anticipated road input frequency range, electronic filters could not be used.

The wheel accelerometer did not encounter as much noise from the engine as the body accelerometer, since some of the vibration was damped out while crossing the dampers. To alleviate the vibration problem, accelerometers were mounted with rubber washers to reduce the engine noise. The body accelerometer was moved several times while searching for a frame location with low engine vibration. Figure 5.3 demonstrates the final sensor mounting locations.

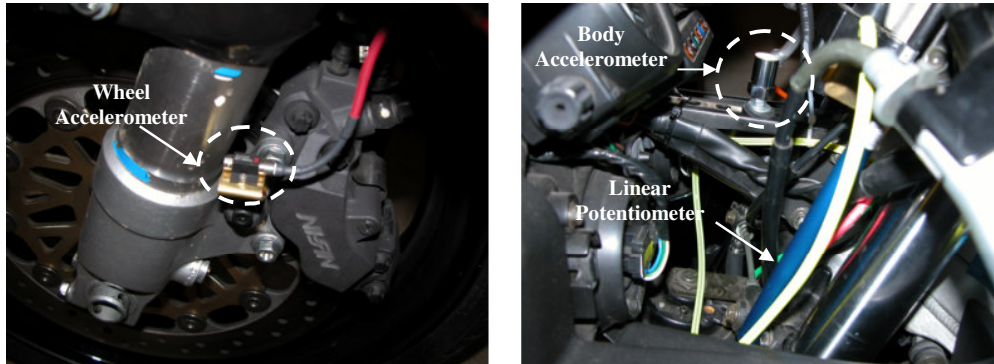


FIGURE 5.3. SENSOR MOUNTING LOCATIONS.

An infrared data storage trigger was also designed and built for the test vehicle's data acquisition system. The data acquisition system must be activated by the laptop prior to each test run, and then must be stopped afterwards. In the interest of conserving storage space and gathering only the course-relevant data, the trigger was designed to activate data storage upon passing an infrared source, and then stop the data storage upon passing a second infrared source. Unfortunately, this device was too sensitive to be used in broad daylight, and was only used for testing near dusk. Figure 5.4 depicts the infrared trigger and infrared emitter modules, while a detailed circuit schematic is shown in Appendix H.

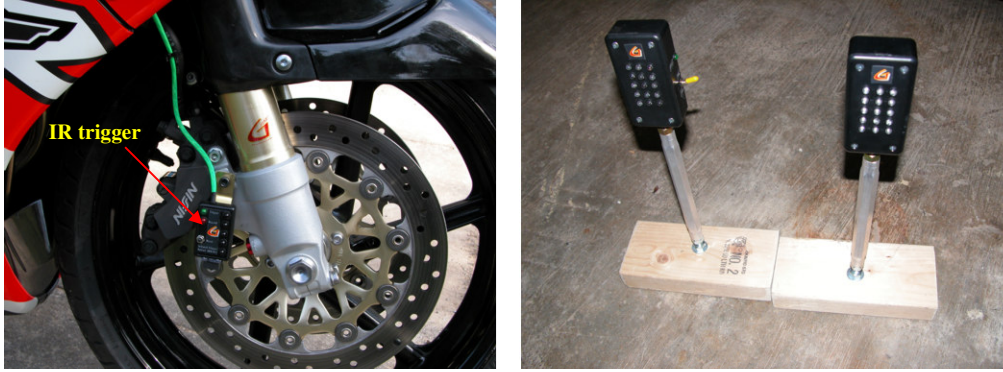


FIGURE 5.4. INFRARED DATA STORAGE TRIGGER (LEFT) AND EMITTERS (RIGHT).

5.2 Procedure

To achieve the field-testing objective—comparing the OEM damper response to that of the MR dampers—a test course was designed. The purpose of the course was to excite the suspension through a series of impulses in the form of road bumps. The corresponding response oscillations, settling time, and frequency content would be analyzed to determine the effectiveness of the MR dampers.

The course designed for this testing was comprised of a series two inch by two inch boards used as the excitation bumps. Boards were arranged to leave enough time between bumps to allow suspension oscillation settling. The first and second bumps were placed 50 feet apart, followed 50 feet later by a series of two bumps, five feet apart. A picture of the test course is displayed in Figure 5.5, while Figure 5.6 illustrates the equivalent input.

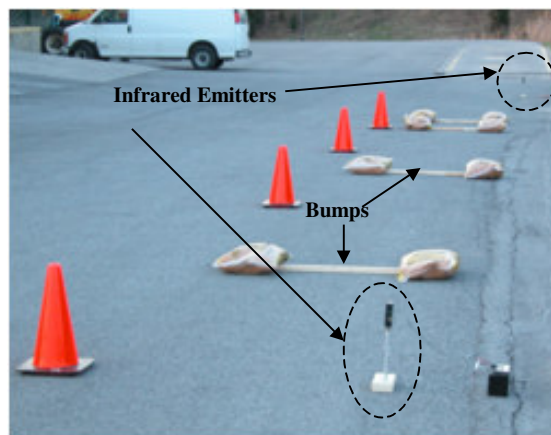


FIGURE 5.5. TEST COURSE.

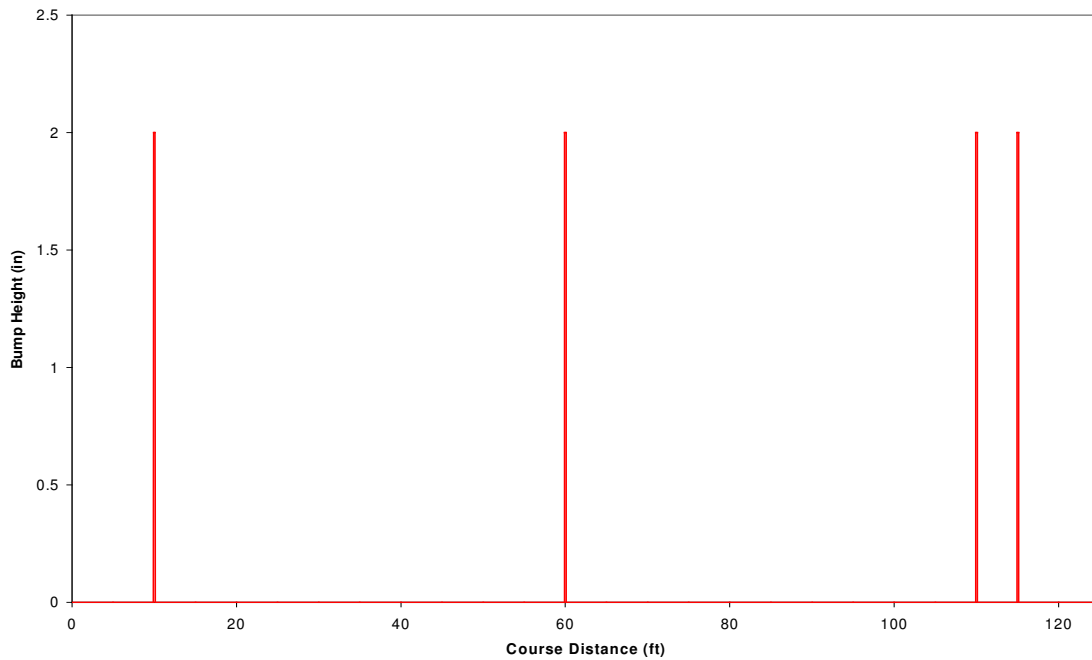


FIGURE 5.6. EQUIVALENT SUSPENSION INPUT GRAPH SHOWING SUSPENSION INPUT VERSUS COURSE DISTANCE.

The motorcycle was driven over the course at a variety of speeds and suspension settings. The speeds tested were 15 mph, 25 mph, and 35 mph, or an equivalent 0.0075 s, 0.0045 s, and 0.0032 s pulse length. Three different suspension tests were conducted at each speed: OEM with stock rebound and compression settings, MR operating in off-state, and MR operating under the skyhook control policy. An additional test was conducted at 15 mph with the MR dampers operating under the displacement control system. All data was then analyzed and compared to determine the effectiveness of each suspension system. Figure 5.7 shows the data acquisition system setup and one vehicle test.



FIGURE 5.7. DATA ACQUISITION SETUP (LEFT) AND VEHICLE TEST (RIGHT)

5.3 Field Test Results

Test results were analyzed in both time and frequency domains. Time domain data was analyzed for maximum suspension displacement and settling time, while the frequency domain data was examined for the magnitude of the frequency content. Accelerometer data was used to determine the level of comfort from the handlebars.

5.3.1 OEM Damper Results

The OEM suspension was tested using stock rebound, compression, and spring pre-load settings, providing a baseline for comparison of the MR dampers. This aids in determining the relative levels of acceleration, displacement, and frequency content of the MR dampers compared to the OEM dampers.

The test vehicle was driven on the course at the three established test speeds with the same OEM damper settings. The data was analyzed for the number of oscillations and settling time after each excitation in the time domain, and the magnitude of the frequency content in the frequency domain. Figure 5.8 illustrates the time domain test results from the OEM damper test at 15 mph.

Suspension displacement settling time for the OEM 15 mph tests was approximately 1.25 seconds, a rather long settling time by any means. High performance suspensions have very quick settling times, on the order of one half second. The peak displacement for the initial response from the impulse neared one inch, while there were about four oscillations of the suspension for every bump hit. The maximum wheel acceleration was approximately 7 gs, while the body acceleration reached a peak of about 4 gs. This information will provide the time domain baseline for which all further tests can be compared.

As shown in Figure 5.8, there are two modes of suspension response: one when the front wheel impacts the bump, and another when the rear wheel impacts the bump. The impulse and response are not limited to the front wheel only. Since this effect is the same throughout the test, settling time is considered a relative comparison for these certain tests conducted at a set speed.

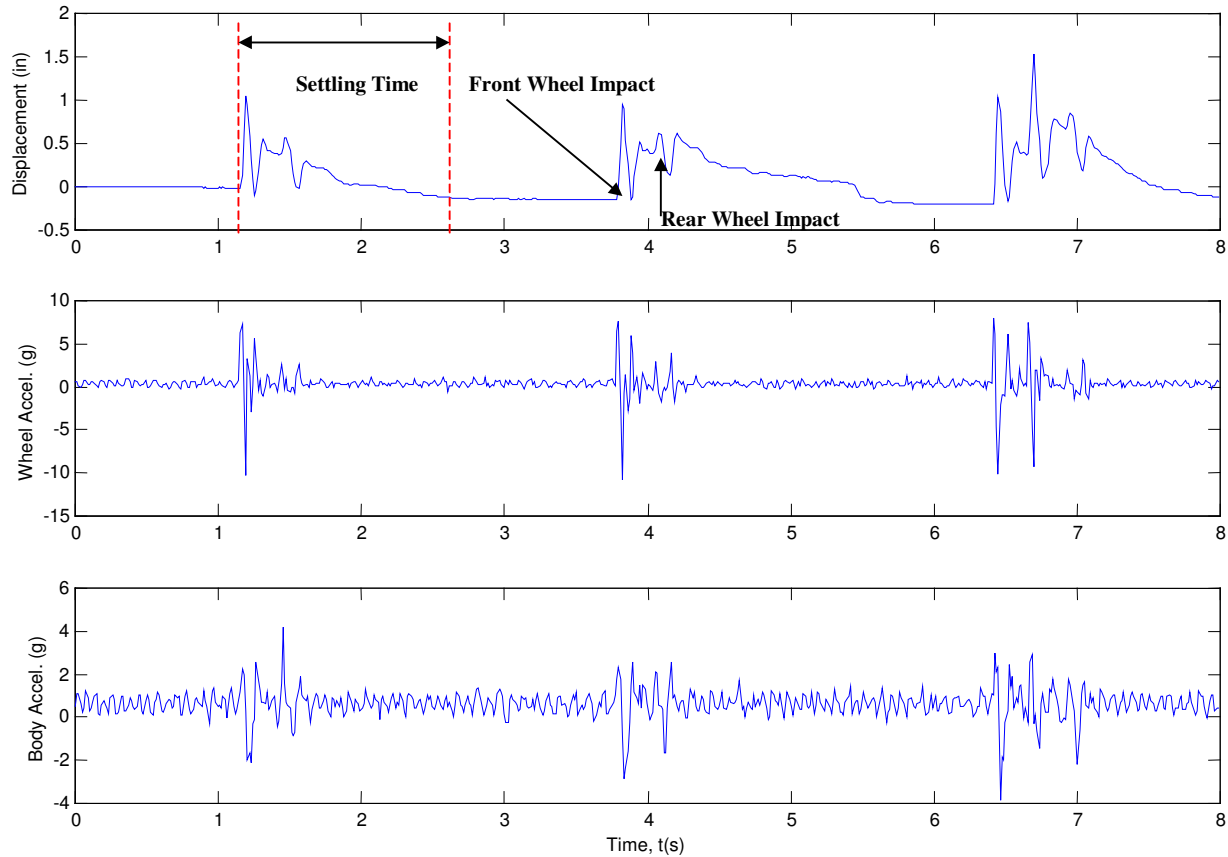


FIGURE 5.8. TIME DOMAIN OEM SUSPENSION PERFORMANCE AT 15 MPH.

Frequency domain analysis is also critical to evaluating the skyhook system performance. Fast Fourier transforms were used to convert the collected data to frequency domain. Since the data lengths of each test varied slightly, the frequency domain analysis was not exact, but the general trend could be extracted and used in analysis. Figure 5.9 displays the frequency domain OEM suspension data collected for the 15 mph test run.

The OEM dampers exhibited significant frequency content in both the damper position and body acceleration from 5 Hz to 15 Hz, in the region of expected road inputs. The wheel accelerometer, on the other hand, demonstrated significant frequency content from 5 Hz to 30 Hz, most likely due to road inputs and slight wheel hop. More often wheel hop is a result of a high spring rate (and/or high tire spring rate) with inadequate damping.

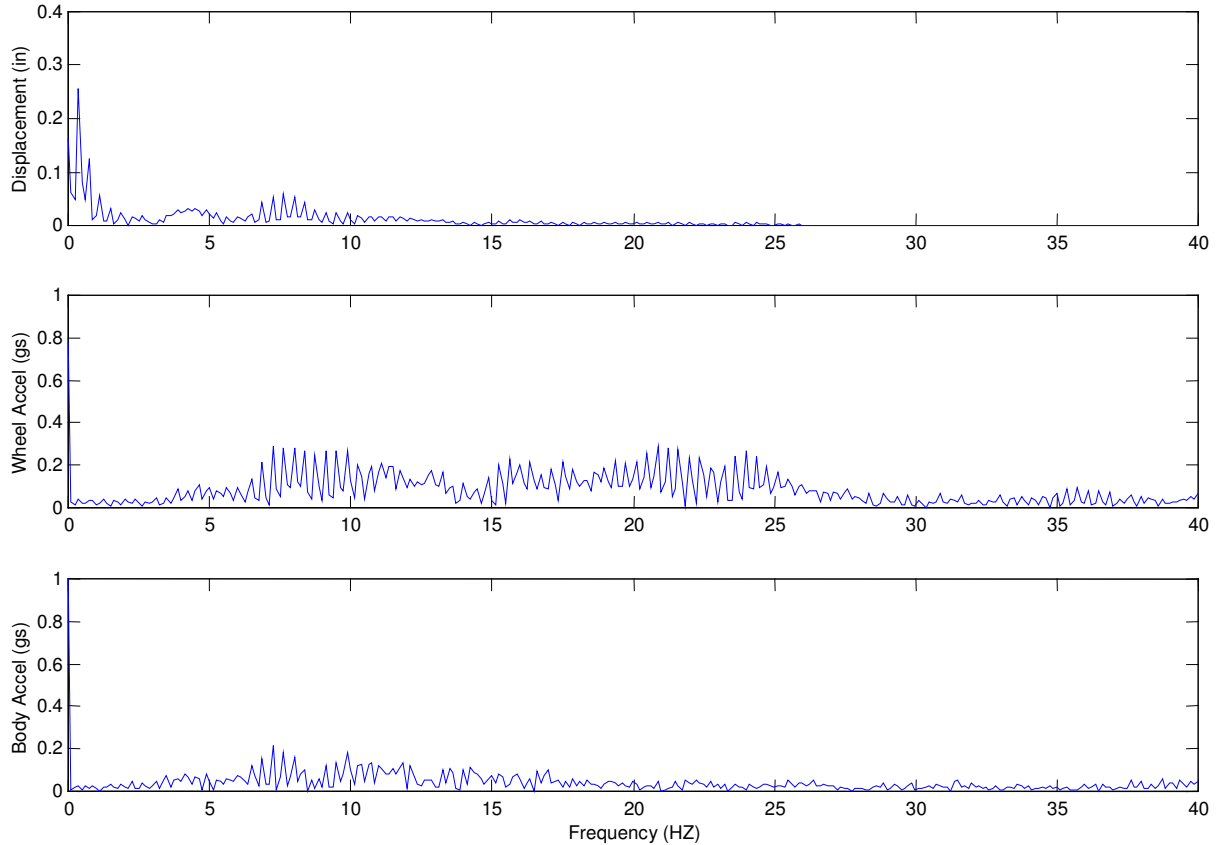


FIGURE 5.9. FREQUENCY DOMAIN OEM SUSPENSION PERFORMANCE AT 15MPH.

5.3.2 MR Damper Results

The retrofit MR damper modules were tested in accordance with the procedure drawn out in Section 5.2. As previously established, the spring rate of the retrofit MR damper forks was much higher than that of the OEM forks. While the spring rate problem could not be eliminated, the MR damper field tests were run regardless. The MR dampers were tested in their off state, with a skyhook control system, and with a displacement-based control system. The off-state tests established a baseline to determine the effectiveness of the skyhook control system and displacement-based control system. The time domain off-state MR damper test data at 15 mph is illustrated in Figure 5.10.

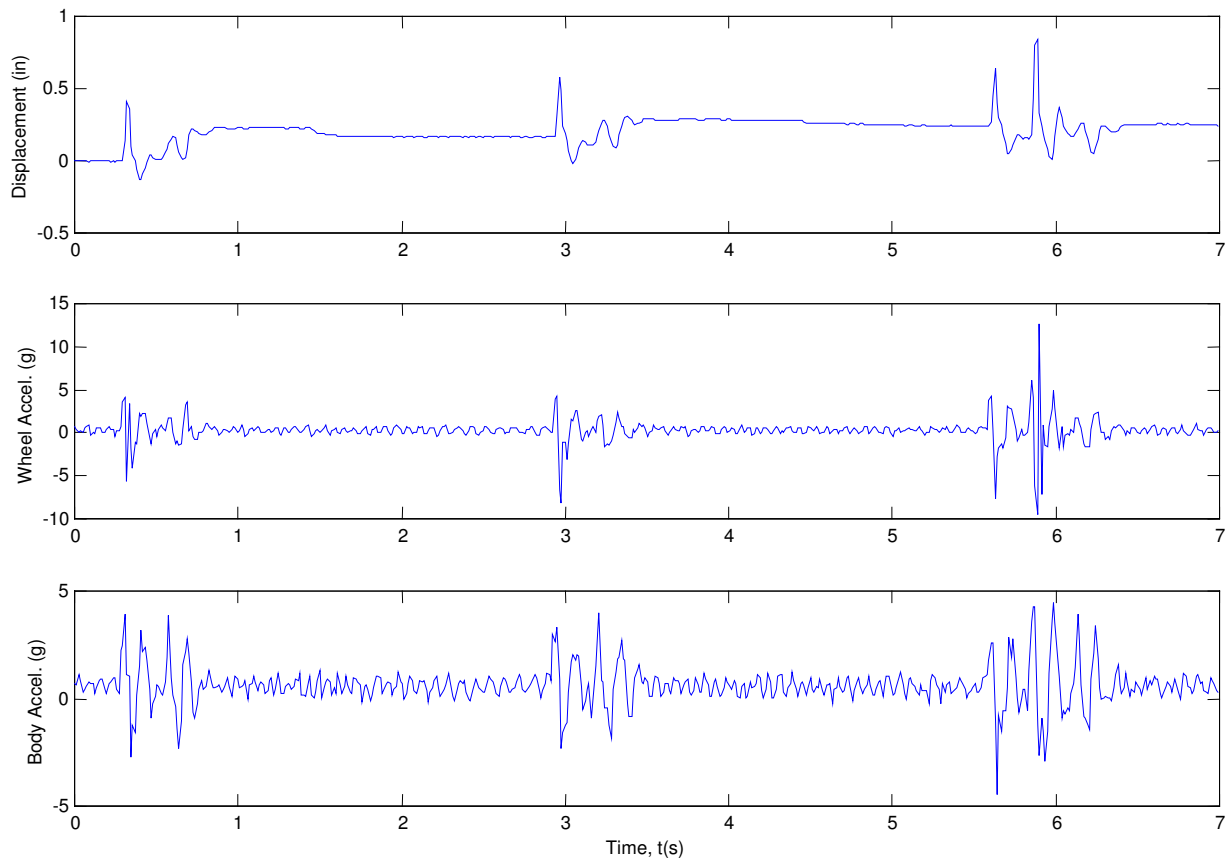


FIGURE 5.10. TIME DOMAIN PERFORMANCE OF MR SUSPENSION IN OFF-STATE AT 15 MPH.

The primary advantage of the MR suspension over the OEM suspension was the reduction of suspension settling time by almost one half second, now down to about 0.75 second. The suspension displacement reduced to half of the OEM's displacement, while the wheel acceleration decreased slightly on the single bumps and increased on the double bumps. The body acceleration decreased very slightly, but not by a noticeable amount. Since rake and trail change when the fork moves causing instability, these initial specifications indicated increased stability and therefore higher performance in cornering situations.

Frequency domain analysis showed a significant reduction in most all frequency content within the collection bandwidth except for one key area, as shown in Figure 5.11. The MR dampers in off state showed a decrease in wheel acceleration except for the 7-8

Hz range. This increase corresponded to a magnitude increase in the body acceleration in the same 7-8 Hz range.

This correlation between the two acceleration signals could possibly be due to a hysteresis effect in both the fork and MR damper. The MR damper has a certain amount of friction to overcome before the shaft will move – this friction can be attributed primarily to the accumulator piston cup seal, piston guide band, and shaft seal. For small displacements, this could lead to a slight stiction in the fork, causing the wheel acceleration frequency content to appear in the body acceleration frequency content. The other possibility for the correlation would be a system natural frequency, though this possibility is rather unlikely when examining the MR suspension settling time.

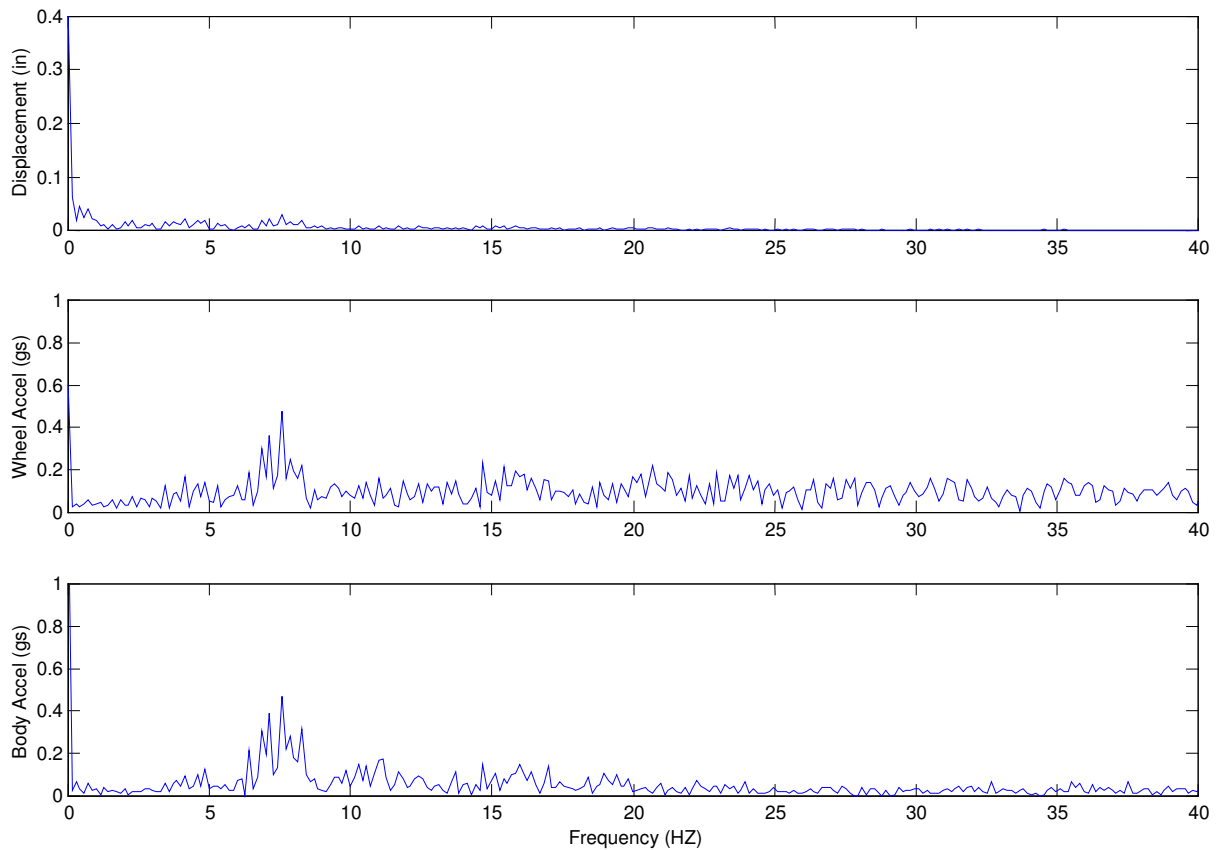


FIGURE 5.11. FREQUENCY DOMAIN PERFORMANCE OF MR SUSPENSION IN OFF-STATE AT 15 MPH.

The second set of MR damper tests to be analyzed was the skyhook controlled system. The time domain data for these tests at 15 mph is shown in Figure 5.12. The settling time for the skyhook controlled system was slightly less than the off state MR suspension, at only 0.6 seconds. The maximum suspension displacement remained the same as the off state MR dampers, while the peak wheel acceleration increased by about fifty percent. The maximum body acceleration decreased by about twenty-five percent, which is a positive sign of the skyhook controller's effectiveness.

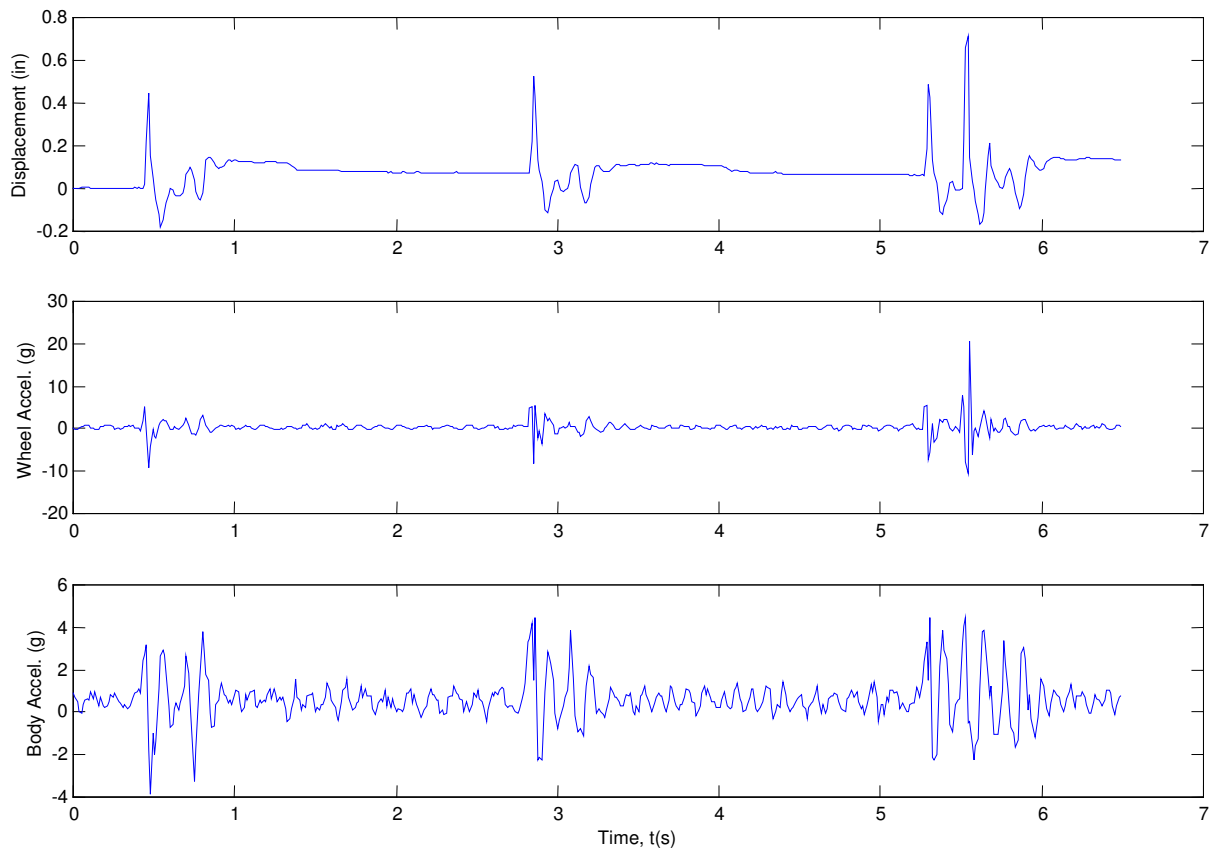


FIGURE 5.12. TIME DOMAIN PERFORMANCE OF MR SUSPENSION WITH SKYHOOK CONTROL AT 15 MPH.

Frequency domain analysis of the skyhook controlled MR damper suspension, displayed in Figure 5.13, showed good results that helps prove the validity of the skyhook control system for MR dampers in motorcycle applications. The wheel acceleration was reduced significantly in the 7-8 Hz range, while the body displacement was slightly

reduced. There is not a drastic difference in the off-state and skyhook control results due to the stiffness of the retrofit MR damper modules—the added spring force creates a much more rigid front suspension. With the stiffer front end, the damper force is no longer proportional to the spring rate, allowing the spring force to do most of the controlling. Therefore, even this slight change in body acceleration is a good sign of the skyhook controller effectiveness on motorcycle applications.

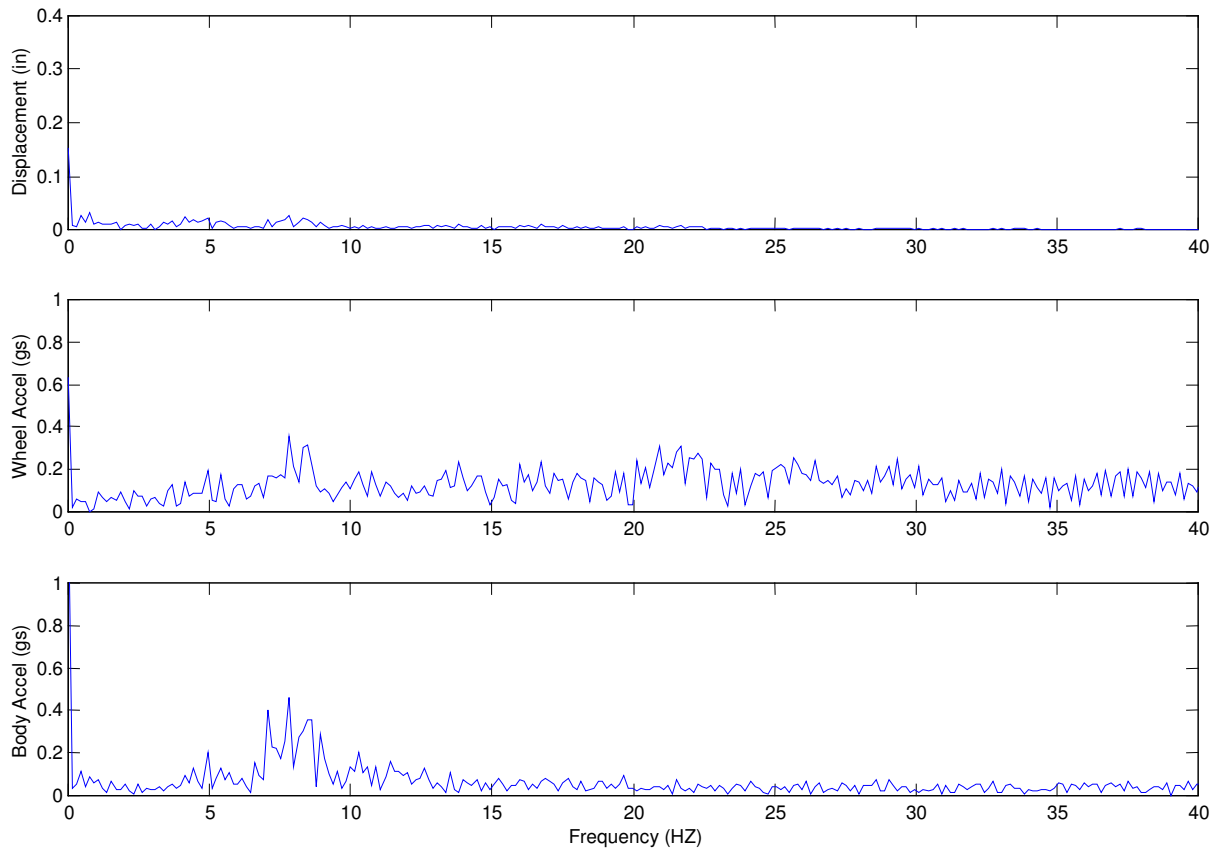


FIGURE 5.13. FREQUENCY DOMAIN PERFORMANCE OF MR SUSPENSION WITH SKYHOOK CONTROL AT 15 MPH.

The final MR control system to be tested was the displacement based control system. This system was designed primarily for smooth road riding (i.e., racetrack), and *not* for the excitation course used in testing. The MR dampers, however, were run through the track once at 15 mph with the displacement based control system. The time

domain data is shown in Figure 5.14. The displacement showed *amazing* settling time, at approximately 0.2 seconds. The rear wheel impact was very obvious in this data, as it was the second main oscillation of the suspension in each set – the front suspension had settled by the time of rear wheel impact. While the acceleration data was not much different than that of the MR system, the ride was uncomfortable upon hitting a bump, likely due to much higher dynamic jerks (derivative of acceleration). This system, however, felt the most stable in cornering situations.

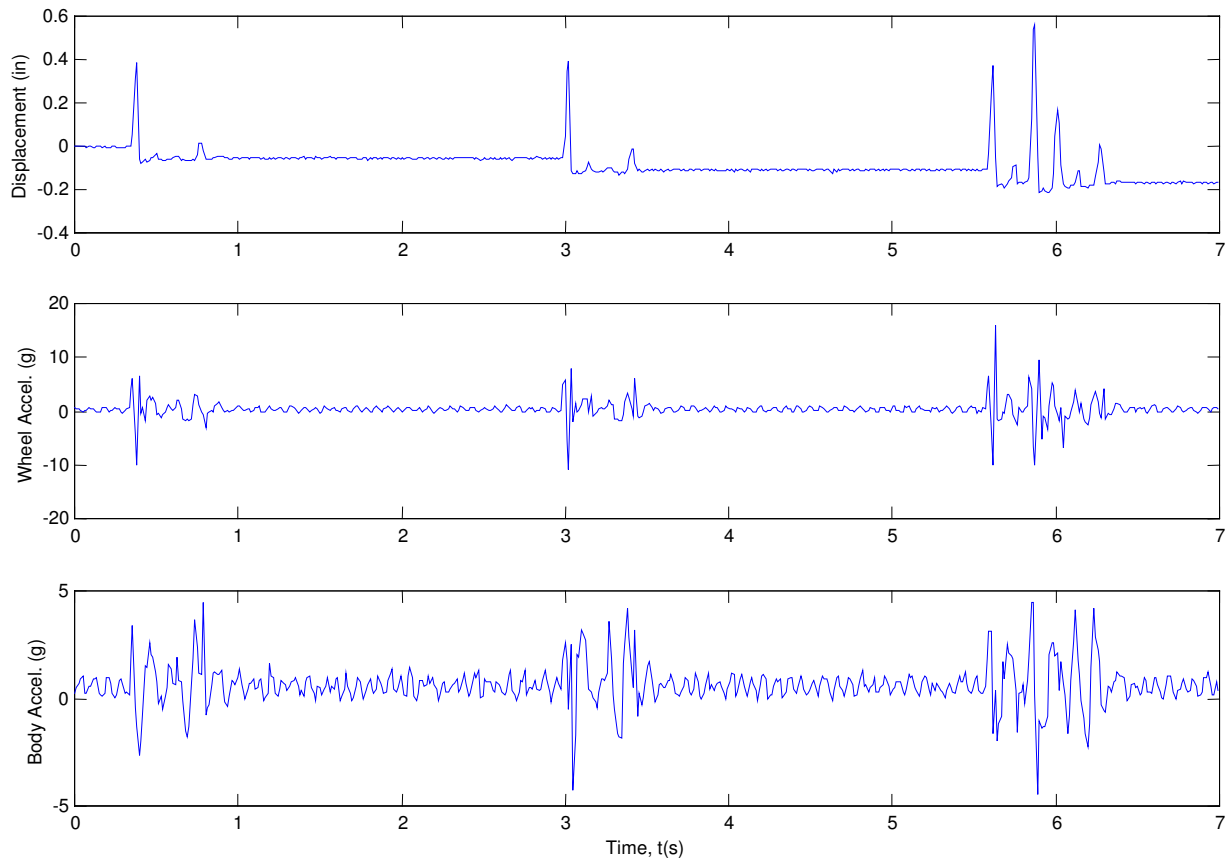


FIGURE 5.14. TIME DOMAIN PERFORMANCE OF MR SUSPENSION WITH DISPLACEMENT CONTROL AT 15 MPH.

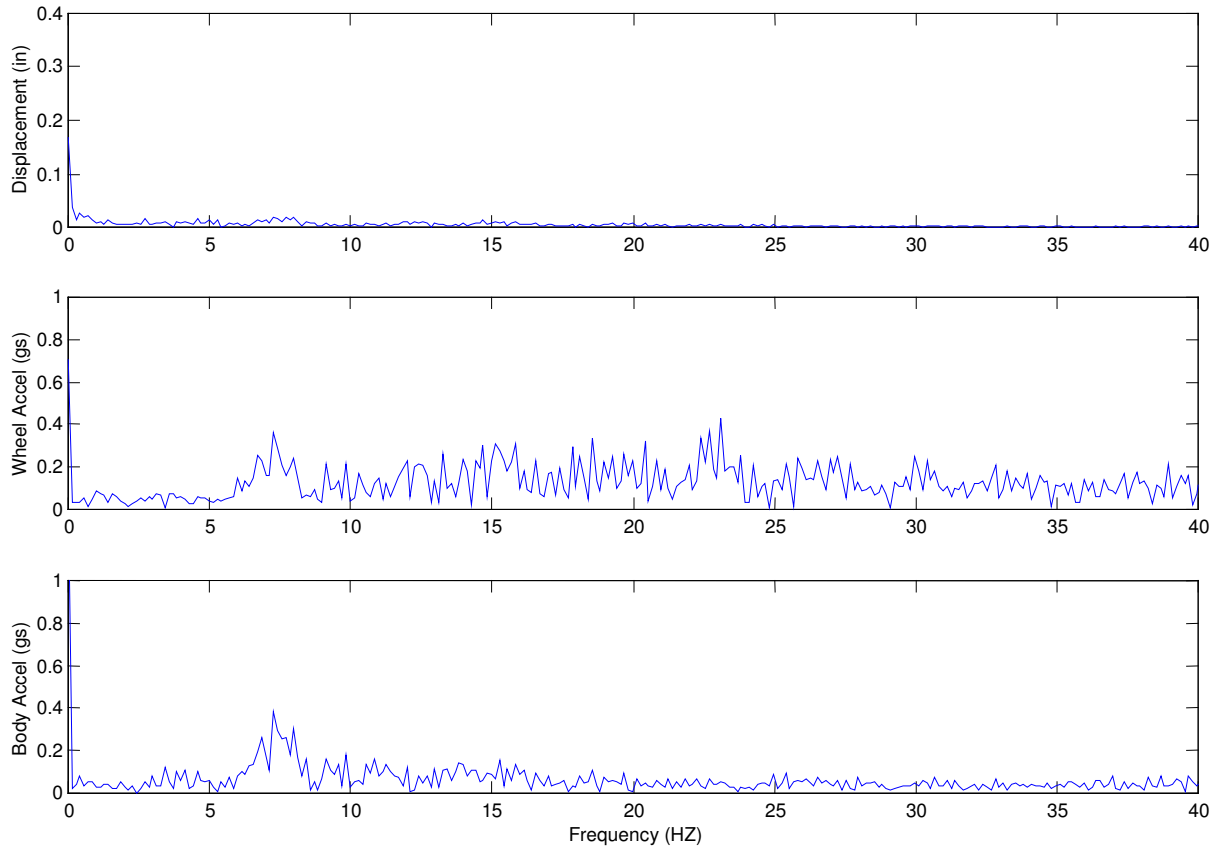


FIGURE 5.15. FREQUENCY DOMAIN PERFORMANCE OF MR SUSPENSION WITH DISPLACEMENT CONTROL AT 15 MPH.

The frequency domain of the displacement based control system test showed the 7-8 Hz peaks associated with all of the MR damper tests, but much like the OEM suspension, the wheel acceleration showed the broad range of 5-30 Hz frequency content.

5.3.3 Performance Comparison

A frequency domain comparison was done between the damper displacement in all of the previously mentioned systems. This was compiled for the purpose of reference in the following subjective opinion of the test rider. Figure 5.16 shows the frequency domain displacement magnitudes for all four 15 mph tests.

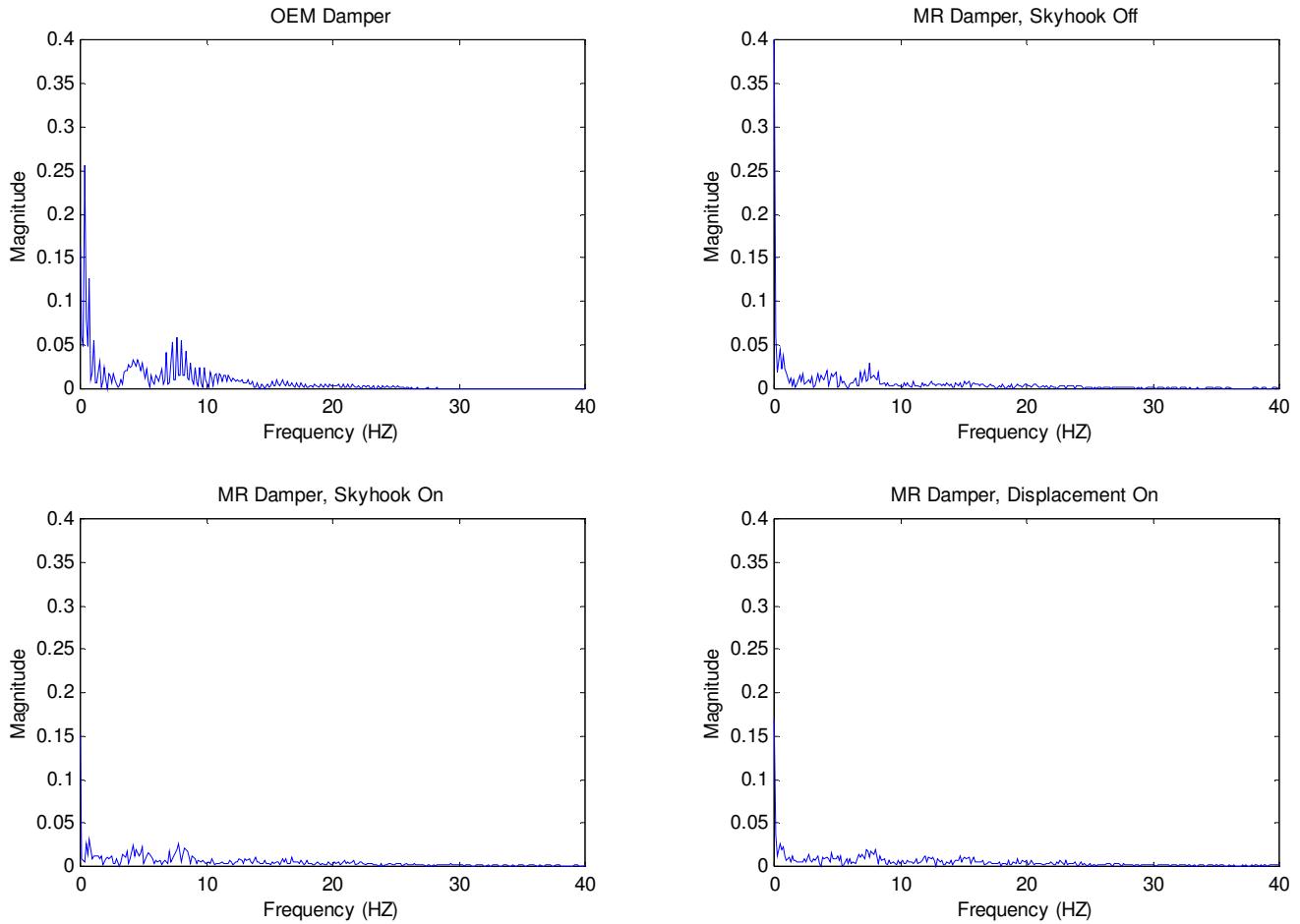


FIGURE 5.16. FREQUENCY DOMAIN COMPARISON OF DISPLACEMENT DATA AT 15 MPH.

The OEM damper had, by far, the highest displacement magnitude, on the order of two to three times more than any other system. The MR damper in off state showed the peak at 7-8 Hz, which was slightly reduced by the skyhook control, and significantly reduced by the displacement-based control. While preferable for performance applications, this displacement magnitude reduction comes at a rather severe price: a reduction in comfort. Figure 5.17 shows a bar chart comparing the OEM and MR damper performance. The OEM damper performance represents the baseline to which the MR dampers are compared.

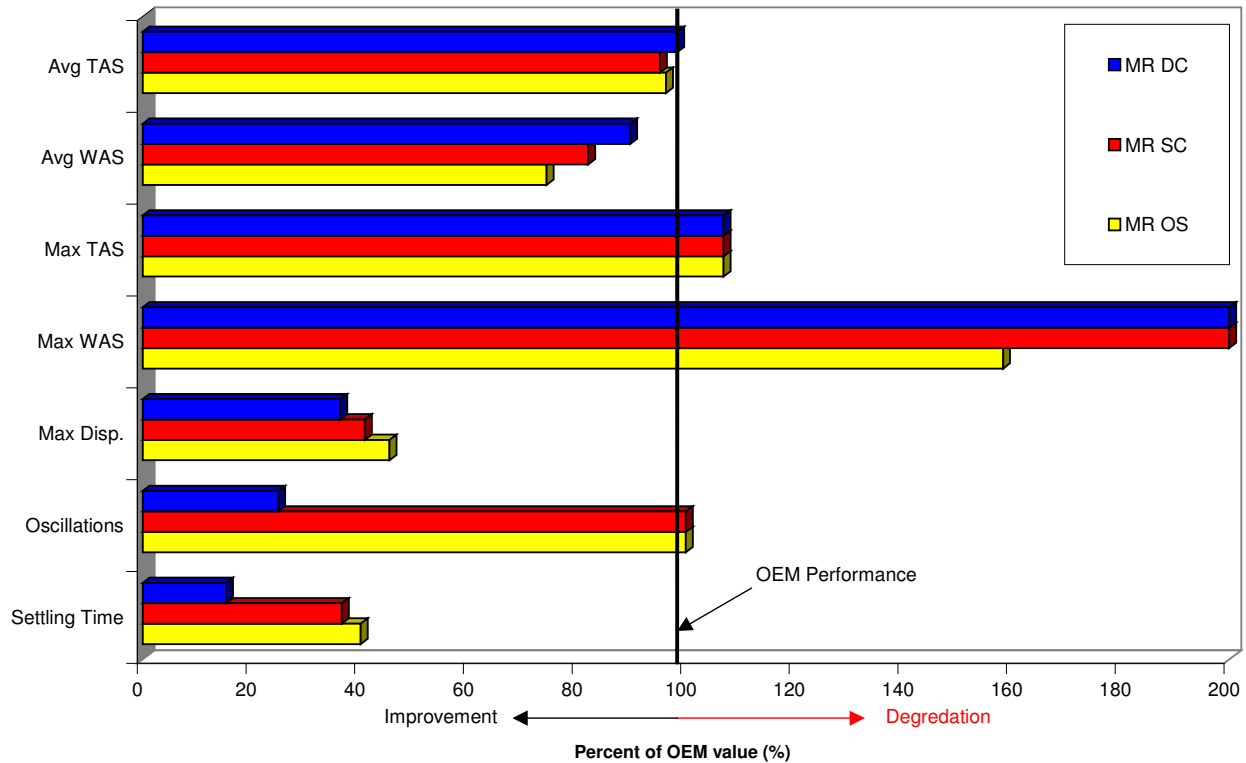


FIGURE 5.17. OEM AND MR DAMPER PERFORMANCE COMPARISON.

5.4 Subjective Opinion of the Test Rider

The author was the sole test rider for all of the field tests conducted for this research, mainly for liability purposes. While completely subjective in nature, this section should enlighten the reader on the test vehicle’s handling that corresponds with the results mentioned in Section 5.3. The author did not confine these subjective opinions to the excitation course – rather, roughly 200 miles were driven on the MR dampers using off state, skyhook control, and displacement-based control. Before the start of the research, the author had over 2000 miles experience on the OEM suspension.

The OEM suspension was rather lacking in both its comfort and performance. The front suspension had a tendency to induce wheel hop after hitting a small bump, causing chatter in the handlebars. This wheel hop could grow very tiresome very quickly. Also, front brake application would cause the OEM suspension to plunge, which can lead to serious control problems. On large bumps, however, the suspension was soft

enough to absorb most of the excitations, but at the same time, the suspension oscillations took too long to settle. This led to instability in cornering which can lead to an aggravated front end, eventually causing a dismount.

The MR suspension in its passive off-state mode seemed to reduce most of the wheel hop oscillations, but made for a much stiffer ride. Brake application no longer caused fork bottoming, due simply to the increased fork spring rate. The suspension seemed to settle out faster over large bumps, but seemed much more uncomfortable in the process, sending larger forces through the handlebars and into the arms and shoulders. The test vehicle seemed more stable cornering, with a much better “feel” of the road. The skyhook controlled MR suspension felt much like the passive mode, and no appreciable difference could be determined between the skyhook control and off state mode.

The displacement-based control of the MR suspension was the most stable suspension system that the author has ever encountered for smooth road riding. It inspired excellent confidence in cornering and superb road feel. The larger bumps posed quite a threat to the arms though, as the suspension would usually rebound before reaching the “soft barrier” where the suspension would go into off state. Therefore, the rider would get the full jolt of the bump, which was, needless to say, very uncomfortable.

Overall, the author believes the MR suspension provides a more stable ride, but the design needs improvement to overcome some of the setbacks of the current design. Should the spring rates of the MR and OEM suspensions been equal, the author believes that the MR suspension with the control systems would have far exceeded both the performance and comfort of the OEM suspension.

Chapter 6

Conclusions

This research was focused on the feasibility of MR dampers for motorcycle front suspension use, and the effectiveness of different types of control systems for the dampers. The design, manufacture, and testing of retrofit MR dampers were accomplished, and the results presented.

6.1 Summary

The primary objective of this research was to determine the feasibility of magneto-rheological dampers for motorcycle front suspension systems. The goal of the use of MR dampers was to allow both comfort and performance with the same suspension package in super sport motorcycles. Providing a background of magneto-rheological technologies and motorcycle suspension history, this paper showed that MR dampers for motorcycles would be a perfect application of the technology. This research was an attempt to prove this idea.

The first phase of this research involved research, testing, and design. Testing and solid-modeling the OEM dampers provided a design envelope for the retrofit MR dampers. The MR damper design proved to be an arduous task, as it required a very slim package with relatively high damping rates, as well as a new system for accumulator charging. MR damper designs were studied and modeled to provide size data and force versus velocity data to facilitate pre-manufacture comparison of both OEM and MR dampers.

The second phase of this research was designated the prototype phase. The retrofit MR dampers were machined and assembled in-house, in entirety, by the author. Following full assembly, the MR dampers were laboratory-tested using a damper dynamometer to provide damper break-in, design verification, and a pre-field testing mechanical check. The retrofit MR dampers showed excellent adjustability with very low power consumption, which nicely lent itself to the design of the rest of the system: the controller and other electronic components. During laboratory testing, an unforeseen

problem became apparent, in that the accumulator's spring rate was too high to allow a good comparison between MR and OEM suspensions in field testing, as the MR system would have a *much* higher spring rate.

In the third phase of research, a series of control systems were designed and assembled. An analog on-off skyhook control unit based on wheel and body accelerometer inputs was designed to show the marriage of comfort and performance with MR dampers in motorcycle applications. An analog displacement-based control system was designed and manufactured to reduce wheel hop and handlebar chatter on smooth road riding via the use of high damping, and allow low damping for larger bumps. This system also employed an anti-bottoming high damping region. The test vehicle was outfitted with appropriate data acquisition equipment including: a laptop computer, a very compact data acquisition unit, two Endevco™ accelerometers, and a linear potentiometer for displacement measurement.

The last phase of the research involved field testing both the OEM and MR damper suspension systems. The MR dampers were tested with on-off skyhook and a displacement-based control scheme that proved to be most effective on smooth roads. A test course was designed for suspension excitation, and was used for all of the ten different tests performed. While testing the full capabilities of the dampers was somewhat hindered by the excessive addition of spring force by the MR dampers, the retrofit MR dampers were successful in increasing the performance aspects of the test vehicle's suspension, as shown in Figure 6.1. Once again, the excessive spring force detracted from our ability to directly compare the ride comfort that can be expected from the MR damper in comparison to the OEM damper.

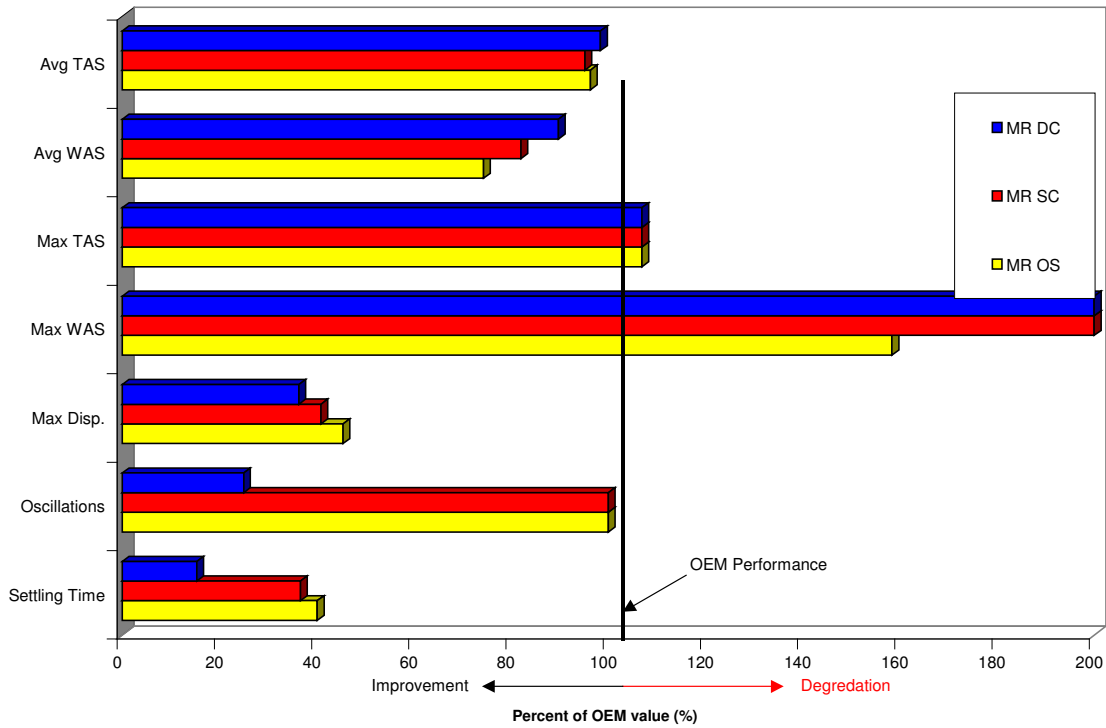


FIGURE 6.1. PERFORMANCE COMPARISON OF OEM AND MR DAMPERS.

While the majority of this research was successful, there are certainly areas that could be improved. The research presented in this paper offers a good start for the future development of magneto-rheological damper technologies for use on all types of motorcycles, from cruisers to super-sport bikes, and in all types of suspension, front and rear. In our opinion, with a few improvements to the damper and control system design, the MR damper technology is capable of revolutionizing the motorcycle suspension industry, provide a vast amount of improvement in performance *and* comfort, in a single package.

6.2 Recommendations

This section will explain some of the shortcomings of the research and designs presented in this paper, and the author's thoughts on how to solve these problems.

6.2.1 Damper Design

The primary problem with this research was the fundamental damper design chosen for the retrofit MR damper design. The OEM dampers were of twintube design with only limited available adjustment. In previous research conducted by Poynor [5], twintube designs did not work well with MR fluids. Since monotube dampers were the most common, compact, and developed MR damper design, they were chosen for the research presented in this paper. While the accumulator spring rate is usually negligible when compared to an automobile's main springs, the same is not the case in designs for MR dampers for motorcycles.

At least three solutions exist for this problem: one, minimizing upward piston area, two, ordering custom springs, and three, choosing a different base damper design. Minimizing upward piston area is probably the quickest "fix" of the accumulator problem. The spring force of the accumulator is based on the area normal to the velocity direction in the upward direction. By minimizing the overall upward area, the spring rate can be reduced. This can be accomplished in the current design by decreasing the shaft diameter. Custom springs are the second option for rectifying this problem – spring manufacturers can make premium custom springs, but expect to pay a premium price for the springs, on the order of \$300 to \$500 for a pair. The third option is to switch damper designs to either a twintube design (which may not work well, according to Poynor [5]) or a double-ended damper design, which requires room for the movement of the rear piston rod as well.

6.2.2 Prediction Model

While the prediction model used in this research held relatively true at low velocities, the effect of the accumulator pressure became apparent at higher velocity. This result showed the need for a more accurate prediction model that takes into account the effect

of the accumulator pressure as a variable in the damper's predicted force versus velocity curve.

6.2.3 Shaft Material & Design

Thomson Industries 60 Case QUICK™ shafts were used for the piston rod in this application. These shafts have extremely hard chrome plating (HRC 60) over a steel core, and exhibit excellent roundness and straightness properties. The chrome plating provides an excellent surface finish that promotes long seal life. While these shafts are excellent for use in dampers, they have a hefty price for motorcycle applications – weight.

A few alternatives to the chrome plated steel shaft exist. McMaster-Carr, for example, offers a ceramic coated aluminum shaft that is less expensive, much lighter, has a Rockwell C hardness of 70, and has an equivalent surface finish to the Thomson shafts. Anodized aluminum shafts are also available from McMaster-Carr with similar specifications. Aluminum 6061-T6 alloy would support the damper forces in this application, and offer an extreme weight savings.

Shaft design should minimize the length of the lead wire conduit hole. The time to machine a hole increases exponentially with the increasing length of the hole. The longer the wire hole, the longer the drill bit must be to machine it, and the slower one must drill. The shaft design was divided into two parts in this design, allowing for a faster machining time. While the bottom of the shaft was made from QUICK™ shaft, the top was made from 7075 aluminum for weight savings.

6.2.4 Housing Materials

The housing material used for MR damper construction was honed inner diameter DOM steel tubing produced by Scot Industries. This material already had a very smooth inner diameter, and required no additional honing. This reduced machining time, and was a much better honing job than the author could have produced himself.

6.2.5 Seals

Seals are of significant importance in MR damper design. As established by Poynor [5], o-rings do not demonstrate high endurance in the presence of MR fluid, since the MR fluid acts as an abrasive. O-rings are acceptable for use in static seals, but the best types of seal to use for dynamic applications in MR dampers are scraper-type seals. Hercules Hydraulics seals were used in this research. A urethane U-seal (U12-0.50-SQB) was used for the piston rod seal.

The accumulator seal used for this application was a Hercules Hydraulics fabric reinforced piston cup seal (9100-050F). The seal provides sealing pressure up to 3,000 psi and is strong enough to withstand MR fluid abuse. This particular seal, however, shows very high friction when installed, which can lead to damper hysteresis or stiction. This is rather critical considering the accumulator spring rate issue with these dampers. For future applications, a less stiff seal such as 8000-series urethane piston cup seal should be used. While this seal provides 1,200 psi sealing capability, it would provide less accumulator piston friction, allowing lower accumulator pressures.

6.2.6 Coil Manufacturing

Coil manufacturing is a rather tedious process, involving machining a coil form, contact and outer band, then winding the wire (150 turns in this case), soldering the wire ends, and sealing and fixing the coil band with epoxy. It is quite possible that the wire could get scared, causing a short or an open circuit. Typically the coil resistance varied by ± 10 percent in the coils in this research.

The best way to implement the coil design would be to have them produced out-of-house. Most coil producers offer hermetically sealed units with two contacts, and give specifications on the maximum duty cycle of the coil. This information is key as to how long a coil can operate at full load without burning out.

6.2.7 Control Units

Control Units of any type should be digitally based, not analog circuits as used in this research. The author's limited knowledge in the field of electronics was used to create these analog control systems only to realize that digital systems would be much more efficient and accurate. Using any one of a variety of programmable integrated circuits (PICs), all signals could be converted from analog to digital and then processed in accordance with the control policy. The output signal could then be converted back to analog form for damper control.

One of the main advantages of digital systems is the ability to preprocess the incoming data. For example, a moving average could be applied to the data to reduce the effects of engine vibration. Signal integration could be performed without the need for drift compensation or a cutoff frequency. Digital systems offer much versatility over analog sensors.

6.2.8 Control Sensors

Motorola MMA1220D accelerometers were used as the control system sensors for this research. These accelerometers are very small, low cost integrated circuits that require only a simple circuit for operation. These sensors work very well for the scope of the control systems in this research.

Accelerometers in motorcycle applications tend to reflect a large amount of chassis vibration from the engine, creating a problem when trying to determine wheel or body velocity, and the relative velocity between the two. Another option for determining the relative fork velocity requires the use of a linear absolute position encoder. The extra shaft length in this design can be marked for recognition by this sensor, which would provide much more accurate relative position data. This data would then aid in determining fork velocities or accelerations. These type of systems have digital output, so the control system would be required to be digital in nature.

6.2.9 Data Acquisition Units

The Dataq Instruments DI-700 data acquisition module used in this research was the perfect size and weight, and met all of the requirements needed. The low cost of this unit also made it very appealing for this research. Unfortunately, the author failed to read the very, very fine print. While the DI-700 unit allows sampling throughput rates (sampling rate for all channels combined) of up to 1,000 Hz, the software included with the unit only allows sampling throughput rates of 244 Hz, allowing only 81 Hz per channel for three channels. The software that would allow the 1,000 Hz sampling rate was an additional \$1500, more than three times the cost of the DI-700 itself. Since this research was primarily self-funded, the author could not afford this expense, and was forced to use the low 81 Hz per channel sample rate. For future reference, be careful when buying data acquisition units that the software included will support the unit's sampling rate.

References

1. Goose, "Motorcycle Suspensions," Direct Parts, Inc.
<http://www.directparts.com/static/goose/suspension.htm>
2. Carlson, J. David, "What Makes a Good MR Fluid?," 8th International Conference on ER Fluids and MR Fluids Suspensions, Nice, July 9-13, 2001.
3. Jolly, Mark R., Bender, Jonathan W., and Carlson, J. David, "Properties and Applications of Commercial Magnetorheological Fluids," SPIE 5th Annual Symposium on Smart Structures and Materials, San Diego, CA, March 15, 1998.
4. Lord Corporation, "Frequently Asked Questions," Lord Corporation, April, 2003.
<http://www.mrfluid.com/faqs.htm>
5. Poyner, James C., "Innovative Designs for Magneto-Rheological Dampers," Advanced Vehicle Dynamics Lab, Virginia Polytechnic Institute and State University, Blacksburg, VA, MS Thesis, August 7, 2001.
6. Lord Materials Division, "Designing with MR Fluids," Lord Corporation Engineering Note, December 1999.
7. Foale, Tony, "Balancing Act," Tony Foale Designs, 1997.
<http://www.ctv.es/USERS/softtech/motos/Articles/Balance/BALANCE.htm>
8. Kanai, Gen M, "Motorcycle Front Suspension Systems: Traditional Problems and Alternative Solutions," SplashMedia, The Unofficial Britten Motorcycle Website, September, 1996. <http://splashmedia.co.nz/users/britten/art3.html>
9. Brooke, Lindsay, "BMW Springs Ahead," Chilton's Automotive Industries, June 1993.
10. Ford, Dexter, "Forward Into The Past: A Short History of Motorcycle Front Suspension," Motorcyclist, July 1989, pp. 64-66.
11. BMW Motorcycles, "Design and Technology Gallery," BMW Motorrad USA, April 2003. <http://www.bmwmotorcycles.com/r1150rdesign.html>
12. Ericksen, Everet Owen, "Study of Magneto-Rheological Fluid (MRF) Dampers and Development of a MRF Shock Absorber for a Motorcycle," University of Nevada, Reno, Dept. of Mechanical Engineering, BS Thesis, 1999.
13. Peck, Kevin L, "Magneto-Rheological Shock Absorber for an off-road motorcycle," California Polytechnic State University, San Luis Obispo, BS Thesis, 2001.

14. Anaconda Wire and Cable Company, “[Wire] Technical Data,” Anaconda Wire and Cable Company, from design catalog; April 1965, pp 3.3-3.5.
15. Carter, Angela K, “Transient Motion Control of Passive and Semiactive Damping for Vehicle Suspensions,” Advanced Vehicle Dynamics Lab, Virginia Polytechnic Institute and State University, Blacksburg, VA, MS Thesis, August 1998.
16. DATAQ Instruments, Inc., “DI-700 USB Data Acquisition System,” DATAQ Instruments, Inc, Akron, OH, April, 2002.
<http://www.dataq.com/products/hardware/di700.htm>
17. Delphi, “Delphi’s Dynamic Duo,” Delphi.
<http://www.delphi.com/news/solutions/monthly/ms6070-11012001>
18. Wang, Jiong, “Mathematical Modeling of MR Dampers,” Advanced Vehicle Dynamics Lab Technical Report; Blacksburg, VA, June 2002.

Vita

John Willie Gravatt was born April 6, 1979 in Petersburg, Virginia. As most young boys his age, he had a quizzical attitude toward the way things worked. At age eleven, he started riding his first motorcycle, a small 80cc dirt bike he bought from his brother. Soon after, John began to discover how motorcycle engines worked. He completed his first engine rebuild at age 13, and the motorcycle successfully ran afterwards. He has been intrigued with motorcycles since then.

In his early teenage years, John had been undecided in a career choice, changing from doctor to nuclear physicist to nuclear engineer and final, his last choice, mechanical engineering. After high school, John decided to pursue this career choice, attending Virginia Tech for four years to obtain a Bachelor of Science degree in Mechanical Engineering.

After undergraduate school, John decided to further his education with a Master's of Science in Mechanical Engineering. In his senior year of undergraduate school, John had become keenly interested in a vehicle dynamics class taught by Dr. Mehdi Ahmadian. The next fall John asked to join Dr. Ahmadian's AVDL lab to do research on magneto-rheological damper applications for motorcycles. And, the rest is history.....

In the future, John will be working for Ingersoll-Rand in the leadership development program in engineering. He hopes to start his own business some day, focusing on motorcycle suspension tuning and data acquisition systems.

